ELUCIDATING THE REGULATORY MECHANISMS OF THE MAMMALIAN TARGET OF RAPAMYCIN COMPLEX 1 (MTORC1) IN PROTEIN HOMEOSTASIS

A Dissertation
Presented to the Faculty of the Graduate School
of Cornell University
In Partial Fulfillment of the Requirements for the Degree of
Doctor of Philosophy

by

Crystal Shana Conn

August 2013

ELUCIDATING THE REGULATORY MECHANISMS OF THE MAMMALIAN TARGET OF RAPAMYCIN COMPLEX 1 (MTORC1) IN PROTEIN HOMEOSTASIS

Crystal Shana Conn, Ph.D.

Cornell University 2013

The proper balance between protein synthesis, maturation, and degradation is crucial for an organism to survive and prosper. Each of these processes is coupled to the cellular environment through a multitude of signaling events to maintain protein homeostasis (proteostasis). The costly process of protein synthesis is partially regulated through the mammalian target of rapamycin in complex 1 (mTORC1). mTORC1 acts as a metabolic hub for the cell monitoring energy levels, nutrients, and amino acid availability in order to increase anabolic processes including initiation and elongation during mRNA translation. Deregulation of mTORC1 signaling can be catastrophic for an organism leading to cancer, obesity, and age-related illness. This work focuses on the molecular events that promote these disease states when mTORC1 is hyperactivated, and further investigates a potential mechanism for the cell to cope with this dys-homeostasis.

Here, I investigated the impact of hyperactive mTORC1 on the proteostasis network by inducing cytosolic and proteotoxic stress within cell cultures. Utilizing fibroblast knockouts, lentiviral knockdowns, plasmid transfections, and mTORC1 inhibitors, I was able to manipulate mTORC1 activity to elucidate its role in mRNA translation and overall proteostasis. I discovered that mTORC1 signaling is necessary for global cap-dependent protein synthesis, but attenuated cap-independent and IRES mRNA translation. Moreover, I demonstrated that the

heat shock protein 70 (*Hsp70*) utilized a cap-independent mechanism of translation through its 5'UTR. Hyperactive mTORC1 signaling prevented the stress-induced preferential translation of HSP70, which inhibited cell recovery leading to cell death. These results uncovered an intimate connection between mTORC1 signaling and the stress response, highlighting how an increase in protein synthesis can imbalance a translational switch necessary to maintain proteostasis.

Correspondingly, a decrease in mTORC1 signaling and protein synthesis can be beneficial to an organism leading to an increase in stress resistance and lifespan. To elucidate this mechanism I further investigated the effects of mTORC1 activity on protein synthesis and discovered an increase in protein quantity altered the quality of newly synthesized polypeptides. I demonstrated that hyperactive mTORC1 signaling decreased translation fidelity through its downstream target S6K, with no apparent influence on the chaperone network or ubiquitin proteasome system. An increase in S6K signaling promoted faster elongation rates, potentially leading to the observed mistranslation. Furthermore, partially inhibiting mTORC1 activity with rapamycin treatment restored protein quality by slowing down mRNA translation. My results reveal a mechanistic connection between protein quality and mTORC1 activity, which strengthen the role of nutrient signaling in proper cell growth and healthy aging.

Collectively, my *ex vivo* results used to manipulate mTORC1 activity uncover molecular events highlighting mTORC1 as a key component of the proteostasis network. mTORC1 signaling favors the development of age-related pathologies and investigating the effects of its activity provides an array of downstream potential drug targets.

BIOGRAPHICAL SKETCH

Crystal Conn was born in Wilmington, DE but spent her early childhood in the quiet suburbia of Lancaster, PA. She began preschool at the age of three and at this early age her mother started her in extra-activities including cheerleading, dance, craft shows, talent shows, hiking and roller-skating every Saturday with her father. At the age of ten, her family moved to the north shore of Long Island to the serene beach town of Shoreham, NY.

With the guidance from her sisters and encouragement from her parents, Crystal remained involved in a multitude of extracurricular activities including lacrosse, yearbook, class committee, honor society, NEXUS volunteer-work, and vocal performing groups to name a few. Her enthusiasm for participation was also present in the classroom. She believed there was no purpose in taking a break period when there was something you could be learning; breakfast was eaten during philosophy and lunch during geography. Throughout high school, Crystal's focus was spread thin between classes, activities, working, and social events. During her senior year, she was awarded the title of 'social butterfly', the technology award, and the art award, while preparing her art portfolio for college, acting as the editor of the yearbook, managing others at work, and supporting teamwork as the captain of the girls lacrosse team. Needless to say, after endless nights of work and days of activities, Crystal realized she needed a career that could keep her curiosity engaged. She put her art portfolio on a shelf and applied pre-med to Penn State University.

Crystal's early experience with multitasking became a true virtue for her in undergrad where she averaged twenty credits a semester, while working over thirty hours a week as a waitress. In her first year of college she accidently

introduced herself to her future mate, Andrew Modzelewski, when she wandered up to him and tried cheering up a stranger. The two became rather inseparable helping each other study through cell biology, organic chemistry, and eventually becoming lab partners in most classes. Crystal also started her research career in her first year where she designed a magnetic-optical trap independently teaching herself physics, CAD programming, and circuit building in Dr. Jiangbing Qi's lab. She was overwhelmed at how behind she was in the Sciences and made it her goal to become the top of her classes, only sometimes surpassed by Andrew. The professors at Penn State including Dr. Ike Shibley, Dr. Lorena Tribe, Dr. Alice Shaparenko, and most importantly Dr. Leonard Gamberg not only nourished their students with knowledge, but engaged Crystal's curiosity in all aspects of Science.

After a successful cooperative intern experience at Johnson & Johnson's McNeil Pharmaceuticals, Crystal changed the course of her future and began accumulating her list of graduate schools. Though being a medical pathologist was an interest of hers, the ability to continuously research novel mechanisms was far more appealing. In her senior year Crystal finally began to apply to graduate school, while also tutoring classmates in Quantum Mechanics and meddling in Biophysics protein purification research under Dr. John Golbeck. In December 2007, Crystal graduated with a B.S. in Biochemical Molecular Biology with minors in Chemistry and Physics.

Directly after graduation, Crystal began working in Litiz, PA for Pfizer pharmaceuticals close to her childhood neighborhood. Andrew was hired shortly after and together they ran manufacturing and set up a world-wide database to be used during Johnson & Johnson acquisition of Pfizer. Luckily their boss, Karen Forsha, allowed them the necessary leave during interview weekends and was enthusiastic to see what graduate school would bring for their future.

Crystal and Andrew jointly accepted an offer to Cornell's Genetic & Development program in Ithaca, NY. They moved into their first home August 1st, 2008 and spent their years in graduate school walking the gorge trails discussing research, contemplating experimental designs, and (as most graduate students do) venting about stubborn experiments. In June 2009 Crystal was honored to be Dr. Shu-Bing Qian's first graduate student where she began investigating the regulation of translation under stress, hyperactive mTORC1 signaling, and co-translation degradation. Her years of leading others in extracurricular activities also came in handy as she trained many graduate and undergraduate students over her four years in the Qian Lab.

Though starting in a new lab can be risky, it gave Crystal a unique glance at the path of academia and the hurdles she may need to leap over during her own future endeavors. Equipped with her new skills in training, learned experiments, and incredible perseverance, Crystal will continue on her next adventure to the sunny coast of California where she hopes to once more flourish near the beach during her postdoctoral training in Dr. Davide Ruggero's laboratory at the University of California, San Francisco.

This piece is dedicated to Hayes & Terri Conn for their guidance, support, and faith in letting me choose my own path; to my sisters Angela Star and Tiffany Lea for helping shape my imagination; to family departed along the way for their love and life lessons we carry on; to Kristie Marks for adventures; Dr. Jeremy Brownstein for sanity/insanity checks; and to Andrew J. Modzelewski, my nemesis and closest friend, that has endured this exploration with me.

Síocháin, Grá, agus Sonas

Sláinte!

ACKNOWLEDGMENTS

First, I would like to express my appreciation to my supervisor, Dr. Shu-Bing Qian. He has not only provided guidance, constructive criticism, and experimental expertise, but he also successfully set up a lab environment for scientific discussion, debate, and research opportunity. During my first year in the lab, Shu-Bing supported my attendance to Cold Spring Harbor laboratory for a conference where I experienced the benefits of scientific collaboration. Within our lab we follow in this style by supporting and guiding one another. Through a few rough patches, Shu-Bing has made me prepare and work to my limit to appease the audience with positive progress and assertive presentation. Overall, Shu-Bing's mentoring has helped me develop into a more efficient and critical scientist, and I am thankful for his contribution to my scientific growth.

I would also like to thank Dr. John Lis and Dr. Siu Sylvia Lee for their research expertise and assistance in my career development. I am particularly grateful to John for creative suggestions, input, and additional moments of shared knowledge over the past four years; including our road trip back to Ithaca in which even after a night of celebration he proceeded to help navigate us home and keep me awake as my lab mates slept in the backseat. I would especially like to thank Sylvia for allowing me to start my first rotation at Cornell in her lab, which reminded me how much I missed research! She was always very patient with me as she mentored me in genetics and experimental design. Outside of the lab, Sylvia also helped me in my career as she introduced me to Shu-Bing when I was trying to find the perfect mammalian signaling lab. In addition, John and Sylvia have become role models for me and I hope to one day achieve even a portion of what they have with their ease and ingenuity.

The MBG department has made Cornell a strong supportive environment. Specifically, I am grateful to Dr. Dan Barbash for answering my e-mail in the spring of 2008 and accepting me into the G&D program sans formal application. Also a special thank you in required for two previous students, Dr. Gizem Rizki and Dr. Raga Krishnakumar, for training me in my first year and letting me see how ambitious strong women succeed in graduate school to master their research. I especially appreciate Dr. Eric Alani and Dr. Paul Soloway for their support and encouragement, which helped me continue on during a few hardships I encountered in my PhD training. Diane Colf and Vicki Shaff have also given endless answers and guidance to the worrying minds of the graduate students and I am very grateful. I also want to acknowledge the custodial staff for their friendship at all times, even when I was sometimes overly exhausted or jumpy working into the wee-early mornings.

The Qian lab members made the environment a home and I am grateful to have such a large extended family. I thank Dr. Jun Sun for training me on transfections when we first began working together to study translation under stress. She was an amazing friend and with her and Dr. Yan Han, lab was always exciting. Even though we all worked, all the time, there was enthusiasm and playfulness throughout -making the lab environment the warmest place in Ithaca! I am grateful to Dr. XingQian (Ben) Zhang for always helping me find reagents, lab stocks, and for suggestions in molecular cloning and cell imaging. The lab could not have had a better founding member. I am also grateful to Botao Lui, Dr. Xiangwei Gao, and R. Alex Coots for insightful discussions and scientific debates. I also want to thank the rotational graduate and undergraduate students past and present for keeping me on my toes with their enthusiasm and contribution to the lab dynamics. A special thank you goes to two of my students, Haerin Paik and

Xiaoxing (Alva) Shen, for working endless hours on the ribosomal project with me. Constructing the lentiviral library, plating endless 96-well plates, and working with each well as a unique cell type, was exhausting and would not have been possible without them. They also became two of my close friends and, with Jun and Yan, created a wonderful lab atmosphere. Finally, I would like to thank our newest members, Elizabeth Ferrie, Ji Wan, Jun Zhou, & Julianna Magdalon, for keeping our research ascending on to new projects waiting to be discovered!

Other students within Cornell have also made the cold rather bearable and I would like to specifically thank Dr. Cornelia Sheitz, Jessica Wagnor, Aziana Ishmail, Mike Dowicki, Carolyn & Jared Hale (G.E.E.K.S.!), Adam & Kelly Brady, Elliot Kahen (Hugs), and the twelve^{+} physics & engineer strangers in a van for the free candy (Ragnarians) especially Veronica Pillar. Each of these individuals has worked extremely hard to remind me that life can exist outside the lab!

Less than ten years ago I entered the abyss of Science, with my loving friends and family worrying for my well-being. Four years later, I came to Cornell with their full support as a graduate student. I am very grateful to my closest friends Angela Star, Tiffany Lea, Kristie Marks & Jeremy Brownstein who have grown with me to become the people we are today. Andrew Modzelewski has played a greater role than he could imagine in my development as a scientist, but more importantly as a person. His sarcasm, humor, and wit has kept me alive and I am always amazed that he puts up with me after living together for a decade. I know I'm eccentric and crazy, thank you. *Ja cię kocham*.

At last, a special thank you goes to my extended family and loved ones I have lost over the years whose own lives, hardships, knowledge, and love has allowed my family to grow. Above all others, my most sincere gratitude goes to my loving parents. I have been blessed with an amazing life that has been planted

and nourished with their guidance. I could never have asked or wanted anything more. I would not be who I am without their life lessons, lectures, and support. Alas, I cannot fully express my appreciation and love for them with words. Thank you for all you do.

TABLE OF CONTENTS

LIST OF FIGURES

LIST OF TABLES

LIST OF ABBREVIATIONS

40S	small subunit of eukaryotic 80S ribosomes
4E-BP	eIF-4E binding protein
5'm7G	5'-7-methyl-guanosine
AKT	serine/threonine-specific kinase (also called PKB)
AMPK	AMP-activated protein Kinase
A-site	Aminoacyl binding site for charged t-RNA in a ribosome
ATP	Adenosine TriPhosphate
CFTR	Cystic Fibrosis Transmembrane conductance Regulator
CDS	Coding sequence
CLIPS	Chaperones Linked to Protein Synthesis
Deptor	Dep-domain mTOR interacting protein
DHX30	ATP-dependent DExD/H family RNA helicase
DNA	DeoxyriboNucleic Acid
DRiPs	Defective Ribosome Products
E3	ubiquitin ligase using ATP, ubiquitin, and protein lysine
eIF3	eukaryotic Initiation Factor 3, associated with 40S
eIF4A	eukaryotic Initiation Factor-4A, has helicase ability
eIF4B	eukaryotic Initiation Factor 4B
eIF4E	eukaryotic Initiation Factor 4E, binds 5'm7G of mRNA
eIF4F	eukaryotic Initiation Factor 4F, a complex including eIF4A, eIF4B, eIF4E, and eIF4G
eIF4G	eukaryotic Initiation Factor 4G
eEF2	eukaryotic Elongation Factor 2, promotes translocation
eEF2K	eEF2 Kinase (also called CaMKIII), inhibits eEF2 activity
ER	Endoplasmic Reticulum, a type of organelle in cell biology
ERK	Extracellular signal-Regulated Kinase
F-Luc or Fluc	Firefly Luciferase
FactSeq	Folding-associated co-translational Sequencing
GβL	G-protein β-subunit Like protein
GFP	Green Fluorescent Protein
GSK3	Glycogen Synthase Kinase 3, serine/threonine-specific
GTP	Guanosine TriPhosphate
GTPase	Guanosine TriPhosphatases
HEK293	Human Embryonic Kidney cells
HSF1	Heat Shock transcription Factor 1
HSP or Hsp	Heat Shock Protein
IGF-1	Insulin-like Growth Factor 1
IRES	Internal Ribosome Entry Site
LKB1	Liver Kinase B1 (or STK11), serine/threonine-specific
LTN1	Listerin E3 ubiquitin protein ligase
NAC	Nascent-polypeptide-Associated Complex
MEF	Mouse Embryonic Fibroblasts

mLST8	mammalian Lethal with Sec-13 protein 8
mRNA	messenger RNA
mSIN1	mammalian Stress-activated kinase interacting protein 1
mTOR	mammalian (or mechanistic) Target Of Rapamycin
mTORC1	mTOR complex 1
mTORC2	mTOR complex 2
P-site	Peptidyl-tRNA binding site in a ribosome
PABP	Poly(A)-Binding Protein, RNA-binding protein
PDCD4	Programmed Cell Death protein 4
PI3K	PhosphoInositide 3-Kinase
PIKK	PI3K Kinase family
pol	Polymerase
PRAS40	Proline-Rich AKT Substrate 40 kDa
Proteostasis	Protein homeostasis
Protor	Protein observed with Rictor
R-Luc	Renilla Luciferase
RAC	Ribosome Associated Complex
Rag	Ras-related small GTP-binding protein
Ragulator	Rag GTPases regulator, a GEF for Rags
Raptor	Regulatory associated protein of TOR
REDD1	Regulated in Development and DNA damage responses 1
Rheb	Ras homolog enriched in brain
Ribo-Seq	Ribosome sedimentation, profiling, and Sequencing
RING	Really Interesting New Gene with zinc finger domain
Rictor	Rapamycin-insensitive companion of TOR
RNA	RiboNucleic Acid
RPF	Ribosome Protected Fragments
RPs	Ribosomal Proteins
RPS6	RP Small subunit 6
RQC	Ribosome Quality Control complex
rRNA	ribosomal RNA
RSK	Ribosomal S6 Kinase, two subfamilies p90rsk and p70rsk
S6K1	p70 ribosomal S6 Kinase 1
Sirt1	NAD-dependent deacetylase sirtuin-1
SKAR	S6K1 Aly/REF-like target
TBC1D7	Tre-2, Bub2p, and Cdc16p 1 Domain family member 7
TOP	Terminal oligo-pyrimidine tract
tRNAs	transfer RNAs
TSC	Tuberous Sclerosis Complex
TSC1	TSC protein hamartin
TSC2	TSC protein tuberin
Ub	Ubiquitin, a small regulatory protein in eukaryotes
UPS	Ubiquitin Proteasome System
UTR	Untranslated Region

PREFACE

The primary emphasis of this dissertation is regulation during protein synthesis, maturation, to degradation and the balance maintained between each stage. This work is composed of five main chapters, each focusing on a different aspect of protein regulation to maintain cellular homeostasis. Part one reviews aspects of protein homeostasis at the ribosome, with emphasis on the role of protein synthesis through mTORC1 signaling. Part two derives from my rotation project and examines the control of protein synthesis under cell stress, identifying attenuation through the insulin-signaling pathway. Part three was the main focus of my graduate work exploring the dynamic effects of mTORC1 regulation of protein quantity and quality. Part four is a new project, which proposes a potential model of maintaining protein homeostasis by quickly disposing of erroneous unstable polypeptides through co-translational degradation. Part five summarizes the connection of these findings, while exploring a few of the unanswered questions which remain.

Extended research in these areas, outside the focus of the main chapters, is examined to a lesser extent and discussed briefly within part five and select unpublished results follow in the appendices.

CHAPTER 1

A sTORy of Protein Homeostasis: Slowing Down for Accuracy

This chapter was written by Conn CS as a literature review on mTOR and its link to protein homeostasis. The article will be revised and submitted for peer-review of co-translational quality control with Qian S-B.

1.1 Abstract

Co-translational regulation for protein quality control is emerging as a primary determinant in maintaining protein homeostasis (proteostasis). The mRNA sequence provides cues for translational regulation with unique motifs for initiation, codon placement for segment pausing, and orientation for polypeptide interactions, while the ribosome is a platform to decode these messages. During synthesis, additional factors assist in monitoring fidelity of the polypeptides and may interact to accurately fold each domain. This quality control of the newly synthesized polypeptides relies on a network of interactions from molecular chaperones to coupled ribosomes complexes for degradation. Furthermore, anabolic processes can only persist with sufficient materials and building blocks for each stage. This review discusses the link between nutrient signaling through mTORC1 with the newly discovered molecular mechanisms monitoring quality control at the ribosome. Without these connections, metabolic dys-homeostasis leads to cellular stress and age-related pathologies, making it critical to untangle the connections of the proteostasis network.

1.2 Introduction

The central dogma of biology traditionally organizes the process of gene expression from DNA, to RNA, to the end product of the native protein. Recent advances suggest the cellular abundance of proteins is predominately regulated at the translational level regardless of transcripts excessive quantity and protein degradation (Schwanhäusser et al., 2011). This allows protein synthesis to swiftly respond to environmental cues and cellular stresses at the level of mRNA translation. However, protein synthesis is the highest error-prone step in gene expression with approximately one in every $\sim 10^4$ codons mistranslated (Kirkwood et al., 1984). It has been proposed that overtime translational errors may create a feedback-loop into the translation machinery causing an exponential increase in errors or rather an "error catastrophe" (Orgel, 1963). To this end, it is not surprising that a decrease in protein synthesis may lead to an increase in stress resistance and lifespan (Pan et al., 2007; Conn and Qian, 2011).

There are several stages during mRNA translation to promote accurate expression of a given gene including recognition for initiation, proof-reading during elongation, and proper protein folding. At the center of this regulation lies multiple cellular pathways interacting in a network to maintain protein homeostasis (proteostasis); the balance between synthesis, maintenance, and degradation of proteins. This network relays information on growth factors, nutrients, energy requirements, and external stress to process accurate mRNA translation. A key metabolic hub integrating these signals is the mammalian (also referred to as mechanistic) target of rapamycin (mTOR). Under stable, nutrient-rich conditions mTOR in complex 1 (mTORC1) activates transcription factors for

ribosome biogenesis, eukaryotic initiation factors for mRNA recognition, and elongation factors necessary for accurate synthesis and speeds (Malik et al., 2013). As these steps occur during protein synthesis, the polymers of amino acids need to fold accurately either during or post-translational elongation. Proper folding may require additional aid from the molecular chaperone network and if errors occur the erroneous polypeptides need to be cleared by the ubiquitin proteasome system (UPS). Deregulation of protein synthesis, maturation, or degradation has been implicated in an array of protein conformational diseases and the abundance of misfolded proteins tends to accumulate in age-related diseases (Hipkiss, 2006; Cohen and Dillin, 2008; Voisine et al., 2010).

The causality between stable proteins and the formation of protein aggregates has therefore been intensely studied, yet the mechanisms of sensing and reacting remain unclear. Recent advances in the field show that the ribosome dynamics and interactions during mRNA translation play a vital role in proteostasis maintenance. Molecular mechanisms and interactions that promote accurate gene expression at the ribosome are reviewed here, highlighting the functional connection between nutrient signaling, the chaperone network, and the UPS in preventing proteostasic disease.

1.3 mTORC1 signaling activates ribosome biogenesis & protein synthesis

The function of mTOR signaling pathways are diverse in cell physiology. This cascade affects ribosome biogenesis, mRNA translation, pyrimidine synthesis, proliferation, mobility, and the activation of multiple transcription factors (Ben-Sahra et al., 2013; reviewed in: Hay and Sonenberg, 2004; Ma and Blenis, 2009; Yang et al., 2009; Oh and Jacinto, 2011; Malik et al., 2013). To cover

this spectrum of cellular processes, mTOR, a serine/threonine kinase from the phosphoinositide 3-kinase (PI3K)-related kinase family forms at least two multi-domain complexes differing in rapamycin sensitivity, function, and molecular composition (Loewith et al., 2002; Foster and Toschi, 2009). Additional factors interact with the core subunits to increase regulation and localization, but only the main complexes are discussed below.

mTORC1 is composed of the catalytic subunit mTOR, regulatory associated protein of TOR (Raptor), mammalian lethal with sec-13 protein 8 also referred to as G-protein β-subunit like protein (mLST8/GβL) and is further regulated with inhibitory partners proline-rich AKT substrate 40 kDa (PRAS40) and Dep-domain mTOR interacting protein (Deptor) (Chen and Kaiser, 2003; Hara et al., 2002; Kim et al., 2002; Sancak et al., 2007; Vander Haar et al., 2007; Peterson et al., 2009). Additionally, mTORC1 is rapamycin sensitive due to the binding of the drug rapamycin to FKBP12, which inhibits Raptor-bound mTOR, while having no direct effects on mTOR in complex 2 (mTORC2). mTORC2 is similarly composed of mTOR, mLST8/GβL, and inhibited by Deptor, but uniquely interacts with rapamycin-insensitive companion of TOR (Rictor), mammalian stress-activated protein kinase interacting protein 1 (mSIN1), and proteins observed with Rictor (Protor1 and 2) (Frias et al., 2006; Pearce et al., 2007; Sarbassov et al., 2004). The exact regulatory mechanisms impinging on mTORC2 are still under investigation, however mTORC2 is known to have a regulatory feedback relationship with mTORC1 (Guertin et al., 2006; Sarbassov et al., 2006). For these reasons we focus on the rapamycin-sensitive mTORC1, which plays a fundamental role in sensing the cellular environment to regulate global protein synthesis (Figure 1).

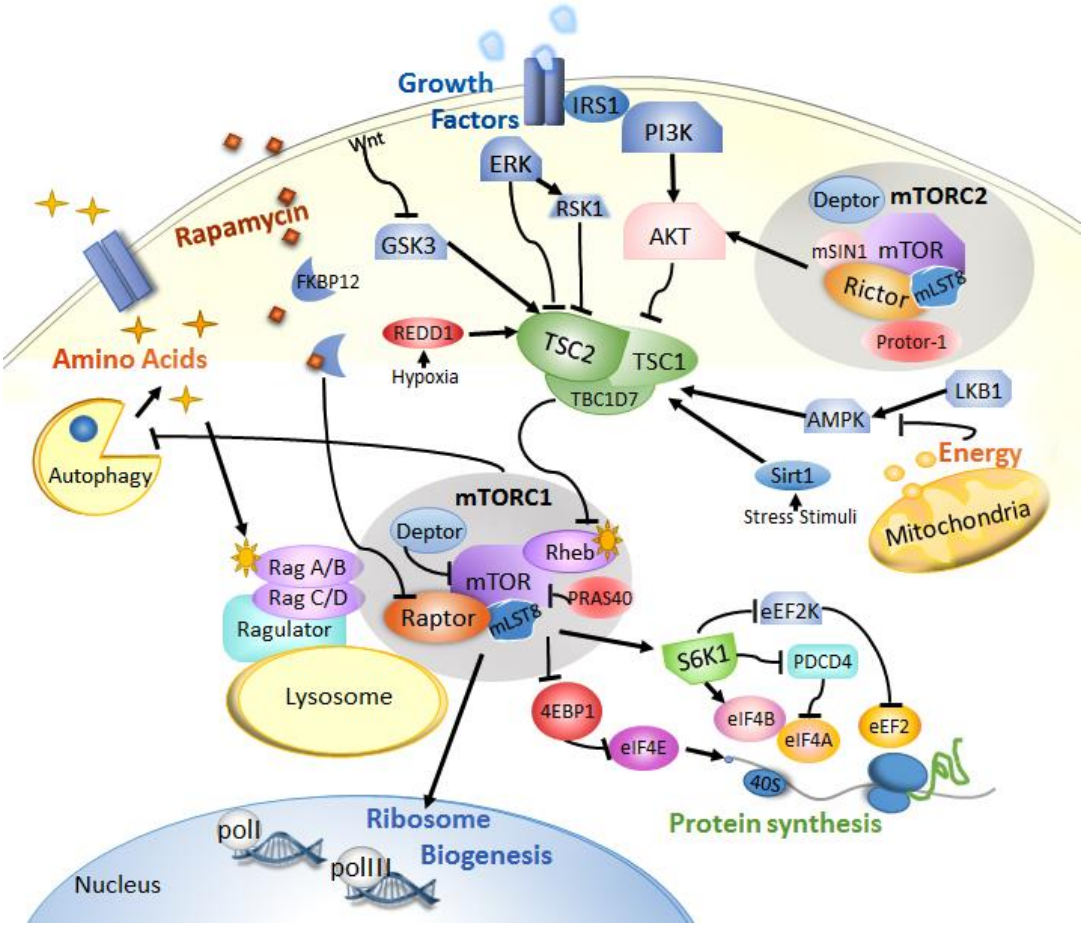

Figure 1-1. **The mTORC1 signaling pathway.** The essential mammalian target of rapamycin (mTOR) is a kinase forming two major complexes in the cell termed mTORC1 and mTORC2. The drug rapamycin, which binds FKBP12 to partially inhibit mTORC1 signaling, is widely studied for organismal benefits while mTORC2 is not directly affected. mTORC2 stimulates mTORC1 through AKT signaling creating a feedback between the two complexes, however these interactions are still under investigation. On the other hand, mTORC1 is well studied as a metabolic hub for the cell monitoring amino acids through interactions with Rags and the Ragulator complex, growth factors including insulin, energy levels through AMP-activate kinase (AMPK) and cellular stress by factors including regulated in development and DNA damage stress response 1 (REDD1). Many cell surface receptors regulate mTORC1 activity through activating or inhibiting the tuberous sclerosis complex (TSC), which acts as a GTP-ase for Rheb. Rheb in the GTP-bound state (sun-star) activates mTORC1 to increase anabolic processes including ribosome biogenesis and protein synthesis, while inhibiting the catabolic process of autophagy.

Regulation of mTORC1 by nutrient signaling and amino acids

The activity of mTORC1 reflects the cellular decision for growth or survival. Several intra- and extracellular cues regulate mTORC1 through the tuberous sclerosis complex (TSC), a GTPase-activating complex composed of hamartin (TSC1), tuberin (TSC2), and a recently identified stabilizing component Tre2-Bub2-cdc16-(TBC)1 domain family member 7 (TBC1D7) (Dibble et al., 2012). TSC works as a tumor suppressor through its inhibition of mTORC1's activator Ras homolog enriched in brain (Rheb) (Inoki et al., 2005). Under optimal cellular conditions, TSC is disrupted allowing Rheb to accumulate to a GTP-bound active state that in turn activates mTORC1. Pathways that phosphorylate TSC2 to activate mTORC1 include PI3K insulin-signaling through AKT and epidermal growth factor signaling through ERK and RSK (Dan et al., 2002; Ma et al., 2005). However, if energy levels are low or there is additional stress, TSC can be activated through AMPK, GSK3, REDD1, and also SIRT1 to inhibit mTORC1 (Brugarolas et al., 2004; Ghosh et al., 2010; Inoki et al., 2006; reviewed by: Rosner et al., 2008). This tight regulation allows cells to rapidly adjust mRNA translation based on cellular homeostasis.

Amino acid abundance is specifically essential for mTORC1 signaling, as the building blocks of proteins, and when limited prevent efficient mTORC1 activation (Hara et al., 1998; Long et al., 2005). The link between amino acids and mTORC1 was strengthened from the identification of Rag GTPases binding Raptor and redirecting mTORC1 to the lysosomal surface where Rheb is thought to reside (Sancak et al., 2008; Sancak et al., 2010). These interactions are stabilized by additional factors in a complex termed the 'Ragulator'. Furthermore, lysosomal proteins at the lumen and amino acid transporters are also thought to play a role controlling mTORC1 activation (Heublein et al., 2010; Zoncu et al.,

2011). Specific amino acids seem to have a larger effect over others (ex. Leucine) and a multitude of other factors are being uncovered for their interaction in this dynamic process (reviewed by: Jewell and Guan, 2013). Overall, with depletion in amino acids, nutrients, or energy levels, mTORC1 activity is inhibited (Figure 1). This necessity is in place due to the substantial amount of cellular materials and energy consumed during protein synthesis.

mTORC1 signaling to promote cap-dependent synthesis & global elongation

Upon activation, mTORC1 stimulates mRNA translation by phosphorylating two well-characterized downstream substrates: the eukaryotic initiation factor 4E (eIF4E)-binding proteins (4E-BP1, 2, and 3) and the ribosomal protein S6 kinases (S6K1 and 2) (reviewed by: Wang and Proud, 2006). 4EBP1 is a binding protein that inhibits the activity of eIF4E. Once phosphorylated (Thr37/46, Ser65, Thr70), 4EBP1 releases eIF4E allowing for it to recognize the 5'-7-methyl-guanosine (5'm7G) cap-structure on mRNA (Yang et al., 2009). eIF4E then recruits scaffolding and helicase factors, eIF4G and eIF4A respectively, in order to complete the eIF4F complex. The completion of eIF4F on the mRNA 5'm7G cap-structure is both rate limiting in translation initiation and tightly regulated (reviewed by: Jackson et al., 2010). Once stabilized, eIF4F helps to recruit the small 40S ribosomal subunit to begin scanning for the translation start site. The other major downstream target of mTORC1, S6K1 is held inactive with the eIF3 translation initiation complex at the 5' untranslated region (UTR) (Holz et al., 2005). Once activated, S6K1 promotes protein synthesis and cell growth presumably by phosphorylating multiple substrates involved in translational control including RPS6 (40S ribosomal protein subunit 6), eIF4B, elongation factor 2 kinase (eEF2K), S6K1 Aly-REF like target (SKAR), and Programmed Cell

Death protein 4 (PDCD4) (Richardson et al, 2004; Shahbazian et al., 2006; Wang et al., 2001; Yang et al., 2003). Through these interactions, downstream of mTORC1 signaling, these factors unite to recruit the 60S ribosomal subunit to proceed with protein synthesis.

S6K1 phosphorylation of eIF4B allows for an increase in elongation as the initiation factor stimulates the helicase eIF4A to unwind secondary structures for proper decoding (Shahbazian et al., 2006). Protein synthesis proceeds through initiation to elongation as the ribosome moves one codon relative to the mRNA; this process requires elongation factors eEF1 and eEF2. eEF2 allows for translocation of the ribosome to promote the peptidyl-tRNA migration from the A-site to the P-site allowing newly synthesized polymers of amino acids to grow. The activation of eEF2 is regulated by eEF2K phosphorylation within its GTP-binding domain (Wang et al., 2006). As stated above, S6K1 phosphorylates eEF2K inactivating the kinase and releasing eEF2 to promote elongation. The effects of mTORC1 activity in elongation and cap-independent synthesis are discussed further in the following sections.

mTORC1 activation of ribosome biogenesis

Ribosomes are composed of multiple ribosomal RNAs (rRNA) and, in mammals, seventy-nine distinct ribosomal proteins (RPs). Ribosome biogenesis requires RNA polymerase (pol) I to produce rRNAs, pol II for mRNAs encoding RPs, and pol III to produce 5S rRNA. mTORC1 monitors nutrient availability to promote ribosomal RNA synthesis and translation of RPs (reviewed by: Xiao and Grove, 2009). The transcription of ribosomal DNA is catalyzed by RNA pol I within the nucleolus, which requires at least three transcription factors for activity (TIF-1A, TIF-1B, and UBF). Upon phosphorylation at serine 44 (S44), TIF-

1A interacts with TIF-1B to recruit pol I to rDNA promoters to form the transcriptional complex. By inactivating mTOR with rapamycin treatment or mutating S6K1, TIF-1A loses phosphorylation at S44 and the formation of the transcription initiation complex is lost (Tsang et al., 2003; Hannan et al., 2003). Rapamycin treatment and amino acid deprivation also cause TIF-1A to re-localizes to the cytoplasm (Mayer et al., 2004; Li et al., 2006) and a loss of TIF-1B binding to rDNA promoter due to UBF dephosphorylation (Hannan et al., 2003).

Studies have further identified mTORC1 regulation of pol III transcription and identified mTOR binding at both pol I and pol III promoters (Tsang et al., 2010). Tsang *et al* used chromatin immunoprecipitation to identify mTOR as a chromatin-associated kinase binding the 45S rDNA promoter, 5S rRNA, and tRNAs under optimal growth conditions. This direct interaction allows for a rapid response to changes in cellular homeostasis at the transcriptional level to regulate global protein synthesis. It is intriguing to consider that mTORC1 may even play a conserved role in remodeling chromatin to prevent transcription, as observed in yeast (Tsang et al., 2003), but current roles for mTOR in transcription regulation are still under investigation.

Ribosome biogenesis is further regulated at the translational level. RP transcripts contain a unique 5' terminal oligo-pyrimidine (TOP) sequence regulated by mTORC1 activity. The 5'TOP allows for strict regulation followed by nutrients; under serum starvation, mRNAs are poorly translated and after stimulation with nutrient-rich conditions they associate in polysome fractions of sucrose gradients (Warner, 1999). Unlike the transcriptional regulation of ribosome biogenesis, which is affected by rapamycin treatment and S6K1, the translational regulation of the 5'TOP and TOP-like sequences rely on signaling through 4EBP to eIF4E (Hsieh et al., 2012; Thoreen et al., 2012).

Recent reports utilized polysome profiling with sequencing, Ribo-Seq (Ingolia et al., 2009), to monitor mTORC1 specific translation with or without mTOR inhibition by ATP-site inhibitors and found that TOP mRNAs were most affected. Furthermore, 4EBP deficient cells still show 5'TOP protein synthesis even when mTORC1 activity is completely inhibited by the drug Torin 1 (Thoreen et al., 2012) and abolishing P-S6rp by over-expressing a S6K1 negative mutant had no effect on 5'TOP mRNA translation (Tang et al., 2001). These recent advances in the field suggest eIF4E plays a key role in RP translation, but other 5'TOP binding factors may also be necessary (Damgaard and Lykke-Andersen, 2011). It could be that S6K1 has a greater effect on the transcriptional aspects of ribosome biogenesis, while signaling through 4EBPs is necessary for RP mRNA translation. Either way, perturbations in mTORC1 activity can be detrimental not only to 5'TOP protein synthesis, but globally due to effects on the translational apparatus during ribosome biogenesis and throughout elongation.

1.4 Ribosomes aid in nascent chain processing & quality control

Upon assembly, the ribosome is an intricate macromolecular complex providing support as a platform for decoding each messenger RNA to give rise to a unique three dimensional polypeptide. The small subunit is positioned for deciphering the transcript, while the large subunit contains the active peptidyl-transferase center for completing peptide bond formation. Variation in protein synthesis by codon usage, secondary structures, and additional binding partners allows for precise regulation at the ribosome (Kramer et al., 2009; Pechmann et al., 2013). The ribosome, as a ribonucleoprotein complex, also provides structure to initiate folding starting within the exit tunnel during elongation (Fedyukina

and Cavagnero, 2011). As the newly synthesized polypeptides are decoded, it is believed that they have already started on a pathway of intermediate steps to reach their native state (Levinthal, 1968). Though many components have been identified to interact or bind newly synthesized polypeptides, the direct co-translational mechanisms have just started to be revealed.

Nascent chains interact with ribosomal pausing for efficient folding

Local discontinuous translation, ribosome pausing, temporally separates the translation of segments within the peptide chain and actively coordinates their co-translational regulation (Komar, 2009). The cellular environment coupled with the gradual emergence of the ribosome-bound nascent chains enforce conformational restraints on a proteins folding landscape that differ from historically isolated proteins stimulated to fold *in vitro*. In order to examine co-translational folding, nascent chains are historically labeled to monitor their movements while bound to a stable ribosome. Recent advances using NMR spectroscopy have allowed for studying the conformation of a polypeptide chain by labeling a sequence isotopically *in vivo* and viewing different fractional lengths corresponding to the protein on an isotopically silent ribosome (Cabrita et al., 2009). This approach generated a series of snapshots of the folding nascent chain, revealing the existence of partially folded ribosome-bound intermediates.

To view global translational pausing of the ribosome in relation to co-translational folding *in vivo*, Han *et al* developed a novel approach utilizing ribosome profiling and sequencing. Folding-associated co-translational sequencing, FactSeq, allowed them to monitor folding at single codon resolution. By comparing features of RPFs (ribosome protected fragment) distribution and density along mRNA sequences of interest, they provided direct evidence of

domain-wise measurements for the efficiency of folding (Han et al., 2012; Liu et al., 2012). However, folding is a complex task requiring further regulation of aberrant mRNAs, mistranslated polypeptides, and misfolded species.

Ribosome associated chaperones aid in co-translational folding

As newly synthesized polypeptides emerge from the ribosome exit tunnel they allow their exposed amino-terminus to interact within the cellular environment. Though most small cytosolic proteins are able to assemble into the correct confirmation, the majority of proteins require further assistance to acquire their distinctive structure either by a co- or post-translational mechanism. In eukaryotes, cytosolic chaperones facilitate both mechanisms by chaperones linked to protein synthesis (CLIPS) and also heat shock proteins induced during cell stress to maintain proteostasis.

CLIPS directly associate with the translational apparatus during optimal conditions. The exit tunnel of the ribosome provides a platform for newly synthesized polypeptides to interact with rRNA and CLIP factors. These chaperones provide co-translational interactions to sort, fold, and modify the exposed amino acid residues (Kramer et al., 2009; Hartl and Hayer-Hartl, 2009). The ribosome-associated complex (RAC) is a heterodimeric chaperone complex of the CLIPS network that plays a functional role with co-translational protein folding without directly associating with the nascent chains. RAC is composed of a J-domain HSP40- and HSP70-based system. Eukaryotic RACs directly bind to ribosomes through the J-domain proteins and co-chaperones stimulate the ATPase activity of their CLIPS HSP70 homologs. Recent work identified that mRAC specifically interacts with HSP70 stimulating ATPase activities, but not with the 85% identical homolog HSC70 (Jaiswal et al., 2011). The ability to bind

ATP allows a regulatory mechanism to monitor cellular energy status for direct chaperone coupling with the ribosome. When energy sources are depleted, the chaperones are no longer recruited to the translational machinery and likely assist in additional protein quality control mechanisms. In addition to RAC, an essential heterodimeric nascent polypeptide-associated complex (NAC) is also present at the exit tunnel directly contacting the nascent polypeptides during non-stress conditions (Rospert et al., 2002; Kirstein-Miles et al., 2013). However, when proteostasis is imbalanced, NAC also relocalizes to aggregates playing a typical chaperone role, which also leads to a loss of the translational capacity.

There has been recent evidence that the ribosome requires these chaperones not only to ensure proper folding, but for maintaining global protein synthesis. With an imbalance in proteostasis, caused by heat shock or induced protein misfolding, there is translational pausing at an early elongation stage. This stalling of the ribosomes appears to be regulated by HSP70 in cell culture studies (Liu et al., 2012; Shalgi et al., 2012). HSP70s are central organizers of the chaperone network, directing subsets of proteins to additional chaperonins including TRiC/CCT for coupled folding or HSP90 for conformational regulation (Wegele et al., 2004; Yam et al., 2008). Interestingly, hyperactive mTORC1 signaling inhibits paused translation after stress and attenuates the stress-induced translation of HSP70 required for cell recovery (Sun et al., 2011; Conn and Qian, 2011). The inhibition of cap-independent *hsp70* translation prevents the cytosolic stress response and eventually causes cell death. Therefore, HSP70 is key component of the molecular chaperone and proteostasis networks, essential for refolding polypeptides as well as playing a novel role in stalling protein synthesis during proteotoxic stress (Liu et al., 2012).

Ribosome associated factors monitor protein quality for co-translational degradation

Aberrant mRNAs and faulty ribosome decoding can also lead to defective polypeptide products unable to reach functional native structures regardless of chaperone assistance. It has been estimated and debated that as high as 30% of all newly synthesized polypeptides are targeted for degradation as defective ribosome products (DRiPs) by UPS (Schubert et al., 2000; Qian et al., 2005; Yewdell and Nicchitta, 2006). Of polypeptides targeted for degradation, approximately 50% are estimated to be degraded by a co-translation mechanism monitored using elegant reporter constructs for stability (Turner and Varshavsky, 2000). The extent of co-translational degradation has recently been re-evaluated by monitoring ubiquitin (Ub) on a proportion of nascent polypeptides *in vivo* with a drastic range in Ub levels on ribosome-bound polypeptides with levels as low as 1.1% in *S. cerevisiae* and up to 15% in mammalian cell culture (Duttler et al., 2013; Wang et al., 2013).

Ribosome sedimentation allowed both groups to sequester polypeptides at the ribosome that could then be monitored by either a polyUb-affinity capture after radioactive pulse or biotin-conjugating puromycin label to evaluate peptides targeted for degradation, both co- and post-translation. Wang *et al* determined both cytosolic and ER-bound polysomes target newly synthesized polypeptides with Ub. In addition, using an *in vitro* assay, they showed both stalled and active translation complexes can accumulate Ub, with 2/3 from actively translating ribosomes. Both groups evaluated how co-translation folding mechanism influence co-translational degradation. Indeed blocking HSP70 or ribosome bound NAC components induced ribosome stalling and enhanced Ub at nascent peptides by 50% in human cell lines. Duttler *et al* specifically looked at mRNA features to identify particular structures that may be targeted for

degradation. They found that co-translational Ub preferentially targets longer peptides that are derived from highly expressed and rapidly translating mRNAs. These results highlight the cooperation of co-translational folding for quality control at the ribosome that can lead to ubiquitylation for misfolded and erroneous nascent peptides, but what chain of events lead to their degradation?

Co-translational degradation processes target defective mRNA and aborted translation. Utilizing non-stop mRNA reporter proteins in a screen allowed for the identification of multiple components required for the non-stop mRNA decay pathway (Wilson et al., 2007). One of these candidates, Listerin/LTN1, was further characterized to determine its role as a RING-domain-type E3 ubiquitin ligase that associates with ribosomes for quality control of non-stop mRNAs (Bengston and Joazeiro, 2010). Ltn1 was further identified as a component of a ribosome quality control complex (RQC) recently identified to stably interact with the 60S ribosomal subunit to trigger degradation of polypeptides during stalled synthesis (Brandman et al., 2012). Components of RQC and localization with the ribosomes were identified by immuno-precipitation, mass spec, and electron microscopy. Single and double mutants of RQC components in *S. cerevisiae* further elucidated their unique roles, specifically identifying Tae2 for monitoring translation-stress and signaling to the heat shock factor 1 (HSF1). These recent reports place interconnections of the proteostasis network from synthesis, to maintenance, and degradation all beginning at the ribosome even for eliciting the cellular stress response (Figure 2).

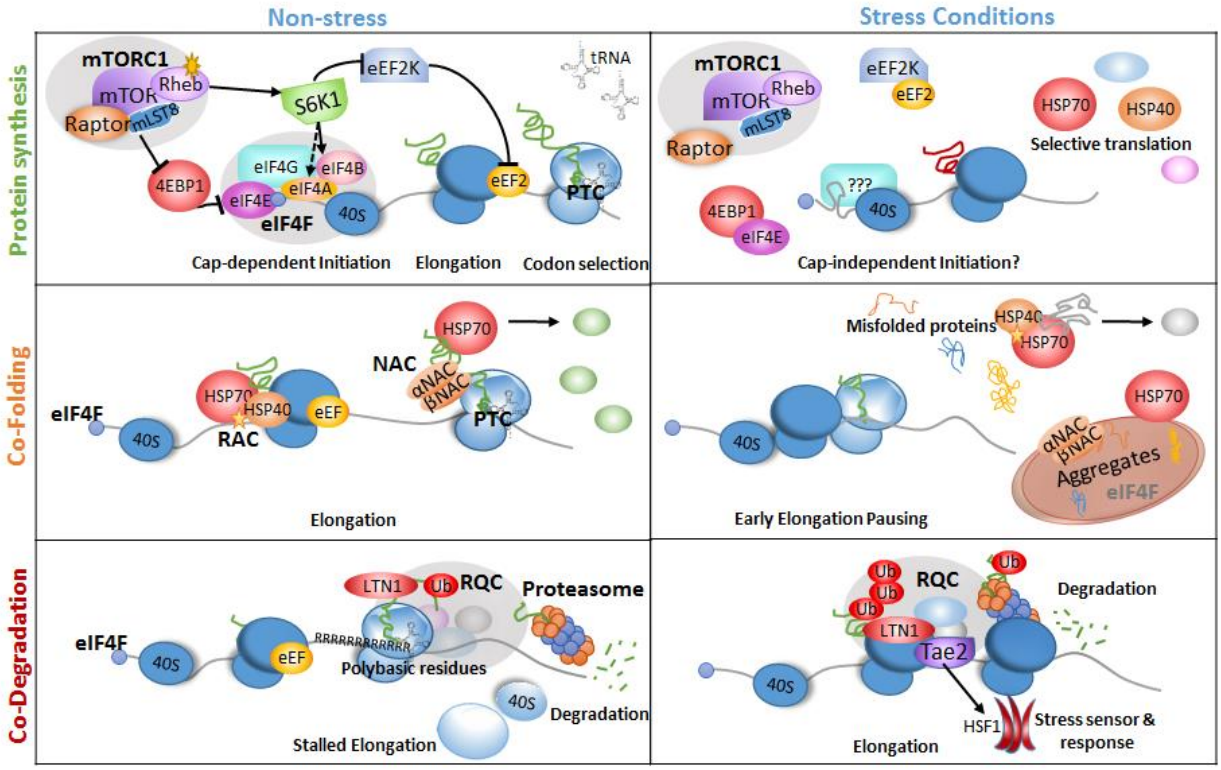

Figure 1-2. **Protein quality control at the ribosome.** *Upper:* mTORC1 signaling increase translation initiation and elongation for accurate protein synthesis. Disruptions is mTORC1 activity can impair accurate codon selection altering translation fidelity. Under stress conditions, mTORC1 activity is decreased allowing for selective translation potentially by unique mRNA selection and initiation mechanisms. *Middle*: Chaperones linked to protein synthesis included the ribosome-associated complex (RAC) and the nascent polypeptide-associated complex (NAC), either of which can utilize or interact with HSP70 to promote accurate protein folding. Under stress, these complexes dissociate from the ribosome to refold proteins and clean-up protein aggregates. The loss of chaperones associated with the ribosomes, creates an early elongation pause as the newly synthesized polypeptide emerges into the cellular environment without assistants. *Lower*: Aberrant mRNAs can induce ribosome stalling and slipping during elongation. These ribosomes are targeted by the ribosome quality control complex (RQC), where LTN1 acts as an E3 ligase to ubiquinate the stalled polypeptide chain for degradation. Under stress, there is an increase is nascent chain ubiquitination, degrading the targeted polypeptides at the ribosome. The RQC complex component Tae2 also signals to the stress sensor HSF1 to induce the stress response and promote cell recovery.

1.5 Elongation speeds affect translation fidelity

Transient pausing or dwelling of ribosomes can affect a variety of co-translational processes, including protein targeting, folding, and potentially degradation as discussed above. Many have reviewed how codon usage controls ribosome speed, fine-tuning translation to increase efficiency and accuracy of protein synthesis (Gingold and Pilpel, 2011). Elongation rates in eukaryotes are thought to be globally constant under optimal conditions with ~3-8 amino acids translated per second (Mathews et al., 2000). However, the overall speed of translation relies on initiation, elongation, and termination with the general agreement that 'less leads to more'. It has been shown that slowing translation speeds using mutant ribosomes in *E. Coli* enhanced eukaryotic protein folding efficiency, leading to higher yields of native recombinant proteins (Siller et al., 2010). The consensus is that faster elongation will create greater conformational possibilities for the emerging polypeptides that may disrupt chaperone assistance, but how does the ribosome know when to slow down and what regulatory elements are in place for this controlled synthesis to prevent stalling?

Codon usage alters ribosomal pausing for efficient folding

Varying codon placement along the mRNA not only varies rates of polypeptide emergence from the ribosome, but influences the capacity to fold toward the native state (O'Brien et al., 2012; Ciryam et al., 2013). Spencer et al. derived a formula based on predicting relative codon translation speeds of *E. Coli* tRNA information using values from measured rates of individual codons. To measure newly synthesized elongation rates they used pulse-chase analyses *in vivo* and showed that sequence engineering, based on their predictions, modulates translation rates in a manner not only based on codon usage

frequency, but more so on tRNA availability and wobble content for proper folding of the encoded polypeptide (Spencer et al., 2012). If they modulated their designed sequence to accelerate translation, they correspondingly saw a decrease in folding yields suggesting elongation rates are critical for a protein to reach the accurate confirmation. Their equation generates predicted translation speed profiles for any mRNA, in any organism, with known tRNA gene content. These findings further support a model where each protein follows a particular pathway, to fold accurately as the correct codon pairs to influence the nascent chain emerging from the ribosome.

Translation inhibition to increase protein function and maintenance

Inducing chaperones in cells or increasing the activity of the UPS for proper degradation can partially alleviate abnormal proteins that accumulate within cells, but the goal is to prevent them. Slowing down translation can increase accurate folding; furthermore, a partial inhibition of translation can improve folding of mutant proteins (Meriin et al., 2012). Using emetine in a dose-dependent manner creates a mild translation inhibition of ~50% with a significant decrease in aggresome formation, the buildup of newly synthesized aberrant polypeptides. These effects promoted folding of specific polypeptides including disease-related mutants. CFTR-F508Δ disrupts protein folding and trafficking, ultimately leading to cystic fibrosis. A dose-dependent decrease in both translation initiation and elongation lead to the corresponding increase in CFTR-F508Δ folding and activity (Meriin et al., 2012).

Inhibiting specific translation factors has similar benefits in organisms. Knocking-down eIF4G levels decreases global cap-dependent protein synthesis in a mechanism to modulate the rate of translation in response to environmental

cues in *C. elegans* (Rogers et al., 2011). Interestingly, longer mRNAs had a relative increase in translation efficiency even though translation was decreased. The proteome profiles also shifted to genes known to respond to stress and enhance longevity. Similar increases in stress resistance were observed by knocking down other translation factors including eIF4E, S6K, and PABPs (Pan et al., 2007). Stress resistance is closely linked with molecular chaperones and degradation by the UPS and cell autophagy. Each of these pathways is critical for protein quality control in the proteostasis network. Together, it seems that inhibition of translation reprograms cells for somatic maintenance versus cell growth and proliferation.

mTORC1 signaling regulates translation elongation effecting protein quality

mTORC1 activity directly increases global protein synthesis through ribosome biogenesis as well as eIF4E and S6K signaling. Having considered that translation initiation and elongation may influence the quality of products, we recently monitored protein synthesis through hyperactive mTORC1 signaling (Conn and Qian, 2013). An increase in mTORC1 directly increased global newly synthesized polypeptides, as expected, but when looking directly at reporters there was less stable proteins present. Inhibiting the UPS showed an accumulation of newly synthesized proteins within the insoluble fraction of lysates, suggesting an increase in protein aggregation or rather a decrease in protein quality. To monitor translation fidelity, we created a reporter system monitoring mistranslation and read-through errors. Hyperactive mTORC1 lead to an increase in both errors, specifically through S6K downstream signaling. A decrease in translation fidelity is often linked to alterations in elongation rates, which may influence co-translational folding, pausing, modifications, and/or

interactions with binding partners creating an increase in erroneous polypeptides. Using ribosome sedimentation and the translation inhibitor harringtonin, we took snap shots of the polysome run-off to monitor elongation rates. Interestingly, an increase in mTORC1 signaling lead to faster elongation that could be rescued by partial inhibition of mTORC1 with rapamycin treatment. Our results show the drastic effects translation, specifically elongation rates, can have on protein quality reinstating that consensus that 'less can lead to more'.

1.6 Pathway integration for proteostasis and disease prevention

The insulin/insulin-like signaling pathway has been noted for linking protein conformational diseases to the aging process (Cohen and Dillin, 2008). Within this pathway lies mTORC1, which monitors the cellular environment to proceed with the energetically demanding process of protein synthesis (Ma and Blenis, 2009). Due to mTORC1's essential role in each step of translating mRNA to functional protein, an assortment of defects in the mTORC1 signaling pathway can lead to abundant proliferation, tumor formation, and protein aggregate diseases (Averous and Proud, 2006; Dann et al., 2007; Reiling and Sabatini, 2006; Lu et al., 2010). Furthermore, a decrease in TORC1 signaling mirrors that of a decrease in protein synthesis; leading to stress resistance and an increase in lifespan in nearly all model organisms (Syntichaki et al., 2007; Cohen et al., 2009; Harrison et al., 2009; Selman et al., 2009; Stanfel et al., 2009; Zid et al., 2009). Despite the overwhelming experimental evidence, how a reduction in protein synthesis extends stress resistance and lifespan has remained elusive.

It has been postulated that a decrease in translation is beneficial merely because it relieves stress on the folding and degradation machineries necessary

to maintain proteostasis. This situation results in "spare" proteolytic and chaperone function contributing to the observed stress resistance in organisms (Hipkiss, 2008). However, with recent advances in the field, it is now apparent that a decrease in translation additionally allows for accurate binding and maintenance during co-translational events to promote co-translational quality control. This includes regulated pauses between codon sequences and the ribosome, folding by the molecular chaperone network and the stalling HSP70s absence can induce, targeting nascent peptides with modifications, and clearance of aberrant messages to promote proteostasis (Spencer et al., 2012; Liu et al., 2012; Siller et al., 2010; Kirstein-Miles et al., 2013; Duttler et al., 2013; Brandman et al., 2012). Many individual studies also report that these proteostasis mechanisms decline with age, due to absent modifications or misreadings producing defective forms of the proteins necessary for maintenance (Koga et al., 2011). The steps leading to these errors and eventually the overloading of the proteostasis network remain to be clarified (Morimoto and Cuervo, 2009), but with recent advances in the field we can likely state they may occur pre- or at least co-translation at the ribosome.

The ribosome is now viewed as a hub for quality control attributing to pausing and co-translational regulation for an increase in accurate mRNA translation (Zhang et al., 2009; Siller et al., 2010; Tuller et al., 2010; Pechmann et al., 2013). In eukaryotes, the rate limiting step of protein synthesis is mainly determined by the translation initiation complex eIF4F which is partially regulated downstream of mTORC1 signaling. With an increase in TOR activity, there is activation of translation initiation and elongation of the newly synthesized peptides (Browne and Proud, 2004; Hay, 2004). This leads to an increase in the recruitment of ribosomes to mRNA and translocation by eEF2

through S6K signaling, which may skew pausing and co-translational folding required for translation fidelity (Conn and Qian, 2013). Without efficient processing, a cellular burden of erroneously synthesized polypeptides could eventually saturate the chaperone and proteolytic pathways as hypothesized. Furthermore, hyperactive mTORC1 attenuates cap-independent synthesis required for the inducible molecular chaperone, HSP70, which is essential for cell maintenance under stress (Sun et al., 2011; Liu et al., 2012). In time the proteostasis machineries also may become crippled with translational errors, promoting the projected 'error catastrophe' and an acceleration of conformational diseases during aging. To this end, are we left to decrease translation, target the essential pathways leading to the dys-homeostasis, target the exact factors at unique stages of translation, or somehow all of the above?

Previously, our lab has shown that a moderate accumulation of misfolded proteins, and thus a slight reduction of chaperone availability, enhanced mTORC1 signaling (Qian et al., 2010). In addition, we demonstrated that molecular chaperones also regulate mTORC1 assembly in coordination with nutrient availability. These results established that mTORC1 links protein translation with protein quality control (Qian et al., 2010; Conn and Qian, 2011). This also creates a 'chicken and egg' dilemma; does mTORC1 signaling create an accumulation of misfolded proteins with age or do misfolded proteins somehow enhance mTORC1, decreasing translation fidelity? We can imagine that during aging proteins will eventually misfold with a decrease in the chaperone network, but would this derail mTORC1 signaling as well? These insights further strengthen the connection between mTORC1 signaling and its role in maintaining proteostasis, but raise more concerns regarding the role(s) mTORC1 plays in the

balance. Advances in understanding and monitoring these mechanisms with one another will help to untangle protein synthesis within the proteostasis network.

1.7 Conclusions & Outlook

Combining historical methods including sucrose gradients, pulse analysis, and affinity purification with the wealth of bioinformatics data available has allowed for growth in understanding proteostasis. The ability to utilize genome-wide analysis to predict and monitor translation at single-nucleotide resolution has opened the doors to studying various degrees of translational regulation. The historical two-step processed models of folding and denaturing are being replaced with kinetic formulas accessing ribosome dwell-time and wobble-codon selection. Specifically, Ribo-Seq has become vital allowing measurements for proteomics to determine the exact sequence of ribosome pausing and coupling this technology with domain specific antibodies or affinity purification for further identification of co-translational processing *in vivo*.

The approaches touched upon here provide novel insights into individual and global protein synthesis regulation and have opened a new field of ribosome quality control. Monitoring co-translational regulation with these methods will likely shed light on physiological as well as pathological conditions once adapted and utilized widely. Additional *in vivo* research is necessary to understand which mRNA sequences or polypeptides require further assistance, what factors bind for assistance, and when this assistance occurs physiologically during development and disease-related states for future drug targeting.

CHAPTER 2

PI3K-mTORC1 Attenuates Stress Response by Inhibiting Cap-independent Hsp70 Translation

This work was submitted August 2010 and first published on December 22, 2010, doi:10.1074/jbc.M110. 172882. The manuscript was published as Sun J*, Conn CS*, Han Y, Yeung V and Qian S-B. **PI3K-mTORC1 attenuates stress response by inhibiting cap-independent Hsp70 translation.** *J. Biol. Chem*. 2011 Feb 25; 286, 6791–6800. Minor modifications have been made for reprint here. *Both authors contributed equally to this work.

2.1 Abstract

Protein synthesis is a key regulated cellular process that links nutrient availability and organismal growth. It has long been known that some cellular proteins continue to be synthesized under conditions where global translation is severely compromised. One prominent example is the selective translation of heat shock proteins (Hsps) under stress conditions. Although the transcriptional regulation of *Hsp* genes has been well established, neither the specific translation-promoting features nor the regulatory mechanism of the translation machinery have been clearly defined. Here we show that the stress-induced preferential translation of *Hsp70* mRNA is negatively regulated by PI3K-mTORC1 signaling. Despite the transcriptional up-regulation, the translation of *Hsp70* mRNA is deficient in cells lacking tuberous sclerosis complex 2. Conversely, Hsp70 synthesis is enhanced under the reduced PI3K-mTORC1 signaling. We found that the 5' UTR of Hsp70 mRNA contributes to cap-independent translation

without exhibiting typical features of internal ribosome entry site. Our findings imply a plausible mechanism for how persistent PI3K-mTORC1 signaling favors the development of age-related pathologies by attenuating stress resistance.

2.2 Introduction

The eukaryotic translation machinery is a tightly controlled system that regulates protein synthesis based on the availability of growth factors, nutrients, and glucose (Ma and Blenis, 2009; Holick and Sonenberg, 2005; Proud, 2007). A key pathway that integrates and responds to environmental cues involves the mammalian target of rapamycin (mTOR), a member of the PIKK family of protein kinase conserved from yeast to human (Wullschleger et al., 2006; Sarbassov et al., 2005; Inoki and Guan; 2006). Recent studies revealed the existence of two mTOR complexes, named mTORC1 and mTORC2, which differ in molecular composition and cellular functions (Loewith et al., 2002; Kim et al., 2002; Sarbassov et al., 2004). Insulin and insulin-like growth factors are major mTORC1 activators that operate through phosphoinositide 3-kinase (PI3K) and the protein kinase AKT (Hara et al., 2002). Conversely, mTORC1 activity is suppressed by a variety of stress conditions including limited nutrients, hypoxia, and DNA damage (Hay and Sonenberg, 2004).

Activation of mTORC1 positively stimulates cap-dependent mRNA translation via its downstream substrates S6Ks and 4E-BPs (Loewith et al., 2002; Kim et al., 2002; Hara et al., 2002; Chou and Blenis, 1995). S6K1 phosphorylation promotes protein synthesis and cell growth presumably by phosphorylating multiple substrates (e.g. ribosomal protein S6, translational regulators eIF4B and PDCD4) (Ma and Blenis, 2009; Dann et al., 2007). Phosphorylation of 4E-BP1

results in its dissociation from eIF4E, promoting assembly of the eIF4F complex (Gingras et al, 1999). The recruitment of the eIF4F complex to the mRNA 5' cap structure is both rate-limiting in translation initiation and is tightly regulated (Jackson et al, 2010). Translation consumes a substantial amount of cellular material and energy. It is thus not surprising that global translation is reduced in response to most, if not all, types of cellular stress (Holick and Sonenberg, 2005). However, some cellular proteins continue to be synthesized under conditions where global translation is severely compromised, such as during virus infection, stress, and mitosis (Qin and Sarnow, 2004; Clemens, 2001).

Heat shock proteins (Hsps) are known to protect cells against a wide variety of stresses (McClellan et al., 2005; Parsell and Lindquist, 1993; Bukau et al., 2006). Therefore, the regulation of Hsp production is crucial for cell survival. In mammalian cells, heat shock transcription factor 1 (HSF1) is the major transcription regulator of Hsp gene expression (Wu, 1995; Morimoto, 1998; Hahn et al., 2004). HSF1 binding to the heat shock elements results in a rapid increase in the rate of transcription (up to ~200-fold) (Fuda et al., 2009). In addition to the up-regulation of *Hsp70* gene transcription, the *Hsp70* mRNA is also robustly translated under stress conditions despite the slowing of global protein synthesis (Panniers, 1994; Lindquist and Craig, 1988). However, neither the specific translation-promoting features of the *Hsp70* mRNA nor the regulatory mechanism of the translation machinery have been clearly defined.

Persistent mTORC1 activation is associated with diverse pathologies such as inflammation, cancer, and diabetes (Inoki et al., 2005). Conversely, inhibition of mTORC1 prolongs lifespan and increases quality of life by reducing the incidence of age-related pathologies (Vellai et al., 2003; Kapahi et al, 2004; Kaeberlein et al, 2005; Harrison et al., 2009). It has been suggested that the

general reduction of protein synthesis lowers the cellular load of erroneously synthesized polypeptides. This situation results in "spare" chaperone function, which may contribute to the observed increase in organism stress resistance and lifespan (Hipkiss, 2006). In contrast, constitutive active mTOR signaling might increase the burden of chaperone molecules by producing more misfolded proteins. Consistent with this notion, a recent study reported that hyperactive mTOR signaling triggered the unfolded protein response in the endoplasmic reticulum (Ozcan et al., 2008). However, it is unclear whether unrestrained mTORC1 activation also triggers cytosolic stress response.

Here we report our findings that the stress-induced *Hsp70* mRNA translation is deficient in cells with hyperactive mTORC1 activities. Interestingly, although the 5' UTR of *Hsp70* mRNA contributes to the cap-independent translation, it does not behave as the viral IRES. Our results not only reveal novel aspects of cap-independent translation, but also imply a plausible mechanism about how persistent PI3K-mTORC1 signaling favors the development of age-related pathologies by attenuating stress resistance.

2.3 Results

TSC2 Null Cells Are Defective in Heat Shock-induced Hsp70 Expression

TSC2 serves as a GAP for the small GTPase Rheb, which activates mTORC1 (Inoki et al., 2002). Cells lacking a functional TSC-Rheb-GAP exhibit constitutive activation of mTORC1 signaling, which is not increased further by insulin. To test whether TSC deficiency activates cytosolic stress response, we used a luciferase reporter to evaluate the transcriptional activity of HSF1 in TSC2-/- MEFs after heat shock (Qian et al., 2006). After a 1 h incubation at 42 °C, TSC2-/- MEFs

exhibited significantly higher HSF1 activity than did TSC2+/+ MEFs (Fig. 1A). This was not due to the general increase of luciferase protein synthesis, because the control plasmid (CMV-Luc) showed no significant increase in luciferase expression in TSC2-/- MEFs (Fig. 1B).

We next examined protein levels of molecular chaperones in both MEFs after heat shock using immunoblotting. As expected, TSC2+/+ MEFs exhibited a robust induction of Hsp70 and Hsp25 after heat shock (Fig. 1C). To our surprise, there was no Hsp70 induction in cells lacking the *Tsc2* gene. A closer look at the overexposed immunoblotting revealed that Hsp70 was only detectable shortly after heat shock with little accumulation in TSC2-/- MEFs. This deficiency was not due to the lack of *Hsp70* transcription, because the *Hsp70* mRNA levels were comparable in both MEFs as measured by real time PCR (supplemental Fig. S1). Adding proteasome inhibitor MG132 did not rescue the Hsp70 expression in TSC2-/- MEFs (supplemental Fig. S2), excluding the possibility that there is an accelerated Hsp70 degradation in these cells. Further supporting this notion, ectopic expression of *Hsp70* by plasmid showed no difference in both MEFs (Fig. 1D). Notably, the *Hsp70* gene was directly cloned from TSC2-/- MEF cells, excluding the possibility that there are mutations in the endogenous *Hsp70* gene. To further substantiate the role of TSC2 in stress-induced Hsp70 expression, we performed siRNA-mediated TSC2 knockdown in HeLa cells. Despite the high basal levels of Hsp70 in HeLa cells, TSC2 knockdown largely blunted the heat shock-induced Hsp70 expression (supplemental Fig. S3). Therefore, the lack of heat shock-induced Hsp70 expression in TSC2-/- MEFs is likely due to the deficiency of translational regulation.

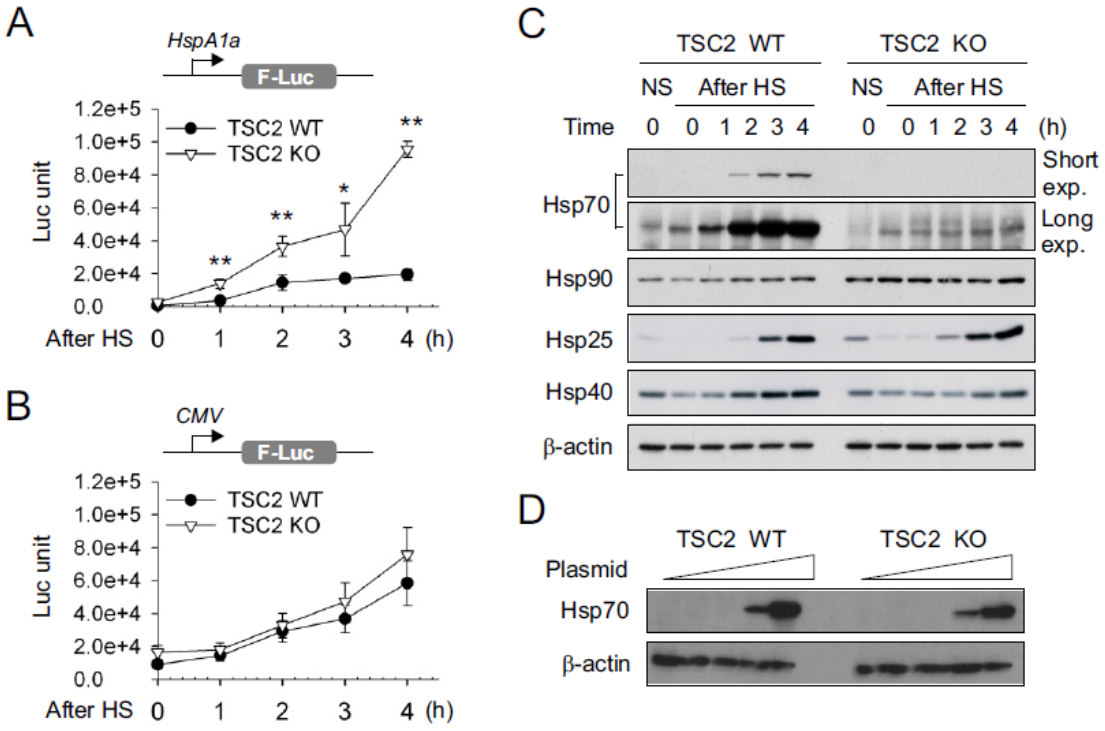

Figure 2-1. **TSC2 null cells are defective in heat shock-induced Hsp70 expression.** A, TSC2 wild type (WT) and knock-out (KO) cells were heat shocked at 42 °C for 1 h and recovered at 37 °C for the times as indicated. HSF1 activity was measured by using a F-Luc reporter driven by the HspA1a promoter. The experiments were repeated 5 times. Error bar, S.E. *, p <0.01; **, p <0.001 (Student's t test, two tails). B, general protein synthesis in cells as A was determined by using a control F-Luc reporter driven by the CMV promoter. The experiments were repeated 5 times. C, molecular chaperone levels in cells as A were determined by immunoblotting analysis using the antibodies as indicated. D, TSC2 WT and TSC2 KO cells were transfected with plasmids encoding Hsp70 with different doses (0, 0.1, 0.5, and 2.5 μg) in a 6-well plate. 24 h after transfection, whole cell lysates were immunoblotted with antibodies as indicated.

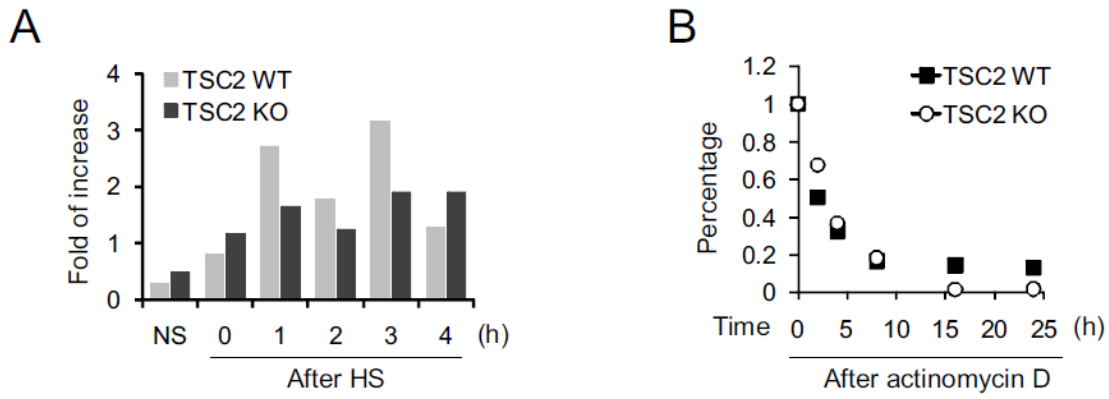

Figure 2-S1. **TSC2 null cells have normal Hsp70 mRNA levels after heat shock.** A, TSC2 wild type (WT) and knockout (KO) cells were heat shocked at 42°C for 1h followed by recovery at 37°C for various times as indicated. Total cellular RNA was extracted followed by reversed-transcription and real-time PCR for Hsp70. B, TSC2 wild type (WT) and knockout (KO) cells were heat shocked at 42°C for 1h followed by recovery at 37°C in the presence of actinomycin D (5 μg/ml) for various times as indicated. Total cellular RNA was extracted followed by reversed-transcription and real-time PCR for Hsp70.

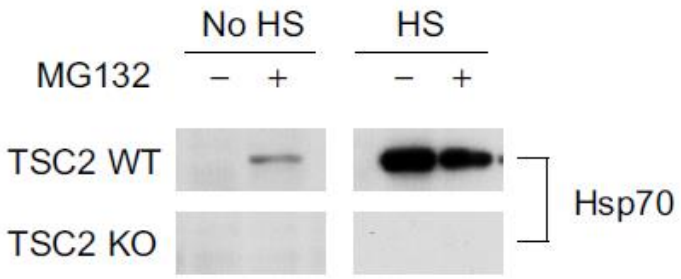

Figure 2-S2. **Deficient Hsp70 expression in TSC2 null cells is not due to accelerated proteasome degradation.** TSC2 wild type (WT) and knockout (KO) cells incubated in the absence or presence of 20 μM MG132 were subjected to heat shocked at 42°C for 1 h followed by recovery at 37°C for 4 h. Whole cell lysates were used for immunoblotting of Hsp70.

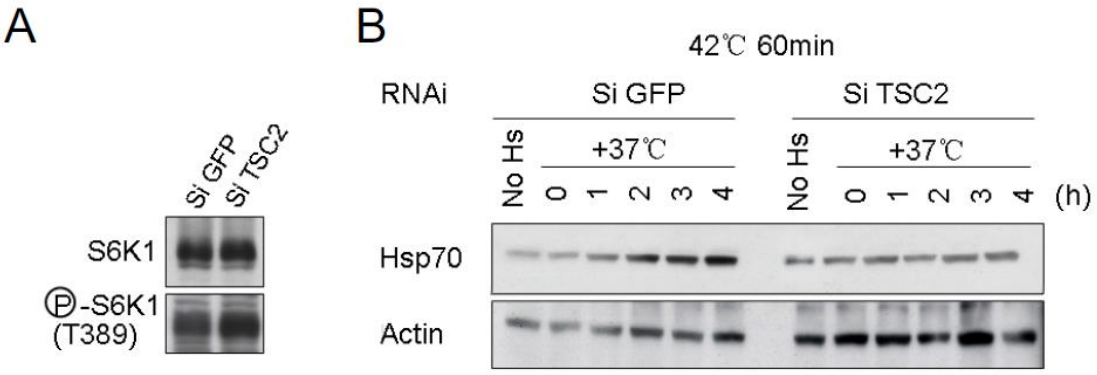

Figure 2-S3. **Effects of TSC2 knockdown on Hsp70 expression in HeLa cells.** A, HeLa cells were transfected with siRNA as indicated. 48 h of siRNA transfection, samples were collected for immunoblotting for S6K1 phosphorylation. B, siRNA-transfected cells were subject to 1 h heat shock at 42°C followed by recovery at 37°C. Immunoblotting was performed using antibodies as indicated.

Deficient Hsp70 mRNA Translation in TSC2 Null Cells after Heat Shock

To examine the translational status of *Hsp70* mRNA before and after heat shock in both MEFs, we performed ribosome sedimentation analysis. Actively translated mRNAs are distributed to polysomes, whereas inactive mRNAs are associated with monosomes (Johannes and Sarnow, 1998). Under normal growth conditions, TSC2-/- MEFs exhibited much more polysome formation than the wild type, with a corresponding decrease of monosome peak (Fig. 2, A and B). This feature is consistent with the increased cap-dependent mRNA translation in cells lacking TSC2. To analyze the polysome localization of specific mRNAs, we performed qPCR for every ribosome fraction. As expected, β-actin mRNA was mainly localized in the heavier polysome fractions of both MEFs (Fig. 2, A and B, grey bar). *Hsp70* mRNA was barely detectable in ribosome fractions because the basal levels were low in both cells under normal conditions (Fig. 2, A and B, black bar).

To investigate the translational status of stress-induced *Hsp70* mRNA, we applied heat shock to both TSC2+/+ and TSC2-/- MEFs. As expected, the polysome formation was largely suppressed in both cell types with higher sensitivity in TSC2-/- MEFs. In line with the efficient *Hsp70* mRNA translation after heat shock (Panniers, 1994; Klemenz et al., 1985), there was an enrichment of *Hsp70* message in polysome fractions of wild type MEFs. However, the ribosome fractions from TSC2-/- MEFs showed only basal levels of *Hsp70* mRNA, despite the total amount of the message was comparable in both MEFs (Fig. 2, triangle). Thus, *Hsp70* mRNA translation was largely deficient in TSC2 null cells, despite up-regulation of HSF1 transcriptional activity after heat shock.

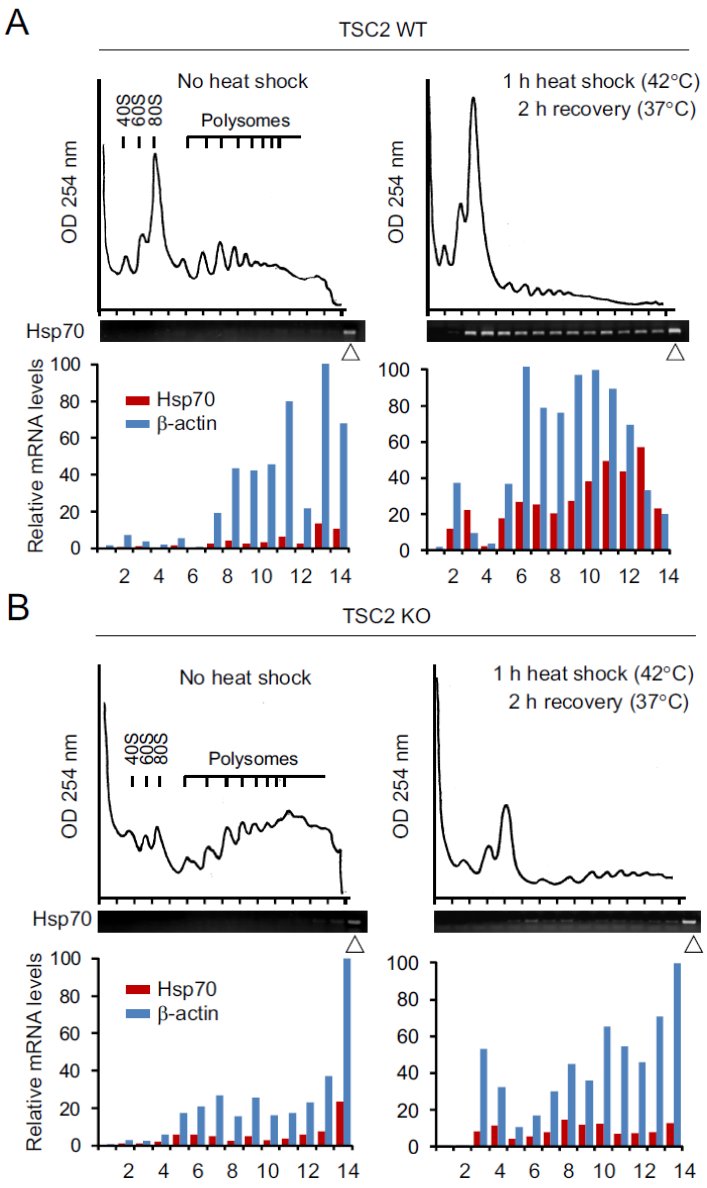

Figure 2-2. **Deficient Hsp70 mRNA translation in TSC2 null cells after heat shock.** A, ribosome profiling of TSC2 WT cells before and after heat shock. Cell lysates were sedimented on a 15–45% sucrose gradient followed by fractionation. The positions of the 40S, 60S, 80S, and polysomal peaks were indicated. Total RNA was extracted from each fraction and subject to RT-PCR and qPCR analysis. Hsp70 RT-PCR results were shown in the middle without concentration normalization. The Hsp70 mRNA levels in whole cell lysates before sucrose gradient are indicated by the triangle. qPCR results of Hsp70 (black bar) and β-actin (grey bar) were normalized based on RNA concentration of each fraction. The highest level was arbitrarily set as 100 and the relative mRNA levels were presented in all polysome fractions. B, ribosome profiling of TSC2 KO cells before and after heat shock. RT-PCR and qPCR were performed as described under A.

PI3K-mTORC1 Negatively Regulates Hsp70 mRNA Translation

Having found the unexpected deficiency of *Hsp70* mRNA translation in cells lacking TSC2, we were interested in assessing whether altered mTORC1 signaling in general affects the translation of *Hsp70* mRNA. We first transfected cells with plasmids encoding *Rheb*, a direct activator of mTORC1 (Yang et al., 2006; Avruch et al, 2006). Indeed, Rheb overexpression enhanced mTORC1 signaling as evidenced by increased phosphorylation of S6K1 at Thr^{389} (supplemental Fig. S4A). Consistent with TSC2 null MEFs, cells overexpressing Rheb showed a significant reduction in Hsp70 expression after heat shock as compared with cells overexpressing β-Gal (Fig. 3A). The Hsp70 transcript levels were indistinguishable in these cells, suggesting that hyperactive mTORC1 signaling inhibits stress-induced *Hsp70* mRNA translation.

We next tested whether decreasing mTORC1 signaling would augment the heat shock-induced *Hsp70* mRNA translation. mTORC1 activity was reduced in cells via siRNA-mediated knockdown of Raptor, a defining component of mTORC1 (Kim et al., 2002). Cells with Raptor knockdown exhibited 90% reduction of Raptor levels and consequently lower levels of S6K1 phosphorylation as compared with cells transfected with control siRNA (supplemental Fig. S4B). As shown in Fig. 3B, cells with Raptor knockdown demonstrated a much higher Hsp70 induction after heat shock. In contrast to Raptor knockdown, we observed no difference in heat shock-induced Hsp70 expression in cells with Rictor knockdown that specifically reduces the mTORC2 signaling (supplemental Fig. S4C).

Rapamycin is a potent mTORC1 inhibitor and can achieve complete attenuation of S6K1 phosphorylation within 5 min of rapamycin treatment (Tee and Blenis, 2005). We expected that the presence of rapamycin should increase

the heat shock-induced Hsp70 expression by suppressing mTORC1 signaling. However, the presence of rapamycin only caused a marginal increase of Hsp70 expression with a slightly faster induction (Fig. 3C). Prolonged rapamycin treatment had little effects in promoting Hsp70 induction (supplemental Fig. S5). In contrast to rapamycin, inhibition of PI3K by LY294002 was able to augment Hsp70 expression after heat shock (Fig. 3D). The discrepancy between rapamycin and LY294002 suggests the existence of rapamycin-resistant mTORC1 function (Choo et al., 2008; Thoreen et al., 2009). Taken together, PI3K-mTORC1 signaling plays a negative role in the regulation of *Hsp70* mRNA translation.

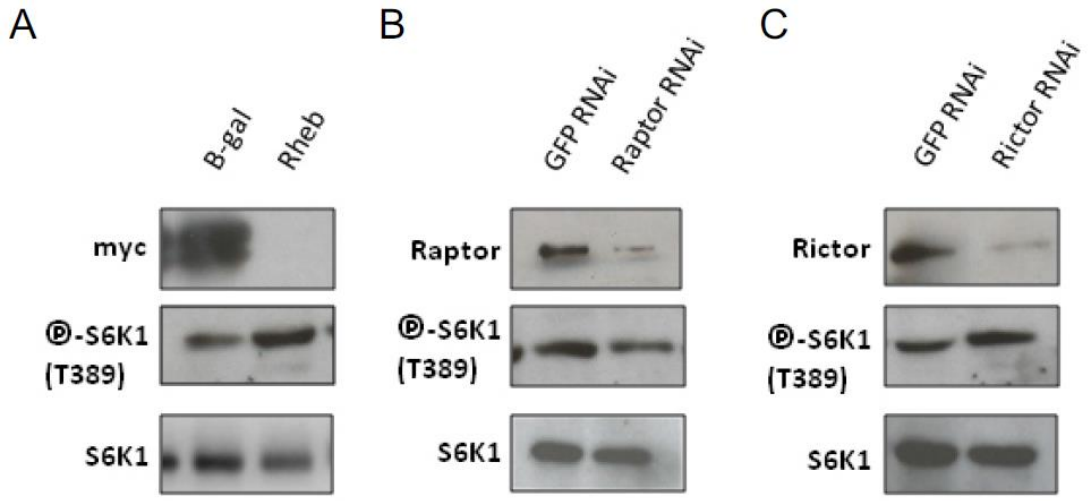

Figure 2-S4. **PI3K-mTORC1 negatively regulates Hsp70 mRNA translation.** A, TSC2 WT cells were transfected with plasmids encoding β-Gal or Rheb. 48 h after transfection, whole cell lysates were immunoblotted using antibodies as indicated. B, TSC2 WT cells were transfected with siRNA targeting Raptor or GFP as control. 48 h after transfection, whole cell lysates were immunoblotted using antibodies as indicated. C, TSC2 WT cells were transfected with siRNA targeting Rictor or GFP as control. 48 h after transfection, whole cell lysates were immunoblotted using antibodies as indicated.

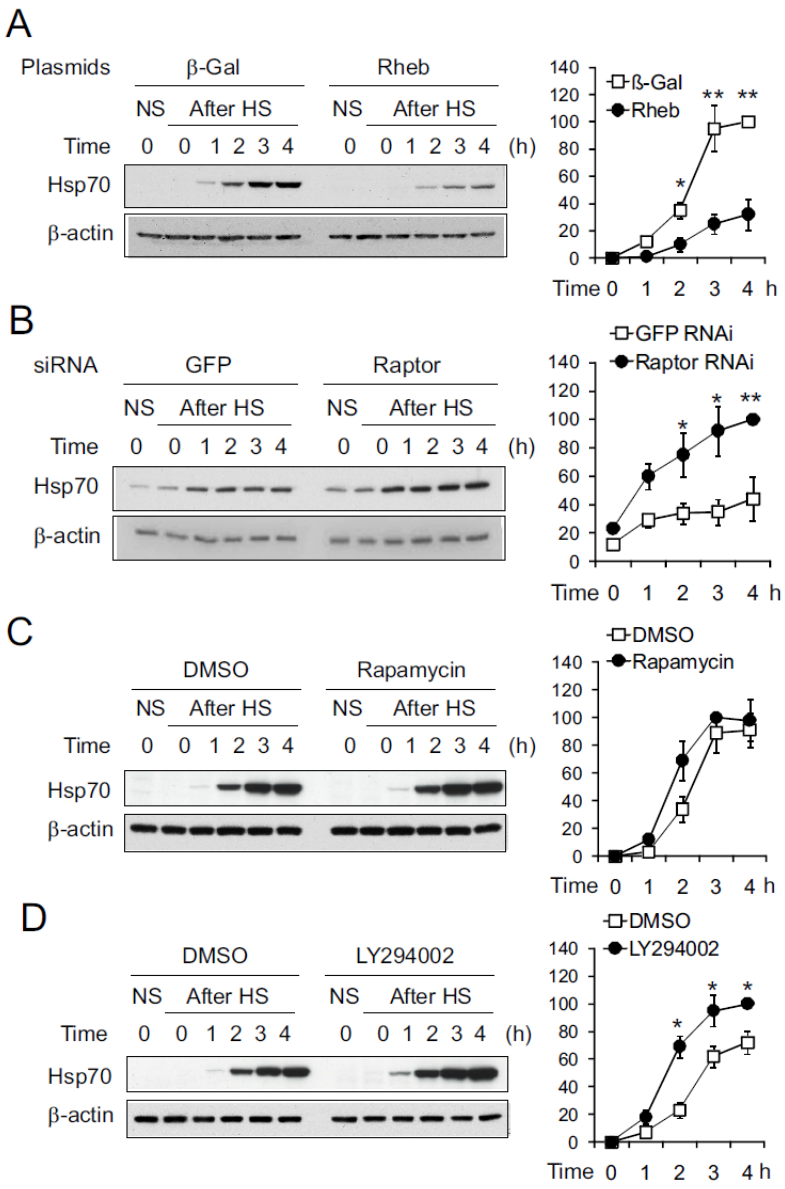

Figure 2-3. **PI3K-mTORC1 negatively regulates Hsp70 mRNA translation.** A, TSC2 WT cells were transfected with plasmids encoding β-Gal or Rheb. 48 h after transfection, cells were incubated at 42°C for the times as indicated. Whole cell lysates were immunoblotted using Hsp70 and β-actin antibodies. B, TSC2 WT cells were transfected with siRNA targeting Raptor or GFP as control. 48 h after transfection, cells were incubated at 42°C for the times as indicated. Whole cell lysates were immunoblotted using Hsp70 and β-actin antibodies. C, TSC2 WT cells were incubated at 42 °C for the times as indicated in the presence of 20 nM rapamycin or DMSO as control. Whole cell lysates were immunoblotted using Hsp70 and β-actin antibodies. D, TSC2 WT cells were incubated at 42°C for the times as indicated in the presence of 50 μM LY294002 or DMSO as control. Whole cell lysates were immunoblotted using Hsp70 and β-actin antibodies. Relative Hsp70 levels were quantitated by densitometry. n=3, error bar, S.E.; **p< 0.01; *p<0.05.

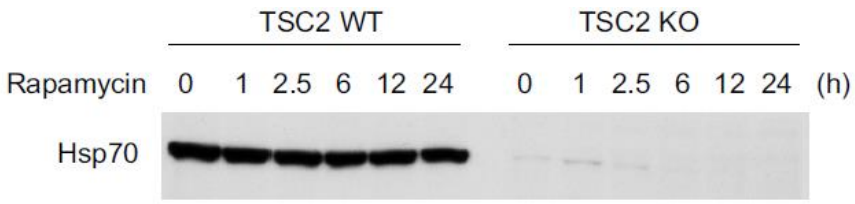

Figure 2-S5. **Rapamycin has limited effects on Hsp70 expression induced by heat shock.** TSC2 wild type (WT) and knockout (KO) cells incubated in the absence or presence of 20 nM rapamycin for various times as indicated. Cells were subjected to heat shocked at 42°C for 1 h followed by recovery at 37°C for 4 h. Whole cell lysates were used for immunoblotting of Hsp70.

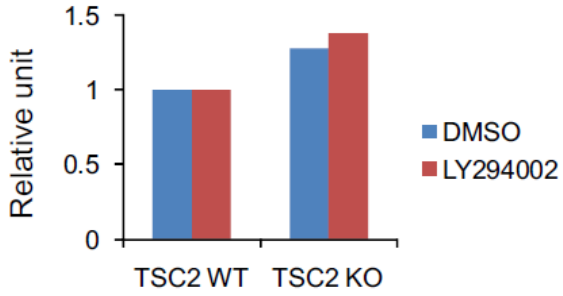

Figure 2-S6. **LY294002 has little effect on the turnover of transfected mRNAs.** Both TSC2 WT and KO cells were transfected with Luc mRNA capped with m7G. qPCR was performed after 3 h of transfection and relative units were presented for both MEFs in the absence or presence of LY294002.

Hsp70 5' UTR Responds to the PI3K-mTORC1 Signaling

In many cases, features in the 5' UTR of mRNAs are important for translational control (McGarry and Lindquist, 1985). To test the role of 5' UTR of *Hsp70* mRNA in responding to PI3K-mTORC1 signaling, we used a real time luciferase reporter assay. In contrast to the conventional end point assays, the real time luciferase assay permits continuous measurement of luciferase activity at multiple time points for the same cells. Thus, it allows us to precisely monitor the translational status of the reporter mRNA (*F-Luc*) in live cells under different PI3K-mTORC1 signaling. In addition, mRNA transfection was selected over plasmid expression as it eliminates any transcriptional variances. To mimic the natural mRNAs in cells, in vitro transcribed *F-Luc* mRNA was capped with m7GpppG at the 5' end followed by polyadenylation at the 3' end. In the absence of 5' UTR, TSC2-/- MEFs showed little increase of luciferase translation as compared with the wild type cells (Fig. 4A, left panel). Remarkably, inclusion of the 5' UTR of *Hsp70* mRNA resulted in ~50% reduction of *F-Luc* translation in cells lacking TSC2 (Fig. 4C, left panel). This reduction was not due to increased mRNA turnover in TSC2-/- MEFs, as qPCR analysis showed the similar turnover of transcripts within 3 h of transfection (supplemental Fig. S6). Further supporting the negative role of mTORC1 signaling in the translation of mRNAs bearing the *Hsp70* 5' UTR, cells overexpressing Rheb exhibited a similar pattern of *F-Luc* mRNA translation as TSC2-/- MEFs (supplemental Fig. S7).

We next examined the effects of reduced PI3K-mTORC1 signaling in the translation of *F-Luc* mRNA. Although the PI3K inhibitor LY294002 significantly inhibited the translation of *F-Luc* in the absence of the Hsp70 5' UTR (Fig. 4B), the same treatment caused a 35% increase of the translation of *F-Luc* bearing the *Hsp70* 5' UTR (Fig. 4D). In agreement with the concept that PI3K acts upstream of

TSC, LY294002 treatment had limited effects on mTORC1 signaling in cells lacking TSC2. For example, control mRNAs without *Hsp70* 5' UTR showed little response to LY294002 treatment in TSC2 KO cells (supplemental Fig. S8). These results indicate that the 5' UTR of *Hsp70* mRNA is responsible for the mTORC1-mediated translational regulation.

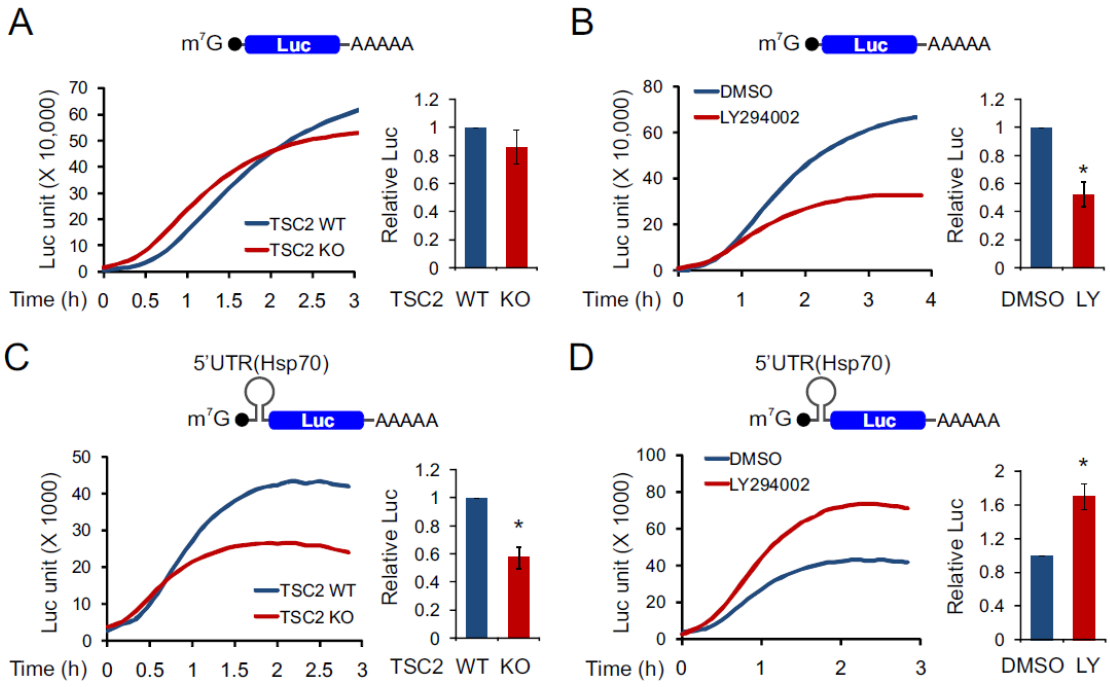

Figure 2-4. **Hsp70 5'-UTR responds to the PI3K-mTORC1 signaling.** A, luciferase mRNA (Luc) was synthesized using in vitro transcription followed by 5' end capping and 3' end polyadenylation. mRNA transfection was performed on TSC2 WT and TSC2 KO cells. Real time luciferase activity was recorded immediately after mRNA transfection (left panel). Relative Luc expression (3 h) in TSC2 KO cells was normalized against the wild type (right panel). B, Luc mRNA transfection was performed on TSC2 WT cells treated with 50 μM LY294002 or DMSO as control. Real time luciferase activity was recorded immediately after mRNA transfection (left panel). Relative Luc expression (3 h) after LY294002 treatment was normalized against the DMSO control (right panel). C, Luc mRNA bearing the Hsp70 5'-UTR was synthesized using in vitro transcription followed by 5' end capping and 3' end polyadenylation. mRNA transfection was performed in cells as in A. D, Hsp70 5'-UTR Luc mRNA transfection was performed on TSC2 WT cells treated with 50 μM LY294002 (LY) or DMSO as control. n=5, error bar, S.E. *, p< 0.01.

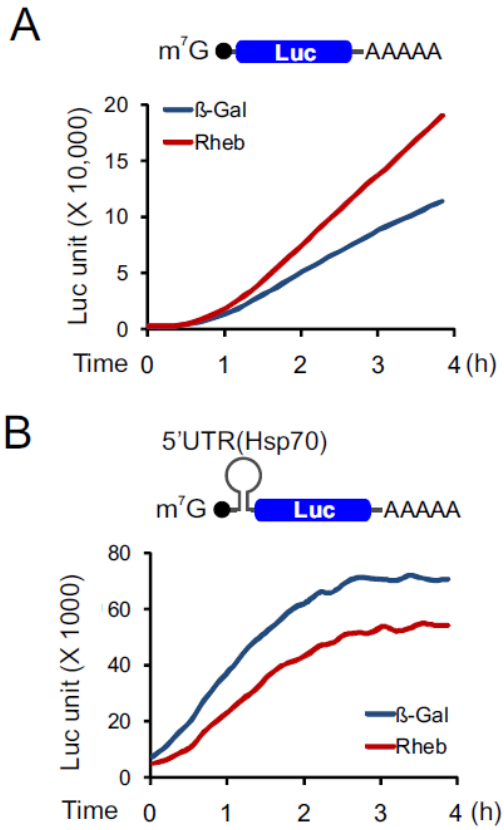

Figure 2-S7. **Hsp70 5'-UTR responds to the hyperactive mTORC1 signaling by Rheb overexpression.** A, Luc mRNA transfection was performed on TSC2 WT cells transfected with plasmids encoding Rheb or β-Gal as control. Real-time luciferase activity was recorded immediately after mRNA transfection. B, Hsp70 5' UTR- Luc mRNA transfection was performed on TSC2 WT cells transfected with plasmids encoding Rheb or β-Gal as control. Real-time luciferase activity was recorded immediately after mRNA transfection.

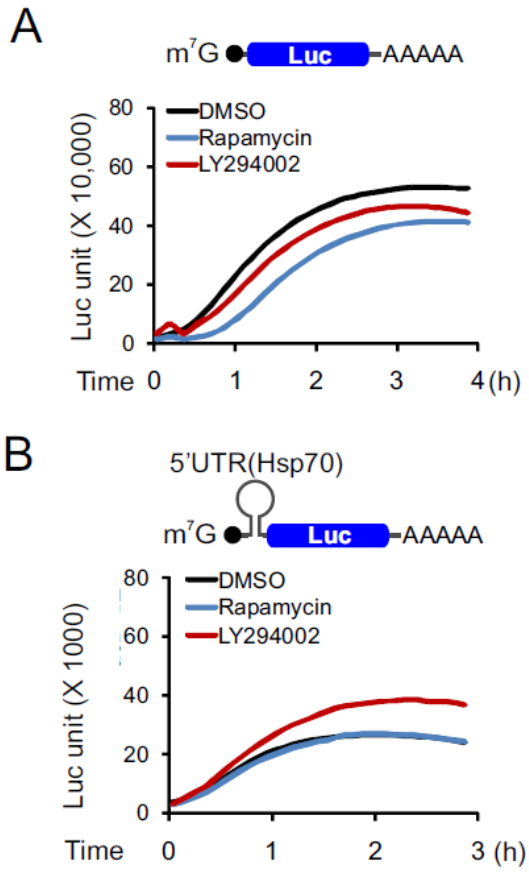

Figure 2-S8. **Hsp70 5'-UTR responds to the PI3K-mTORC1 signaling in TSC2 KO cells.** A, Luc mRNA transfection was performed on TSC2 KO cells treated with 50 μM LY294002, 20 nM rapamycin, or DMSO as control. Real-time luciferase activity was recorded immediately after mRNA transfection. B, Hsp70 5' UTR- Luc mRNA transfection was performed on TSC2 WT cells treated with 50 μM LY294002, 20 nM rapamycin, or DMSO as control. Real-time luciferase activity was recorded immediately after mRNA transfection.

Hsp70 5' UTR Differs from IRES in Mediating Cap-independent Translation

mTORC1 acts a "master regulator" of the cap-dependent translation in cells (Ma and Blenis, 2009). A prevalent hypothesis posits that *Hsp70* mRNA is translated by a cap-independent mechanism (Rubtsova et al., 2003). The cap-independent translation is thought to be mediated by an RNA structure named IRES, which recruits the ribosome independent of both the cap and the entire eIF4F complex (Sarnow et al, 2005). The bicistronic test has been employed as the "gold standard" to demonstrate the presence of an IRES feature for a 5' UTR. In the bicistronic assay, the expression construct is engineered to contain two cistrons with the putative IRES element inserted between them. The first cistron is translated by the cap-dependent scanning mechanism, whereas translation of the second cistron does not happen unless internal initiation at the IRES element occurs. We used a well characterized polio virus IRES (polIRES) as a positive control, in which the IRES element was inserted between *Renilla* luciferase (*R-Luc*) and *firefly* luciferase (*F-Luc*) (Fig. 5A). Consistent with the notion that the IRES-mediated capindependent translation will be selectively up-regulated when the cap-dependent translation is inhibited (Spriggs et al., 2008; Pende et al., 2004), we observed a significant increase in *F-Luc* mRNA translation when PI3K signaling was inhibited by LY294002 (Fig. 5A).

We next replaced the polIRES with the whole 5' UTR of the *Hsp70* mRNA (Fig. 5B). In contrast to the polIRES element, *Hsp70* 5' UTR was unable to drive *F-Luc* expression by either plasmid or mRNA transfection. Furthermore, the presence of LY294002 showed little effect on translation of the *F-Luc* mRNA (Fig. 5B). This result suggests that the 5' UTR of *Hsp70* mRNA does not act as the classic IRES element by internally recruiting ribosome machinery. This finding leaves open the question whether translation of the *Hsp70* mRNA is cap-

dependent or cap-independent. To address this question, we synthesized *F-Luc* mRNA capped with the non-functional analog ApppG. In contrast to normal capped mRNA (Fig. 4), translation efficiency of ApppG *F-Luc* mRNA, with or without *Hsp70* 5' UTR, was extremely low (Fig. 5, D and E), suggesting a strong cap dependence in translation of *F-Luc* mRNA under normal growth conditions. Remarkably, inhibiting PI3K signaling by adding LY294002 significantly increased the translation of ApppG *F-Luc* mRNA bearing the *Hsp70* 5' UTR, but not in the absence of the 5' UTR (Fig. 5E). We conclude that the *Hsp70* 5' UTR differs from IRES in mediating cap-independent mRNA translation.

Hsp70 5' UTR-mediated Cap-independent Translation Is Sensitive to 4E-BP1

To elucidate how PI3K-mTOR signaling controls the balance between cap-dependent and –independent translational mechanisms, we investigated the two well established mTORC1 downstream targets S6Ks and 4E-BPs. We first examined the translation of *Hsp70* mRNA in S6K1/2 double knock-out MEFs (S6K DKO) (Pende et al., 2004), in which general protein synthesis is reduced. However, there was little difference in heat shock-induced Hsp70 expression in these cells (supplemental Fig. S9).

4E-BP1 effectively inhibits cap-dependent translation by binding eIF-4E and inhibiting the formation of eIF-4F. Consequently it frees up the protein synthesis machinery for the selective translation of IRES-containing transcripts (Spriggs et al., 2008). We used a dominant-negative 4E-BP1 with alanine mutations at Thr37/Thr46, which is more potent in inhibiting cap-dependent translation (Li et al., 2002). In cells overexpressing 4E-BP1 (S37A/ S46A), we observed a slight decrease of cap-dependent translation of *F-Luc* mRNA (Fig. 6A). However, translation of *F-Luc* mRNA containing the *Hsp70* 5' UTR was similar in these cells as compared with the ones expressing the GFP control (Fig. 6B).

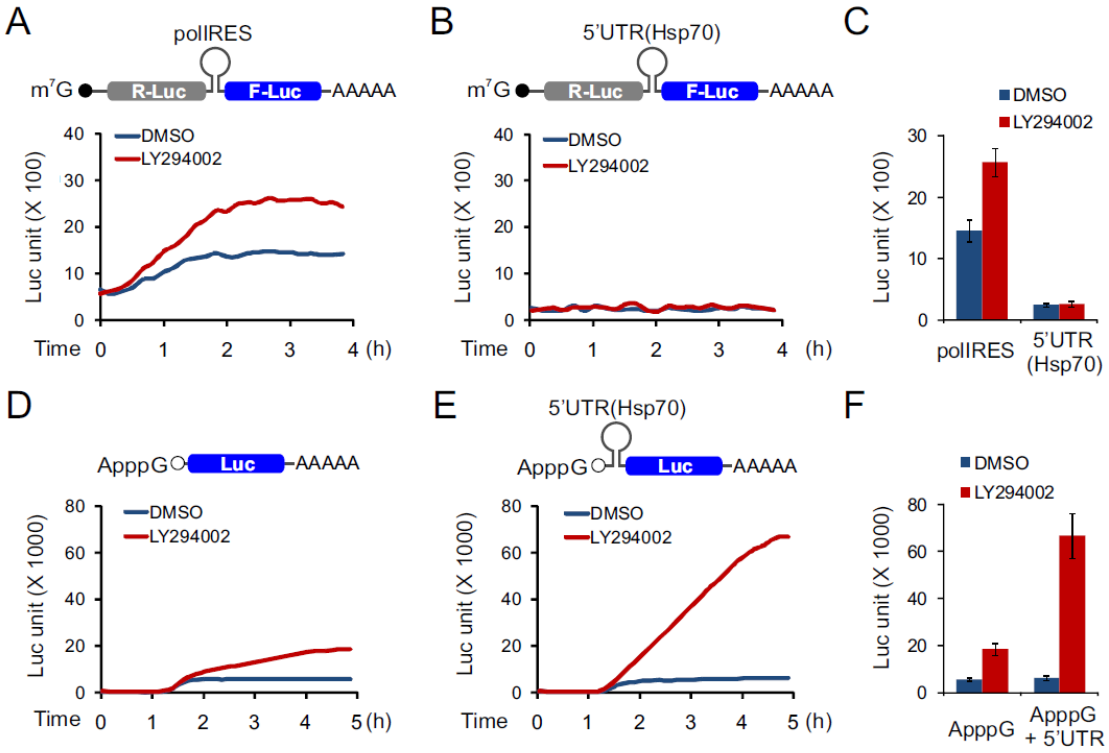

Figure 2-5. **Hsp70 5'-UTR differs from IRES in mediating cap-independent translation.** A, bicistronic Luc mRNA driven by polIRES was synthesized using in vitro transcription followed by 5' end capping and 3' end polyadenylation. mRNA transfection was performed on TSC2 WT cells treated with 50 μM LY294002 or DMSO. Real time luciferase activity was recorded immediately after mRNA transfection. B, bicistronic Luc mRNA driven by Hsp70 5'-UTR was synthesized using in vitro transcription followed by 5' end capping and 3' end polyadenylation. mRNA transfection and real time luciferase measurements were the same as A. C, Luc expression after a 3-h transfection of mRNAs containing polIRES or Hsp70 5'-UTR in the presence or absence of LY294002. Error bar, S.E. D, in vitro synthesized Luc mRNA was capped at the 5' end with a non-functional analog (ApppG) followed by 3' end polyadenylation. mRNA transfection and real time luciferase measurements were the same as A. E, in vitro synthesized Luc mRNA bearing Hsp70 5'-UTR was capped at the 5' end with a non-functional analog ApppG followed by 3' end polyadenylation. mRNA transfection and real time luciferase measurements were the same as A. F, Luc expression after a 3-h transfection of ApppG-capped mRNAs in the presence or absence of LY294002. Error bar, S.E.

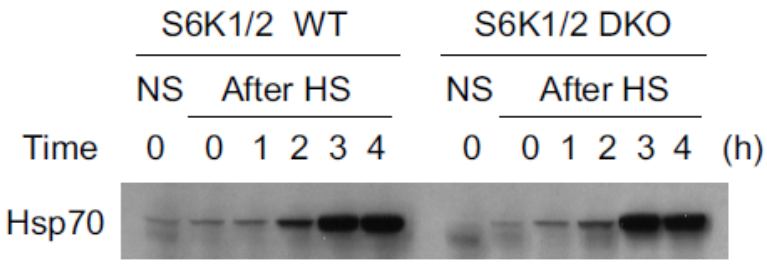

Figure 2-S9. **S6Ks have limited effects on Hsp70 expression induced by heat shock.** S6K1/2 wild type (WT) and double knockout (DKO) cells were heat shocked at 42°C for 1h followed by recovery at 37°C for various times as indicated. Whole cell lysates were used for immunoblotting of Hsp70.

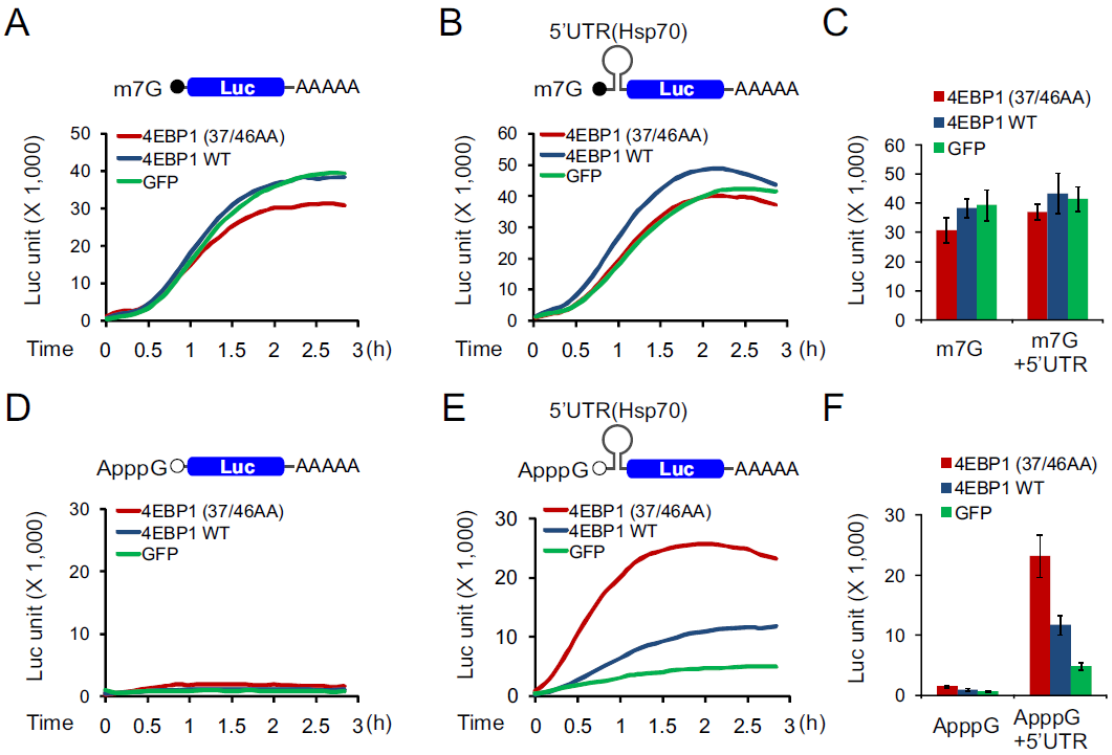

Figure 2-6. **Hsp70 5'-UTR-mediated cap-independent translation is sensitive to 4E-BP1.** A, in vitro synthesized Luc mRNA was capped at the 5' end with a non-functional analog ApppG followed by 3' end polyadenylation. mRNA transfection was performed on TSC2 WT cells pre-transfected with plasmids encoding 4E-BP1 (S37A/S46A), 4E-BP1, or GFP. Real time luciferase activity was recorded immediately after mRNA transfection. B, in vitro synthesized Luc mRNA bearing the Hsp70 5'-UTR was capped at the 5' end with non-functional analog ApppG followed by 3' end polyadenylation. mRNA transfection and real time luciferase measurements were the same as A. C, Luc expression after a 3-h transfection of m7G-capped mRNAs in cells transfected with plasmids encoding 4E-BP1 (S37A/S46A), 4E-BP1, or GFP. Error bar, S.E. D, in vitro synthesized Luc mRNA was capped at the 5' end with non functional analog ApppG followed by 3' end polyadenylation. mRNA transfection and real time luciferase measurements were the same as A. E, in vitro synthesized Luc mRNA bearing the Hsp70 5'-UTR was capped at the 5' end with non-functional analog ApppG followed by 3' end polyadenylation. mRNA transfection and real time luciferase measurements were the same as A. F, Luc expression after a 3-h transfection of ApppG-capped mRNAs in cells transfected with plasmids encoding 4E-BP1 (S37A/S46A) (37/46AA), 4E-BP1, or GFP. Error bar, S.E.

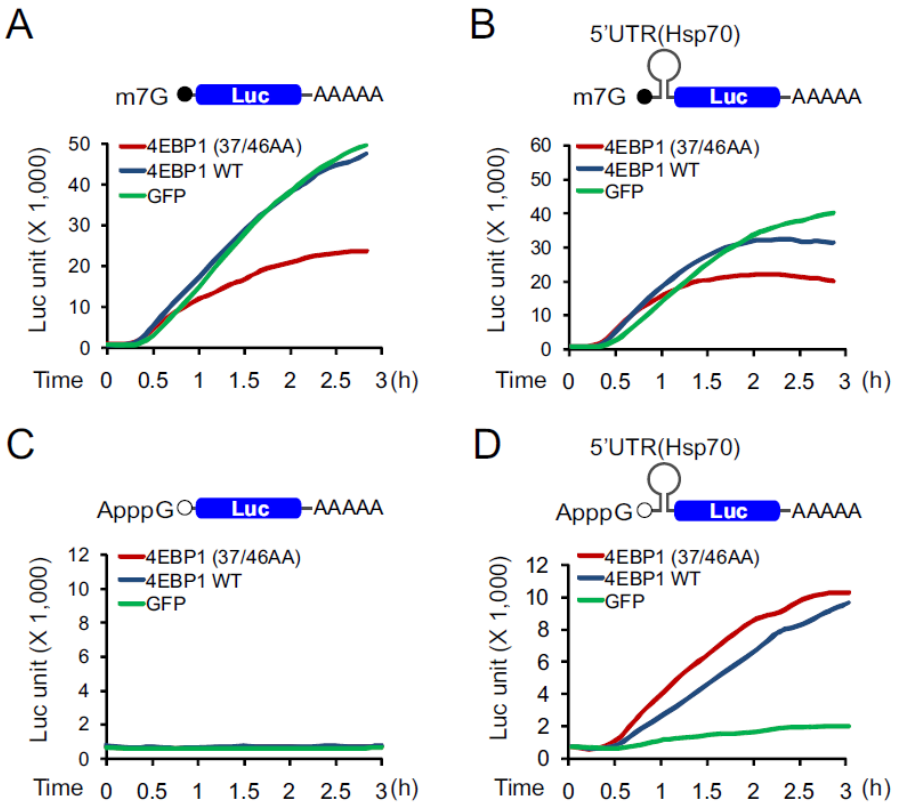

Figure 2-S10. **Hsp70 5' UTR-mediated cap-independent translation is sensitive to 4E-BP1 in TSC2 KO cells.** A, In vitro synthesized Luc mRNA was capped at 5' end with a non-functional analog ApppG followed by 3' end polyadenylation. mRNA transfection was performed on TSC2 KO cells pre-transfected with plasmids encoding 4E-BP1(37/46AA), 4E-BP1, or GFP. Real-time luciferase activity was recorded immediately after mRNA transfection. B, In vitro synthesized Luc mRNA bearing Hsp70 5' UTR was capped at 5' end with a nonfunctional analog ApppG followed by 3' end polyadenylation. mRNA transfection and real-time luciferase measurements were the same as A. C, In vitro synthesized Luc mRNA was capped at 5' end with a non-functional analog ApppG followed by 3' end polyadenylation. mRNA transfection and real-time luciferase measurements were the same as A. D, In vitro synthesized Luc mRNA bearing Hsp70 5' UTR was capped at 5' end with a nonfunctional analog ApppG followed by 3' end polyadenylation. mRNA transfection and real-time luciferase measurements were the same as A.

It is likely that the increased cap-independent translation was masked by the decreased cap-dependent translation when the 5' cap is intact. We then tested the 4EBP1 responsiveness when the normal m7G cap is replaced with the non-functional cap analog ApppG. As expected, no translation occurred in the absence of normal cap for *Luc* mRNA (Fig. 6D). However, the presence of the *Hsp70* 5' UTR was able to drive an efficient translation of *F-Luc* mRNA in cells expressing the dominant-negative 4E-BP1 (S37A/ S46A) (Fig. 6E). Notably, overexpressing wild type 4E-BP1 was also able to boost the translation of *F-Luc* mRNA driven by the *Hsp70* 5' UTR. Similar results were also observed in cells lacking TSC2 (supplemental Fig. S10). Thus, the 5' UTR of *Hsp70* mRNA can efficiently initiate a cap-independent translation mechanism in response to the reduced cap-dependent translation by dominant-negative 4E-BP1.

Deficient Hsp70 Translation Contributes to the Attenuation of Stress Resistance in TSC2 Null Cells

It is well established that Hsp70 molecules protect cells against a wide variety of stresses including heat shock (Balch et al., 2008; Feldman and

Frydman, 2000). TSC mutant cells are also defective in coping with various stresses. We reasoned that the deficient Hsp70 translation might contribute to the attenuation of stress resistance in TSC2 null cells. To test this possibility, we examined the vulnerability of TSC2-/- MEFs to heat shock. After incubation at 45 °C for 1 h, more than 60% of TSC2-/- MEFs were dead as measured by trypan blue staining (Fig. 7A). By contrast, wild type MEFs only showed about 40% cell death ($p = 0.018$). Remarkably, adding back Hsp70, but not Hsp90, using recombinant adenovirus largely rescued the viability of TSC2-/- MEFs after heat shock stress. As Hsp70 protects cells from apoptosis during stress (Mosser et al., 2000), we analyzed the molecular indicators of apoptosis of these cells. In TSC2-/- MEFs, exposure to heat shock resulted in a marked increase in caspase-3 cleavage compared with wild type (Fig. 7B). Once again, adding back Hsp70 largely suppressed the caspase-3 cleavage. These results demonstrated that the deficient Hsp70 translation is responsible for the hypersensitivity of TSC2-/- MEFs to heat shock-induced cell death.

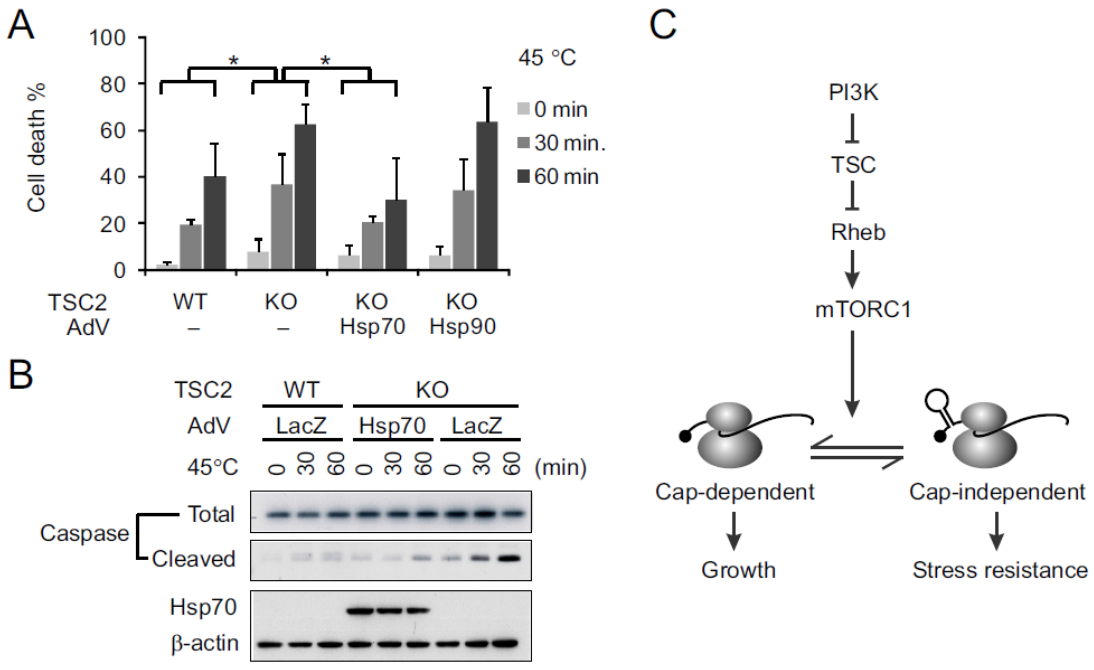

Figure 2-7. **Hsp70 5'-UTR-mediated cap-independent translation is sensitive to 4E-BP1.** Deficient Hsp70 translation contributes to the attenuation of stress resistance in TSC2 null cells. A, TSC2 WT, TSC2 KO, and adenovirus (AdV)-infected TSC2 KO cells were incubated at 45 °C for various times as indicated. Cell viability was measured by trypan blue counting. n=4, error bar, S.E. *, $p<0.05$ (Student's t test, two tails). B, AdV-infected TSC2 WT and TSC2 KO cells were incubated at 45 °C for various times followed by immunoblotting using antibodies as indicated. C, a schematic model for PI3K-mTORC1-controlled translational balance between cap-dependent and cap-independent mechanisms.

2.4 Discussion

Until now it was unclear how PI3K-mTOR signaling regulated the intracellular stress response. A recent study reported that a hyperactive unfolded protein response occurred in the ER of MEFs lacking TSC (Ozcan et al., 2008). It has been suggested that hyperactive mTOR activity triggers the stress response because higher levels of protein synthesis increased the cellular load of erroneously synthesized polypeptides. To our surprise, we observed a defective cytosolic stress response in these cells. Despite the up-regulated HSF1 transcriptional activity, there is a clear deficiency in heat shock-induced Hsp70 expression in MEFs lacking TSC2. In addition, Hsp70 expression is also significantly reduced in cells overexpressing Rheb. Importantly, decreasing mTORC1 signaling by raptor knockdown or PI3K inhibition augments the heat shock-induced Hsp70 expression. Therefore our results demonstrate a critical role for PI3K-mTOR signaling in controlling the synthesis of one of the most prominent stress-inducible chaperones in cells.

Although much is known about chaperone gene transcription in response to heat stress, relatively little is known about post-transcriptional events. The transcriptional regulation of *Hsp70* gene expression has been well established as

a prototype of the evolutionary conserved stress response mechanism (Shi et al., 1998; Mayer et al., 2001). However, many recent studies using comparative genomic and proteomic profiling of cells have documented a lack of correlation between the mRNA and protein levels of numerous genes (Sonenberg and Hinnebusch, 2007). This indicates that post-transcriptional control is more important in the regulation of gene expression than is often assumed. Here we report a clear discrepancy between *Hsp70* transcription and translation in cells with hyperactive mTORC1 signaling. Our results, for the first time, uncovered an intimate connection between nutrient signaling and the stress response.

The untranslated regions of *Hsp70* mRNA have been reported to contain elements important to the post-transcriptional regulation of this key component of the stress response. For instance, the 3' UTR of both the Drosophila and the human *Hsp70* mRNA have been shown to control mRNA stability during heat shock as well as during recovery (Petersen and Lindquist, 1989; Moseley et al., 1993). The 5' UTR of the Drosophila *Hsp70* mRNA allows efficient translation at high temperature when other non-heat shock mRNAs are poorly translated (Klemenz et al., 1985; McGarry and Lindquist, 1985). Interestingly, the 5' UTR of the Drosophila *Hsp70* mRNA is strikingly enriched in adenylic residues (>50%), which suggests a relative absence of secondary structure in this 5' UTR that is imperative for efficient translation. By contrast, the 5' UTR of mammalian *Hsp70* mRNA is generally GC rich (>70%), suggesting a relatively high degree of secondary structure. A relaxed cap dependence of translation of this mRNA strongly suggests a translational feature of IRES (Rubtsova et al., 2003). However, no IRES activity has so far been validated in the Hsp70 mRNA 5' UTR (Andreev et al., 2009). Here we show that the 5' UTR of mouse *Hsp70* mRNA has little effects in driving translation when placed in a bicistronic expression construct. Notably,

all eukaryotic mRNAs are both monocistronic and capped with m7GpppN. Therefore, the bicistronic assay cannot faithfully mimic physiological situations of cap-independent translation.

Cap-independent translation was first established for picornavirus viral mRNAs, which do not possess a cap (Pelletier and Sonenberg, 1988). Examples of cap-independent translation have also been documented for some capped cellular mRNAs (Johannes and Sarnow, 1998). Accumulating evidences indicate that a down-regulation of cap-dependent translation is associated with up-regulation of cellular IRES-dependent mRNA translation in vivo (Spriggs et al., 2008). How does the 5'UTR of Hsp70 mRNA drive the cap-independent translation without acting as an IRES? It is possible that the presence of a 5' proximal mRNA structure (such as in the artificial bicistronic constructs) prevents the direct recruitment of the ribosome by Hsp70 5' UTR. Another interesting question is how Hsp70 mRNA adopts the cap-independent translation when all the eukaryotic mRNAs are synthesized in a capped form. Most recently, it has been reported that the expression of several decapping enzymes was enhanced during heat stress (Neef and Thiele, 2009). This phenomenon could lead to the selective translation of *Hsp70* mRNA due to unique features of the Hsp70 5' UTR in mediating cap-independent translation.

Our findings may have critical implications for the pathologies associated with PI3K-mTORC1 dysregulation. The stress-induced switch between cap-dependent and –independent translation of Hsp70 represents an important cellular adaptation, which is largely disrupted when mTORC1 signaling is dysregulated (Fig. 7C). Significantly, the deficiency of Hsp70 translation in cells with hyperactive mTOR signaling contributes to their stress vulnerability. Unrestrained mTORC1 activity in mammals is associated with the occurrence of

disease states including inflammation, cancer, and diabetes (Inoki et al., 2005). By contrast, decreased mTOR signaling by a genetic approach has been shown to extend the lifespan in a variety of organisms (Vellai et al., 2003; Kapahi et al, 2004; Kaeberlein et al, 2005; Harrison et al., 2009). Interestingly, a robust stress response is required for lifespan extension in these organisms (Hsu et al., 2003; Morley et al., 2004; Powers et al., 2006). We demonstrate that reducing PI3K-mTOR signaling increases stress resistance by promoting cap-independent Hsp70 translation, thereby increasing the availability of proteolytic and chaperone functions that may contribute to the observed increase in organism stress resistance and lifespan. With the demonstration of the mechanistic connection between nutrient signaling and stress resistance, our findings will shed light on therapeutic interventions of aging and age-associated pathologies.

2.5 Materials & Methods

Cells and Reagents—TSC2+/+ and TSC2-/- MEFs were kindly provided by Dr. David J. Kwiatkowski (Harvard Medical School) and maintained in Dulbecco's modified Eagle's medium (DMEM) with 10% fetal bovine serum (FBS). The polio IRES luciferase construct was a generous gift from Peter Bitterman (University of Minnesota). The plasmid expressing Rheb was kindly provided by Dr. Kun-Liang Guan (University of California at San Diego). Rapamycin and LY294002 were purchased from Sigma. Anti-Hsp70 (SPA-810), anti-Hsp90 (SPA-830), anti-Hsp25 (SPA-801), and anti-Hsp40 (SPA-400) antibodies were purchased from Stressgen; antibodies for phosphorylated and total S6K1, 4E-BP1, Raptor, and Rictor from Cell Signaling. siRNA targeting Raptor and Rictor were purchased from Santa Cruz.

Plasmids—The 5' UTR of mouse *Hsp70* were amplified by RT-PCR using total RNA extracted from TSC2-/- MEFs. The *Hsp70* 5' UTR was cloned into HindIII and BamHI sites of pcDNA3.1 (Invitrogen). The *firefly luciferase* gene was directly removed from pCDNA3-rLuc-polIRES-fLuc into the pcDNA3.1/*Hsp70* 5' UTR using BamHI and XbaI restriction sites. For IRES constructs containing the *Hsp70* 5' UTR, the polIRES cassette in the bicistronic vector pcDNA3/rLuc-polIRES-fLuc was replaced by the full-length of *Hsp70* 5' UTR cloned from TSC2-/- MEFs (231 bp, NM_010479).

Transfections—Plasmid and siRNA transfections were performed using Lipofectamine 2000 (Invitrogen), according to the manufacturer's instructions.

Immunoblotting—Cells were lysed on ice in TBS buffer (50 mM Tris-HCl (pH 7.5), 150 mM NaCl, 1 mM EDTA) containing protease inhibitor mixture tablet (Roche Applied Science) and 1% Triton X-100. After incubating on ice for 30 min, the supernatants were heated for 5 min in SDS-PAGE sample buffer (50 mM Tris-HCl (pH 6.8), 100 mM dithiothreitol, 2% SDS, 0.1% bromphenol blue, 10% glycerol). Proteins were resolved on SDS-PAGE and transferred to Immobilon-P membranes (Millipore). Membranes were blocked for 1 h in TBS containing 5% blotting milk, followed by incubation with primary antibodies. After incubation with horseradish peroxidase- coupled secondary antibodies, immunoblots were developed using enhanced chemiluminescence (Amersham Biosciences).

Ribosome Profiling—Sucrose solutions were prepared in polysome gradient buffer (10 mM HEPES, pH 7.4, 100 mM KCl, 5 mM MgCl2, 100 μg/ml of cycloheximide, 5 mM DTT, 20 units/ml of SUPERase_In). Sucrose density gradients (15– 45% w/v) were prepared in SW41 ultracentrifuge tubes (Fisher) using a BioComp Gradient Master (BioComp Instruments) according to the manufacturer's instructions. Cells were lysed in ice-cold polysome lysis buffer

(10 mM HEPES, pH 7.4, 100 mM KCl, 5 mM MgCl2, 100 μg/ml of cycloheximide, 5 mM DTT, 20 units/ml of SUPERase_In, 2% Triton), about 650 μl of supernatant was loaded onto gradients, followed by centrifugation for 100 min at 38,000 x g at 4 °C in an SW41 rotor. Gradients were fractionated at 0.375 ml/min using a fractionation system (Isco), which continually monitored OD254 values. Fractions corresponding to 60 s intervals were collected.

RT-PCR and qPCR—Total RNA was extracted from whole cell lysates or fraction samples using TRIzol reagent (Invitrogen) according to the manufacturer's instructions. Reverse transcription was performed using Superscript III kit (Invitrogen). PCR was performed under the following conditions: 30 s, 94 °C; 30 s, 55 °C; 30 s, 72 °C, 22 cycles. The primer pair for the *Hsp70* gene was 5'-GCAAGGCCAACAAGATCACCAT-3' and 5'-GGCGCTCTTCATGTTGAAGGC-3'. The primer pair for β-actin gene was 5'-TTGCTGACAGGATGCAGAAG-3' and 5'-ACTCCTGCTTGCTGATCCACAT-3'. For real-time PCR analysis, a SYBR Green PCR kit (Invitrogen) was used on a LightCycler 480 II Q-PCR machine (Roche Applied Science). Raw data were analyzed using the Light- Cycler 480 Software (version 1.5.0, Roche Applied Science).

mRNA In Vitro Transcription—mRNAs with normal m7G cap or analog ApppG were synthesized using the mMessage mMachine T7 Ultra kit (Ambion), followed by purification using the MEGAclear kit (Ambion), according to the manufacturer's instructions.

Luciferase Reporter Assay—For the non-real time luciferase assay, transfected MEFs were lysed and luciferase activity was measured using a luciferase reporter assay system (Promega) on a SynergyTM HT Multi-detection Microplate Reader (BioTek Instruments). For real time luciferase assay, cells were plated on 35-mm dishes and transfected with plasmid or mRNA containing

the luciferase gene. Immediately after transfection, luciferase substrate D-luciferin (1 mM) was added into the culture medium. Luciferase activity was recorded at 37 °C with 5% CO2 using Kronos Dio Luminometer (Atto).

Cell Viability Assays—TSC2+/+ and TSC2-/- MEFs were grown to 90% confluence, followed by incubation at 45 °C for various times. Cells were then returned to 37 °C for a 20 h recovery. The cells were then counted via trypan blue staining. For the rescue experiment, MEFs were infected with recombinant adenoviruses expressing Hsp70, Hsp90, or GFP control using 20 multiplicity of infection 24 h after infection, cells were heat shocked and viability was measured via cell counting.

2.6 Acknowledgements

We thank Dr. John T. Lis (Cornell University) for critical discussion. We are also grateful to Drs. David J. Kwiatkowski (Harvard Medical School) for providing TSC2 MEFs, Kun- Liang Guan (University of California at San Diego) for Rheb plasmid, Peter Bitterman (University of Minnesota) for the polio IRES luciferase construct, and Patrick Stover (Cornell University) for access to the gradient fractionation system. **Funding:** this work was supported, in whole or in part, by a National Institutes of Health grant and the Ellison Medical Foundation (to S.-B. Q.).

CHAPTER 3

Nutrient Signaling in Protein Homeostasis: An Increase in Quantity at the Expense of Quality

This work was submitted August 2012 and the manuscript was published as Conn CS and Qian S-B. **Nutrient Signaling in Protein Homeostasis: An Increase in Quantity at the Expense of Quality.** *Sci. Signal.* 2013 April 16; 6(271), ra24. Minor modifications have been made for reprint here.

3.1 Abstract

The discovery that rapamycin extends the life span of diverse organisms has triggered many studies aimed at identifying the underlying molecular mechanisms. Mammalian target of rapamycin complex 1 (mTORC1) regulates cell growth and may regulate organismal aging by controlling mRNA translation. However, how inhibiting mTORC1 and decreasing protein synthesis can extend life span remains an unresolved issue. We showed that constitutively active mTORC1 signaling increased general protein synthesis but unexpectedly reduced the quality of newly synthesized polypeptides. We demonstrated that constitutively active mTORC1 decreased translation fidelity by increasing the speed of ribosomal elongation. Conversely, rapamycin treatment restored the quality of newly synthesized polypeptides mainly by slowing the rate of ribosomal elongation. We also found distinct roles for mTORC1 downstream targets in maintaining protein homeostasis. Loss of S6 kinases, but not 4E-BP family proteins, which are both involved in regulation of translation, attenuated

the effects of rapamycin on the quality of newly translated proteins. Our results reveal a mechanistic connection between mTORC1 and protein quality, highlighting the central role of nutrient signaling in growth and aging.

3.2 Introduction

The mammalian target of rapamycin (mTOR) is a highly conserved serine/threonine kinase that is named for its inhibition by the drug rapamycin (Wullschleger et al., 2006; Laplante and Sabatini, 2012). mTOR assembles into two functionally and structurally distinct complexes in the cytoplasm: mTORC1 (mTOR complex 1) and mTORC2. As a major hub that integrates multiple signaling pathways, mTORC1 is a master regulator of protein synthesis that couples nutrient signaling to cell growth and proliferation (Ma and Blenis, 2009; Sonenberg and Hinnebusch, 2009). In mammalian cells, mTORC1 is positioned downstream of the tumor suppressors tuberous sclerosis complex 1 (TSC1) and TSC2. The TSC1/2 complex inhibits mTORC1 by acting as a guanosine triphosphatase (GTPase)–activating enzyme (GAP) for Ras homolog enriched in brain (Rheb), which binds to and activates mTORC1 (Inoki and Guan, 2006; Huang and Manning, 2008). Cells lacking functional TSC exhibit constitutive activation of mTORC1 signaling, resulting in increased protein synthesis and cell size (Kwiatkowski and Manning, 2005). The phenotypes associated with *TSC* deficiency can be rescued by rapamycin treatment (Goto et al., 2011). In further support of the critical role of mTORC1 in cell growth and proliferation, dysregulation of mTORC1 has been implicated in many disease states including cancer, metabolic disorders, and aging (Zoncu et al., 2011).

The role of mTORC1 in aging has received increasing attention owing to its mechanistic connection with other pathways in longevity studies. In many model organisms, longevity is regulated by the conserved insulin and insulin-like growth factor 1 (IGF-1) signaling pathway (Kenyon, 2005). Reducing the activity of phosphoinositide 3-kinase (PI3K), an upstream signaling of mTORC1, promotes longevity (Cohen et al., 2009). In addition, caloric restriction increases life span in various organisms and is proposed to function by inhibiting mTORC1 (Fontana, 2009). Direct inhibition of mTORC1 signaling also increases life span (Kapahi et al., 2004, 2010; Kaeberlein et al., 2005), and administration of rapamycin to adult mice substantially extends life span (Harrison et al., 2009). A consequence of mTORC1 suppression is the general attenuation of protein synthesis. Indeed, partially inhibiting the translation machinery also increases life span in various organisms (Pan et al., 2007; Hansen et al., 2007; Syntichaki et al., 2007). Thus, reduced mRNA translation might be a common mechanism to extend life span in multiple species under different conditions.

How can reducing protein synthesis extend life span? Protein homeostasis refers to a delicate equilibrium between synthesizing proteins, maintaining protein conformations, and removing damaged proteins from cells (Balch et al., 2008) and has been postulated to play a critical role in growth and aging (Morimoto, 2008). This balance is maintained by molecular chaperones, the ubiquitin-proteasome system, and the autophagy pathway (Bukau et al., 2006). A robust stress response is often associated with life span extension, which supports a critical role for protein homeostasis in growth and aging. We previously reported that constitutively active mTORC1 attenuates the expression of genes encoding chaperones at the translational level during stress conditions

(Sun et al., 2011). However, how mTORC1-controlled mRNA translation influences the quality of translational products is not fully understood.

mTORC1 stimulates protein synthesis by phosphorylating several translational regulators. Two well-characterized downstream targets are the eukaryotic initiation factor 4E binding proteins (4E-BPs) and the p70 ribosomal S6 kinases (S6Ks) (Ma and Blenis, 2009; Jackson et al., 2010). The nonphosphorylated 4EBPs bind and sequester eIF4E, a key rate-limiting factor for cap-dependent mRNA translation initiation. mTORC1 phosphorylates 4E-BPs, thereby derepressing eIF4E and promoting formation of the translation initiation complex. mTORC1-mediated phosphorylation of S6K promotes protein synthesis through multiple substrates, including the translation initiation factor eIF4B and the elongation regulator eEF2K (Dann et al., 2007; Proud, 2011). Ribosome profiling analysis indicates that 4E-BPs are the master effectors of mTORC1 in controlling translation of mRNAs containing 5′ terminal oligopyrimidine tract (TOP) and TOP-like sequences (Hsieh et al., 2012; Thoreen et al., 2012). This finding raises the question regarding the role of S6Ks in mTORC1-mediated translational regulation. Notably, the phosphorylation of S6Ks is rapamycin-sensitive, whereas mTORC1-mediated phosphorylation of 4E-BPs is largely rapamycin-resistant (Choo et al., 2008). This finding suggests that the antiaging effects of rapamycin might be mediated by the target of S6Ks rather than 4E-BPs. Supporting this notion, deletion of S6K1 in mice leads to increased life span and resistance to age-related pathologies (Selman et al., 2009). However, the differential effects of mTORC1 downstream targets on mRNA translation remain poorly understood.

Here, we sought to dissect the role of mTORC1 in various aspects of protein homeostasis. We found that persistent activation of mTORC1 signaling

led to less functional proteins. The defective ribosome products were mainly due to reduced translation fidelity as a result of increased elongation speed. Rapamycin treatment largely restored protein homeostasis in these cells. The differential effects of mTORC1 downstream targets on translation fidelity further support the critical role of elongation in the quality of translational products. Our results provide mechanistic insights into the molecular connection between nutrient signaling and protein homeostasis and may offer new opportunities for treating age-related diseases.

3.3 Results

Constitutively active mTORC1 signaling reduces the stability of synthesized polypeptides

To monitor the quality of translational products, we used firefly luciferase (Fluc) as a reporter, whose activity can be measured by a luminescence-based assay with exquisite sensitivity. Fluc folds rapidly upon translation on eukaryotic ribosomes and does not require posttranslational modification for its activity (Frydman et al., 1999). Its sensitivity to various stress conditions makes it an ideal molecule to evaluate intracellular protein homeostasis (Gupta et al., 2011). To monitor the biosynthesis of synthesized Fluc in cells with altered mTORC1 signaling, we used a real-time luminometer that allows continuous measurement of Fluc activity in live cells (Sun et al., 2011). Shortly after transfection with plasmids encoding Fluc, luciferase activity progressively accumulated in a mouse embryonic fibroblast (MEF) cell line (Fig. 1A). Unexpectedly, MEFs lacking TSC2 showed less Fluc activity with about 50% reduction by 15 hours after transfection. This was not due to a difference in transfection and transcription

efficiency because *Fluc* mRNA abundance was comparable between these two sets of MEFs (fig. S1). To further exclude the possibility of altered transcription, we synthesized *Fluc* mRNA and performed mRNA transfection. Consistent with the plasmid transfection, TSC2 null cells showed lower Fluc activity than wild-type cells (Fig. 1B). Thus, constitutively active mTORC1 signaling reduces the functionality of synthesized Fluc.

Because mTORC1 is believed to promote protein synthesis, it was surprising to find reduced Fluc activity in TSC2 knockout cells. Immunoblotting of whole-cell lysates revealed that the steady-state amounts of Fluc were significantly lower in TSC2 knockout cells than in wild-type MEFs (Fig. 1C), which is consistent with the reduced Fluc activity measured in live cells. We then treated the transfected cells with the proteasome inhibitor MG132 to examine whether the reduced Fluc quantity was due to increased degradation. Proteasome inhibition by MG132 had minimal effects on translation initiation factors such as eIF2a (fig. S2). In comparison to wild-type cells, TSC2 knockout cells showed increased Fluc abundance after MG132 treatment with the majority recovered in the insoluble fraction (Fig. 1C). This result suggests that a substantial proportion of synthesized Fluc is short-lived in cells with increased mTORC1 signaling.

To examine the feature of other proteins under constitutively active mTORC1 signaling, we expressed green fluorescent protein (GFP), which is relatively stable in cells. Similar to Fluc, GFP also showed decreased steady-state amounts in TSC2 knockout cells with an increased accumulation after MG132 treatment (fig. S3). Proteasome inhibition leads to an accumulation of endogenous substrates in the form of polyubiquitin conjugates (Qian et al., 2002). We measured the abundance of polyubiquitinated species after MG132 treatment

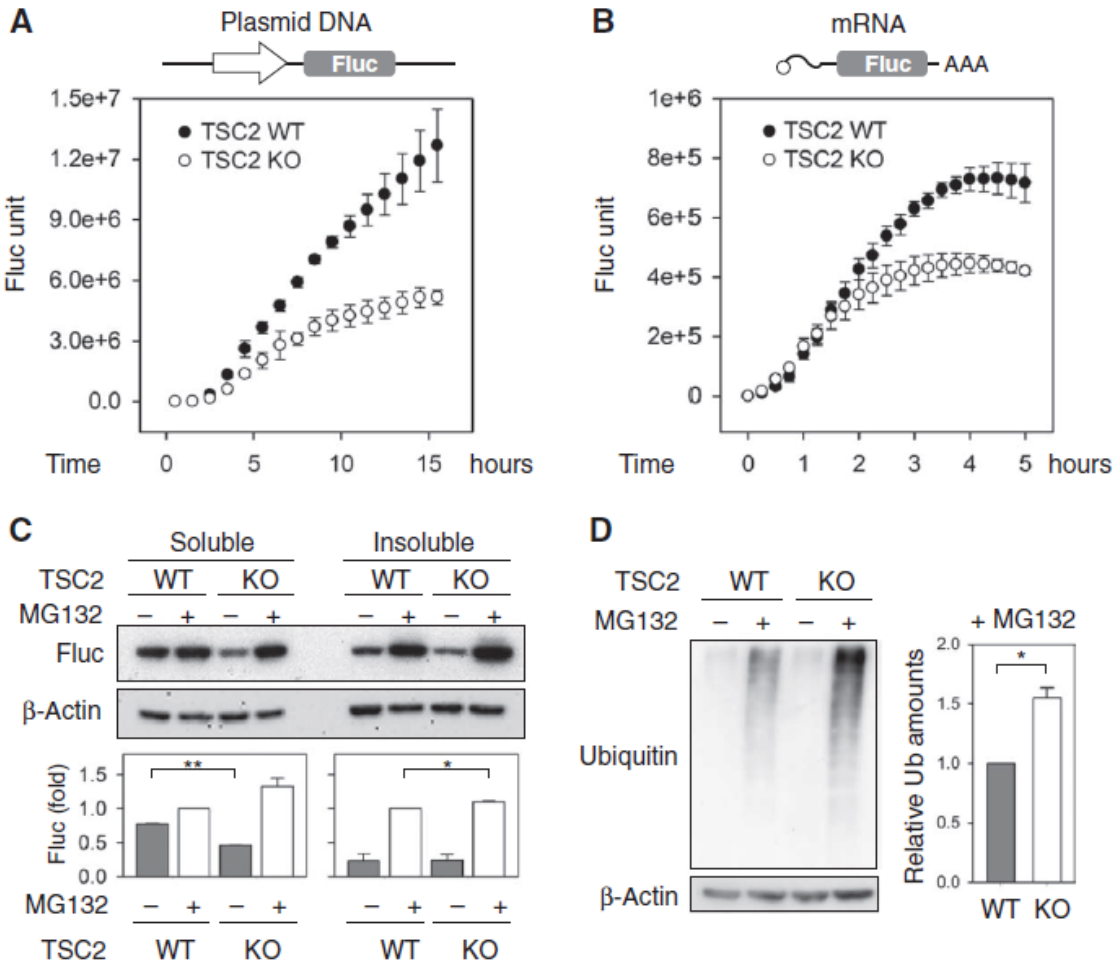

Figure 3-1. **Constitutively active mTORC1 reduces the stability of synthesized polypeptides.** (A) Wild-type (WT) and TSC2 knockout (KO) cells were transfected with Fluc plasmids, and the Fluc activity was monitored continuously (means ± SEM; n = 6 independent experiments). (B) Similar to (A) except that the cells were transfected with Fluc mRNA (means ± SEM; n = 3 independent experiments). (C) WT and TSC2 KO cells transfected with Fluc plasmids were treated with MG132. Whole-cell lysates were separated into soluble and insoluble fractions followed by immunoblotting using antibodies as indicated. Bottom panel shows quantification of Fluc amounts (means ± SEM; n = 3 independent experiments; *P < 0.05, **P < 0.01, ratio paired t test). (D) MG132-treated WT and TSC2 KO cells were immunoblotted with the indicated antibodies. Right panel shows quantification (means ± SEM; n = 3 independent experiments; *P = 0.014, ratio paired t test).

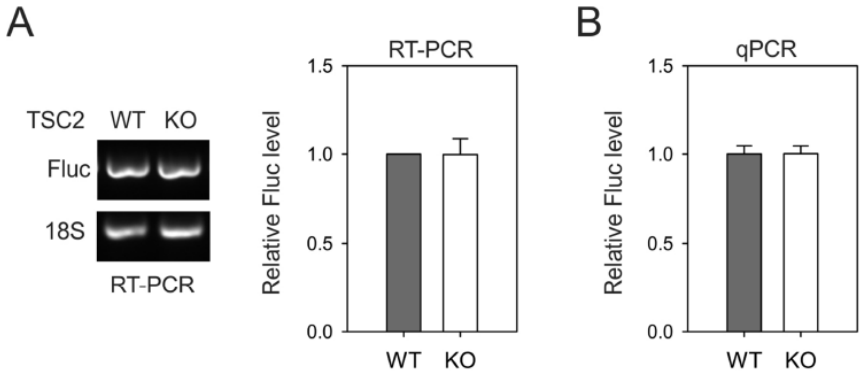

Figure 3-S1. **Quantification of Fluc mRNA abundance in wild-type and TSC2 knockout cells.** (A) Total RNA was extracted from TSC2 wild-type and knockout MEFs transfected with Fluc plasmids followed by RT-PCR with Fluc and 18S primers (left panel). Quantification of Fluc mRNA abundance is normalized to 18S rRNA (right panel) (mean ± SEM; n=3 independent experiments for PCR). (B) RNA was extracted as in (A) and quantitative RT-PCR used to measure abundance of Fluc mRNA normalized to β-actin (mean ± SEM; n=3 independent experiments for qPCR).

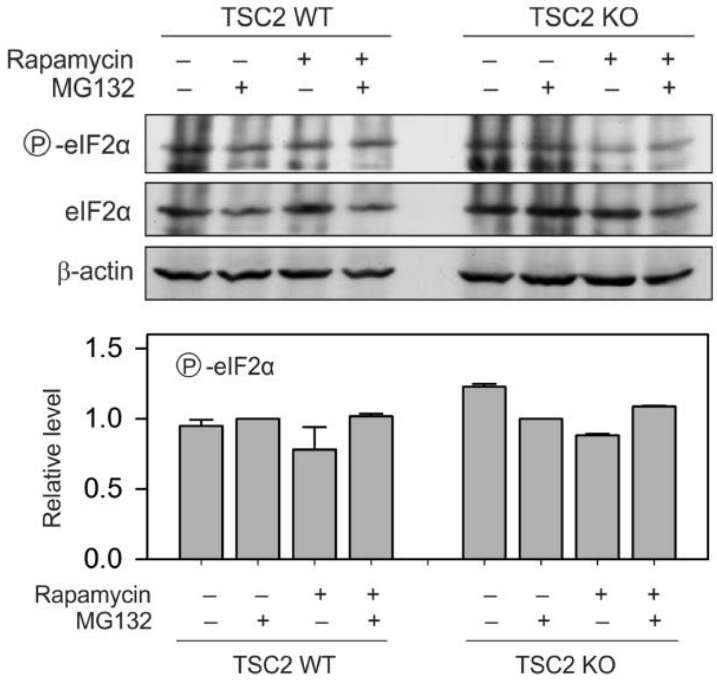

Figure 3-S2. **Phosphorylation status of eIF2α in wild-type and TSC2 knockout cells.** TSC2 wild-type and knockout cells were treated with 10 nM Rapamycin and/or 5 μM MG132 for 15 hours. Whole cell lysates were immunoblotted using antibodies as indicated (top panel). Phosphorylation of eIF2α was normalized to total eIF2α (mean ± SEM; n=3 independent experiments).

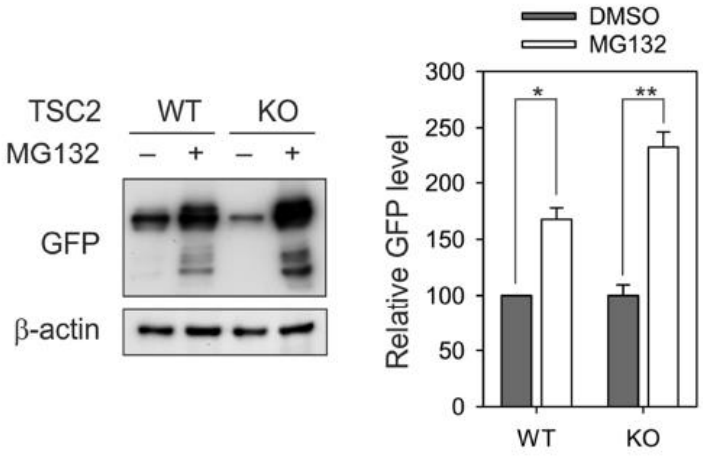

Figure 3-S3. **Features of GFP in wild-type and TSC2 knockout cells.** TSC2 wild-type and knockout cells transfected with myc-GFP plasmids were treated with 5 μM MG132 for 15 hours. Whole cell lysates were immunoblotted as indicated (left panel). The abundance of GFP was normalized to that of β-actin (mean ± SEM; n=3 independent experiments for blot; *P = 0.022, **P = 0.0077, Paired t-test).

in cells with unrestrained mTORC1 signaling. Compared to wild-type cells, TSC2 knockout cells demonstrated a substantial increase of polyubiquitin signals with MG132 treatment (Fig. 1D). Together, these results suggest that mTORC1 signaling disrupts the stability of synthesized polypeptides.

Rheb overexpression reduces the stability of synthesized polypeptides

To independently confirm that uncontrolled mTORC1 signaling contributes to the reduced stability of translational products, we transfected human embryonic kidney (HEK) 293 cells with plasmids encoding Rheb, a direct activator of mTORC1. Rheb overexpression enhanced mTORC1 signaling in a dose-dependent manner as evidenced by increased RpS6 phosphorylation (Fig. 2). Consistent with TSC2 null cells, Rheb overexpression also resulted in a decrease of Fluc steady-state amounts in transfected HEK293 cells. MG132 treatment largely rescued the loss of Fluc, indicating a higher turnover of synthesized Fluc under Rheb overexpression. These cells also showed a higher accumulation of polyubiquitinated species in the presence of MG132 (Fig. 2, bottom panel). Thus, an increase in mTORC1 activity by Rheb overexpression also reduces the stability of synthesized polypeptides.

Suppressing mTORC1 restores the stability of synthesized polypeptides

Having found that an increase in mTORC1 signaling reduced the stability of translational products, we next asked whether suppressing mTORC1 signaling by rapamycin could restore the stability of synthesized polypeptides. Although treating wild-type cells with rapamycin slightly reduced Fluc expression, the presence of rapamycin increased the steady-state Fluc amounts in TSC2 knockout cells (Fig. 3A). This was not due to an increased translation rate in the presence of rapamycin because the abundance of synthesized Fluc under proteasome

inhibition remained consistent after rapamycin treatment (Fig. 3A). The presence of rapamycin also substantially decreased the amount of polyubiquitinated species accumulated after proteasome inhibition by MG132 (Fig. 3B). Therefore, suppressing mTORC1 signaling decreases protein synthesis but increases the stability of synthesized polypeptides.

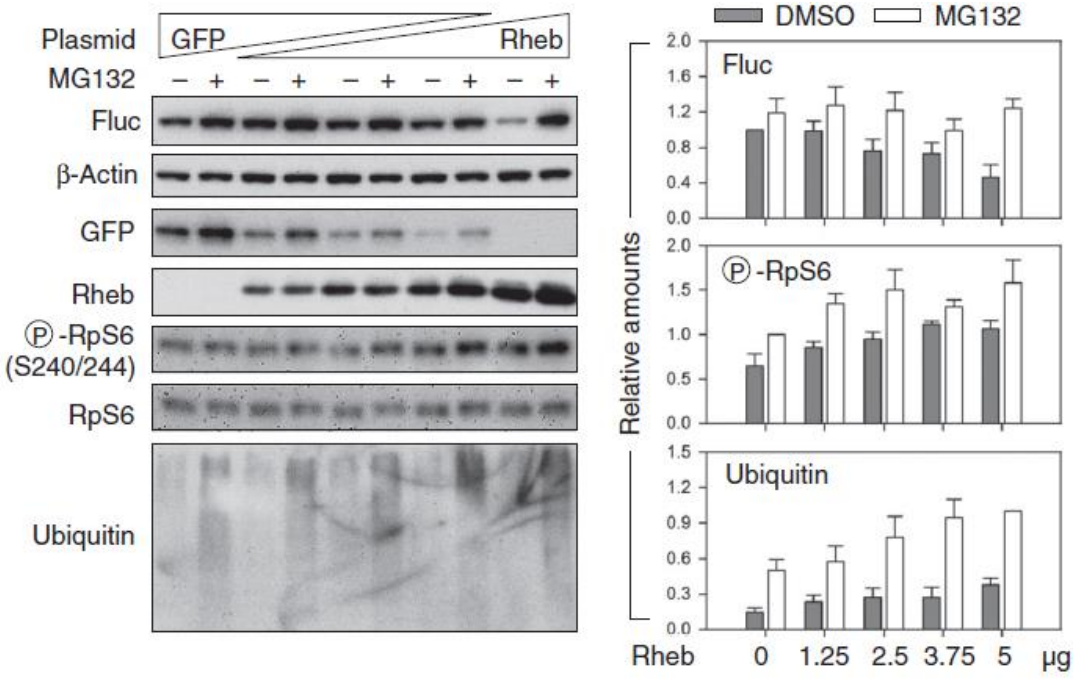

Figure 3-2. **Rheb overexpression reduces the stability of synthesized polypeptides.** MG132-treated HEK293 cells cotransfected with plasmids encoding Fluc and Rheb, supplemented with GFP, were immunoblotted with the indicated antibodies (left panel). Fluc and polyubiquitinated species were quantified after normalizing to b-actin abundance (right panels). Phosph-orylated RpS6 was normalized to total RpS6 protein abundance (means ± SEM; n = 3 independent experiments).

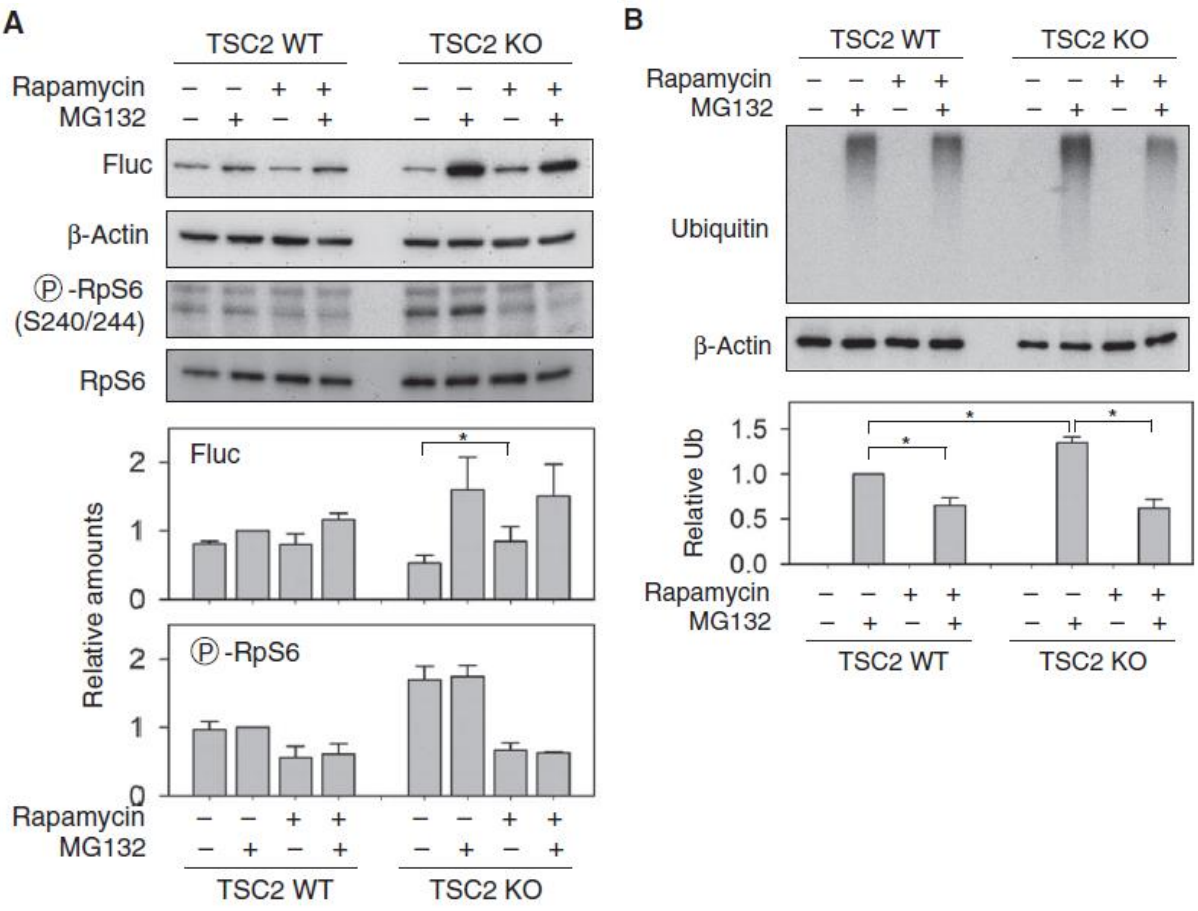

Figure 3-3. **Suppressing mTORC1 restores the stability of synthesized polypeptides.** (A) WT and TSC2 KO cells transfected with Fluc were treated with rapamycin in the absence or presence of MG132 followed by immunoblotting with indicated antibodies. Middle panels show quantification of Fluc protein normalized to β-actin before and after rapamycin treatment. Lower panel is the quantification of phosphorylated RpS6 normalized to total RpS6 protein abundance (means ± SEM; n = 3 independent experiments; *P < 0.05, ratio paired t test). (B) Cells in (A) were immunoblotted using antibody against polyubiquitinated species. Lower panel shows quantitation of ubiquitin before and after rapamycin treatment normalized to b-actin (means ± SEM; n = 4 independent experiments; *P < 0.05, mixed model with random blots and fixed treatment using normalized values; P values are adjusted with a Bonferroni correction).

mTORC1 does not primarily affect chaperone and proteasome activities

The reduced stability of translational products under constitutively active mTORC1 signaling suggests a lower quality of newly synthesized polypeptides, or saturation of the protein quality control system in cells. Molecular chaperones and the ubiquitin-proteasome system are two major mechanisms that maintain intracellular protein homeostasis (Morimoto, 2008; Hartl and Hayer-Hartl, 2011; Sherman and Goldberg, 2001). We previously demonstrated that mTORC1 inhibited the cap-independent Hsp70 translation induced by heat shock stress (Sun et al., 2011). However, it remains unknown whether the chaperone network is adversely affected by persistent mTORC1 signaling under a nonstressed condition. To directly measure the chaperone activity in wild-type and TSC2 knockout cells, we used whole-cell lysates to refold heat-denatured Fluc. This in vitro refolding assay revealed that the chaperone activities in both cells were comparable (Fig. 4A). Furthermore, Rheb overexpression in HEK293 cells also had no appreciable effects on cellular chaperone activities (fig. S4A).

The ubiquitin-proteasome system is the main pathway for elimination of damaged proteins in eukaryotes, and its increased activity might contribute to lower steady-state protein abundance in cells with constitutively active mTORC1 signaling. To compare the proteasome activity between wild-type and TSC2 knockout cells, we used a cell-based proteasome assay in which the chymotrypsin-like activity of the proteasome can be directly measured using a luminogenic substrate (Proteasome-Glo). We observed similar chymotrypsin-like activity in both cell types (Fig. 4B). Consistently, Rheb overexpression in HEK293 cells also did not affect the proteasome activity (fig. S4B). Thus, mTORC1 does not primarily affect the intracellular proteasome system.

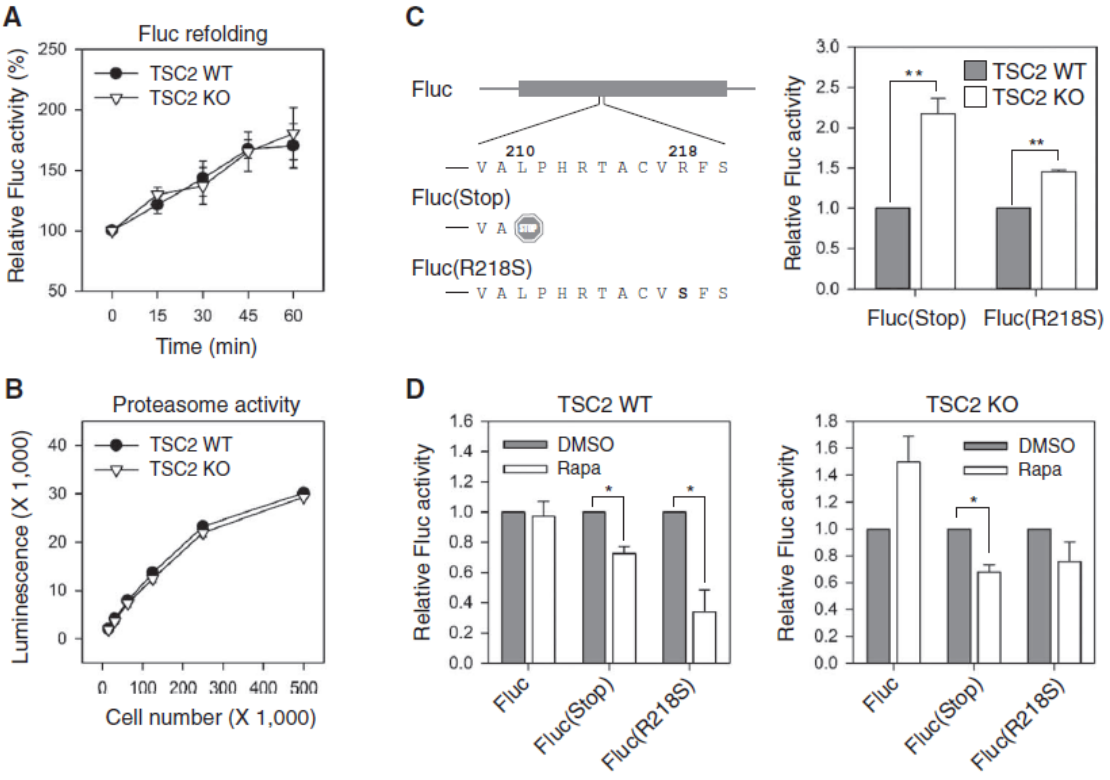

Figure 3-4. **mTORC1 primarily affects translation fidelity**. (A) Heat-denatured Fluc proteins were incubated with whole-cell lysates derived from TSC2 WT and KO cells at room temperature. Fluc refolding was monitored by measuring Fluc activities at the time points indicated. Relative Fluc activity is presented (means±SEM; n=3 independent experiments). (B) The intracellular chymotrypsin activities in TSC2 WT and KO cells were measured by luminescent reagent (Proteasome-Glo) (means±SEM; n=3 independent experiments). (C) Schematic diagram of Fluc mutants Fluc(Stop) and Fluc(R218S) (left panel). TSC2 WT and KO cells were transfected with plasmids encoding Fluc mutants followed by measurement of Fluc activity. Relative Fluc activities were normalized to WT Fluc (means±SEM; n=4 independent experiments; **P < 0.01, paired t test). (D) WT (left panel) and TSC2 KO cells (right panel) transfected with plasmids encoding Fluc mutants as in (C) were treated with rapamycin (Rapa) followed by measurement of Fluc activity. Relative Fluc activities were normalized to WT Fluc with dimethyl sulfoxide (DMSO) (means±SEM; n=4 independent experiments; *P < 0.05, paired t test).

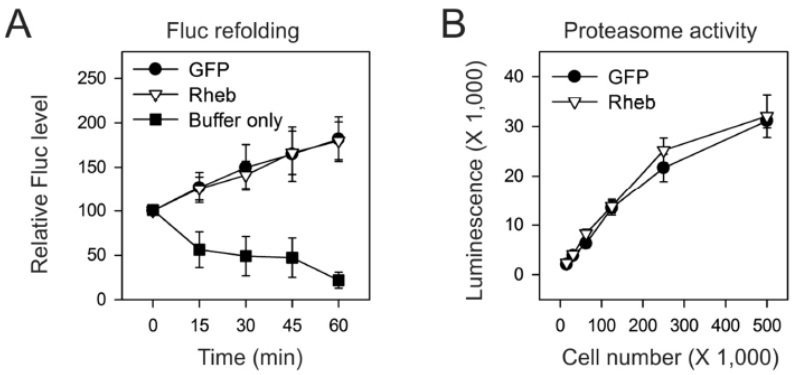

Figure 3-S4. **Chaperone and proteasome activity in cells expressing Rheb.** (A) Heat-denatured Fluc proteins were incubated with whole cell lysates derived from HEK293 cells expressing myc-GFP or myc-Rheb at room temperature. Fluc refolding was monitored by measuring Fluc activity at the time points indicated. Relative Fluc activities are presented (mean ± SEM; n=3 independent experiments). (B)HEK293 cells expressing myc-GFP or myc-Rheb were plated at the indicated concentrations and the intracellular chymotrypsin activity was measured by the luminescent reagent Proteasome-Glo (mean ± SEM; n=3 independent experiments).

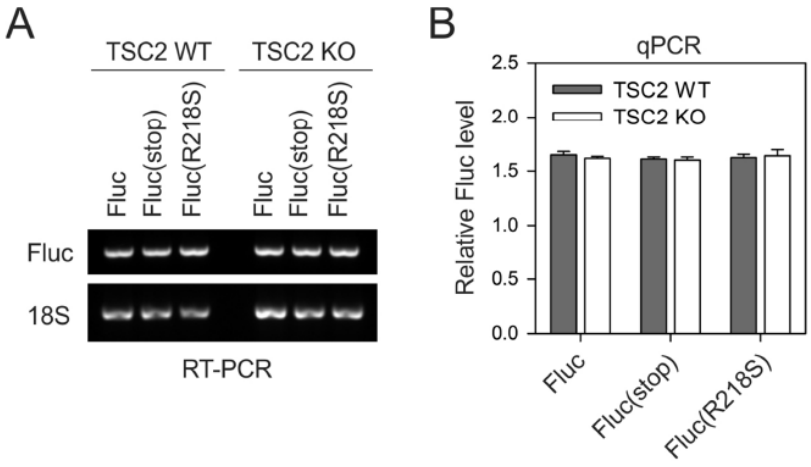

Figure 3-S5. **Quantification of mRNA abundance of Fluc mutants in wild-type and TSC2 knockout cells.** (A) RNA was extracted from TSC2 wild-type and knockout cells expressing wild-type or mutant Fluc plasmids followed by RT-PCR with Fluc and 18S primers. (B) RNA was extracted as in (A) and quantitative RT-PCR used to measure abundance of Fluc mRNA normalized to β-actin (mean ± SEM; n=3 independent experiments for qPCR).

mTORC1 decreases translation fidelity

With no apparent influence on either chaperone or proteasome function in cells, how does constitutively active mTORC1 signaling decrease the stability of synthesized proteins? Nascent chains are synthesized during elongation, and folding generally begins during translation on the ribosome (Fedorov and Baldwin, 1997; Komar, 2009). Thus, the efficiency of cotranslational folding is influenced by translation fidelity during elongation (Buchan and Stansfield, 2007). We reasoned that dysregulated mTORC1 signaling might decrease translation fidelity and increase the generation of defective ribosomal products. To test this hypothesis, we generated two Fluc reporters to assess translational fidelity. One reporter, Fluc(Stop), has leucine at position 210 replaced with a stop codon, which leads to the synthesis of a truncated and enzymatically inactive protein product. This reporter has previously been used to assess readthrough errors occurring during translation (Rakwalska and Rospert, 2004). To evaluate the potential of misincorporation during translation, we mutated the arginine at the active-site position 218 into serine, which renders the resultant Fluc(R218S) mutant devoid of enzymatic activity. As expected, both Fluc(Stop) and Fluc(R218S) mutants showed less than 1% of the enzymatic activity of the wild-type Fluc; however, TSC2 knockout cells showed a significant increase in Fluc activity for both Fluc(Stop) and Fluc(R218S)when compared to wild-type cells (2- and 1.5-fol increase, respectively) (Fig. 4C). Again, this relative increase was not due to a difference in transfection efficiency between these two cells, because quantitative polymerase chain reaction (qPCR) revealed comparable amounts of Fluc mRNA (fig. S5). Consistent with the findings in TSC2 knockout cells, overexpressing Rheb in HEK293 cells also led to a higher rate of readthrough and misincorporation errors during translation of Fluc mutants (fig. S6).

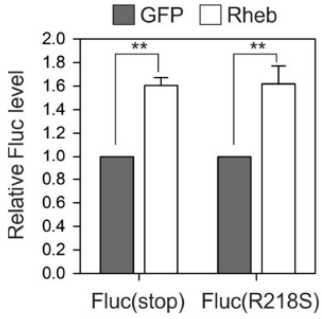

Figure 3-S6 **Translation fidelity in cells expressing Rheb.** HEK293 cells expressing myc-GFP or myc-Rheb were transfected with plasmids encoding Fluc mutants for 24 hours. Relative Fluc activity was normalized using wildtype Fluc (mean ± SEM; n=5 independent experiments; **p < 0.01, Ratio paired t-test).

Because rapamycin treatment increases the stability of synthesized proteins, we examined whether repressing mTORC1 signaling would restore translation fidelity. Indeed, rapamycin treatment decreased the functionality of Fluc mutants in both wild-type and TSC2 knockout cells (Fig. 4D). The effect of rapamycin on promoting translation fidelity in TSC2 knockout cells is an underestimate because wild-type Fluc in these cells showed increased activity in the presence of rapamycin (Fig. 4D). This is consistent with the finding that rapamycin rescues the stability of Fluc under persistent mTORC1 signaling (Fig. 3A). Therefore, repressing mTORC1 signaling increases the stability of newly synthesized polypeptides by promoting accurate mRNA translation.

mTORC1 downstream targets exhibit distinct roles in translation fidelity

Two well-established mTORC1 downstream targets are 4E-BPs and S6Ks. Although 4EBP family proteins are the master effectors of mTORC1 in controlling translation of TOP and TOP-like mRNAs (Hsieh et al., 2012; Thoreen et al., 2012),

the phosphorylation of 4E-BPs is resistant to rapamycin treatment. Because rapamycin effectively abolishes phosphorylation of S6Ks, we suspected that rapamycin might act through S6Ks to restore translation fidelity. Indeed, enzymatic activities of transfected Fluc(Stop) and Fluc(R218S) mutants were significantly reduced in S6K1 and S6K2 double-knockout MEFs when compared to wild-type cells (Fig. 5A). This result indicates increased translation fidelity in the absence of S6Ks. In contrast, MEFs lacking both 4E-BP1 and 4E-BP2 showed comparable activity for both Fluc mutants (Fig. 5B). Considering that 4E-BPs mainly act on translation initiation, the critical role of S6Ks in translation fidelity supports the notion that ribosomal elongation may be responsible for the quality of translational products.

To substantiate the finding that rapamycin acts through S6Ks in restoring translational fidelity, we examined how rapamycin influences the translation of Fluc mutants in MEFs lacking either S6Ks or 4E-BPs. Rapamycin treatment significantly reduced the activity of transfected Fluc mutants in wild-type cells but showed no effects in S6K double-knockout cells (Fig. 5C). In contrast, the presence of rapamycin equally restored the translation fidelity in both 4E-BP wild-type and double-knockout MEFs as evidenced by the suppressed activity of Fluc mutants, in particular Fluc(Stop) (Fig. 5D). These results confirm the distinct roles of mTORC1 downstream targets in controlling the quality of translational products.

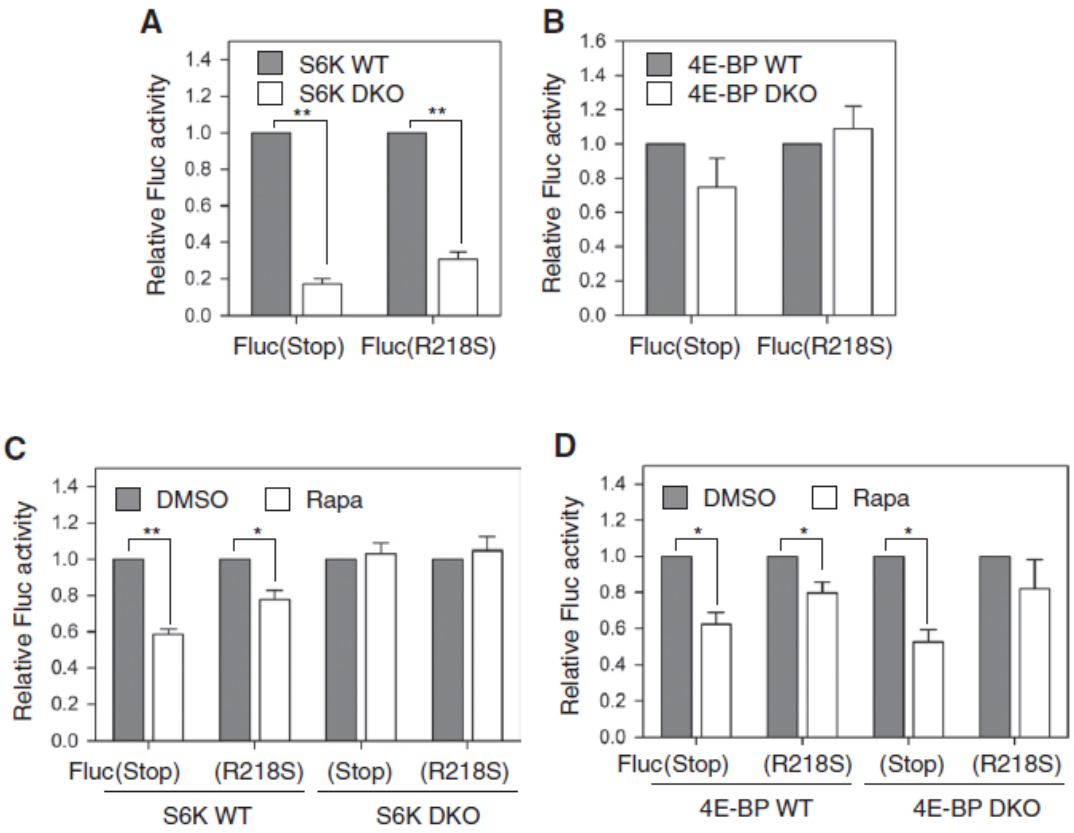

Figure 3-5. **Distinct roles of mTORC1 downstream targets in translation fidelity**. (A) WT and S6K double-KO (DKO) cells were transfected with plasmids encoding Fluc mutants. Relative Fluc activities were normalized to WT Fluc (means ± SEM; n = 4 independent experiments; **P < 0.001, paired t test). (B) WT and 4E-BP DKO cells were transfected with plasmids encoding Fluc mutants. Relative Fluc activities were normalized to WT Fluc (means ± SEM; n = 4 independent experiments). (C) WT and S6K DKO cells transfected as in (A) were treated with rapamycin. Relative Fluc activities were normalized to WT Fluc (means ± SEM; n = 3 independent experiments; *P < 0.05, **P < 0.001, paired t test). (D) WT and 4E-BP DKO cells transfected as in (B) were treated with rapamycin. Relative Fluc activities were normalized to WT Fluc (means ± SEM; n = 4 independent experiments for WT and n = 3 independent experiments for DKO; *P < 0.05, **P < 0.001, paired t test).

mTORC1 increases ribosome speed during translation elongation

Translation fidelity is influenced by multiple factors. For instance, defective ribosome biogenesis reduces the accuracy of amino acid incorporation (Belin et al., 2009). However, both TSC2 wild-type and knockout cells showed a similar ratio of 28S to 18S ribosomal RNAs (rRNAs) (fig. S7). The accuracy of codon-anticodon recognition is also susceptible to ribosome dynamics during elongation. In addition to translation initiation, mTORC1 promotes elongation through S6K-mediated eEF2K phosphorylation (26). We hypothesize that constitutively active mTORC1 signaling might potentially compromise the fidelity of the decoding process by increasing the speed of elongation. To evaluate the ribosome dynamics in both TSC2 wild-type and knockout cells, we performed ribosome sedimentation analysis. Consistent with an increase in cap-dependent mRNA translation, TSC2 null cells exhibited higher polysome formation than wild-type cells, and the monosome peak was correspondingly reduced (Fig. 6A). Although this feature is consistent with more efficient translation initiation in cells with increased mTORC1 signaling, the snapshot of polysome profiles does not offer insight into ribosome dynamics during elongation.

The translation inhibitor harringtonine stalls initiating ribosomes at the start codon while allowing elongating ribosomes to run off the transcript (Ingolia et al., 2011). The time required for polysome depletion correlates with the global translation elongation speed. By treating cells with harringtonine for various times, we evaluated the average elongation speed (fig. S8). Compared to wild-type cells, TSC2 knockout cells showed an earlier polysome runoff, indicating faster ribosome movement during elongation (Fig. 6B).

Because rapamycin treatment essentially restored translation fidelity in TSC2 knockout cells, we examined the effect of rapamycin on ribosome dynamics.

As a specific mTORC1 inhibitor, rapamycin suppresses translation initiation. Supporting this notion, the monosome peak was increased after rapamycin treatment (Fig. 6A). Intriguingly, we observed a slight increase rather than a decrease of polysome formation in TSC2 knockout cells in the presence of rapamycin. Under this condition, the retained polysome is a strong indication of ribosome slowing down during elongation. Indeed, application of harringtonine showed delayed depletion of polysomes in the presence of rapamycin (Fig. 6C). These results support the interpretation that mTORC1 decreases translation fidelity by increasing ribosome speed.

Because rapamycin treatment essentially restored translation fidelity in TSC2 knockout cells, we examined the effect of rapamycin on ribosome dynamics. As a specific mTORC1 inhibitor, rapamycin suppresses translation initiation. Supporting this notion, the monosome peak was increased after rapamycin treatment (Fig. 6A). Intriguingly, we observed a slight increase rather than a decrease of polysome formation in TSC2 knockout cells in the presence of rapamycin. Under this condition, the retained polysome is a strong indication of ribosome slowing down during elongation. Indeed, application of harringtonine showed delayed depletion of polysomes in the presence of rapamycin (Fig. 6C). These results support the interpretation that mTORC1 decreases translation fidelity by increasing ribosome speed.

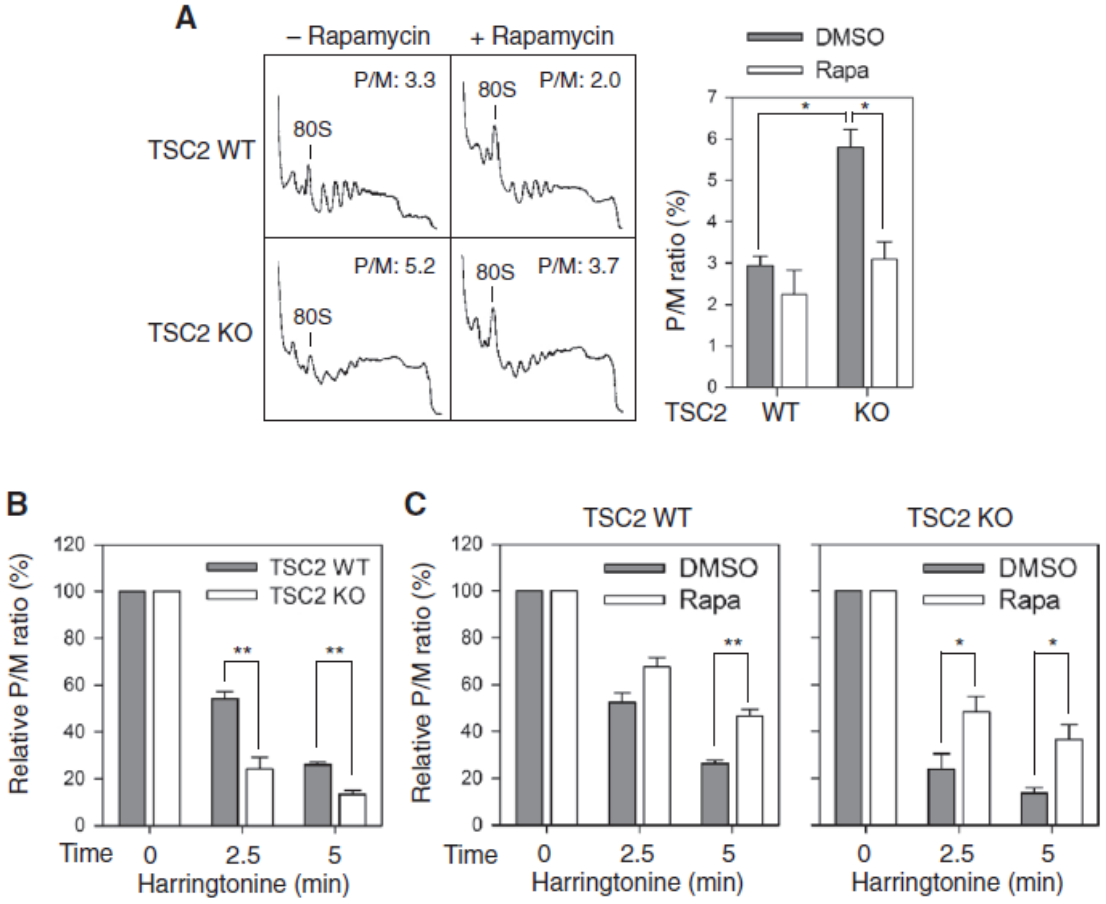

Figure 3-6. **mTORC1 alters ribosome dynamics during translation elongation.** (A) Polysome profiles of WT and TSC2 KO cells in the presence of rapamycin were determined using sucrose gradient sedimentation. The P/M (polysome/monosome) ratio was calculated by measuring the areas under the polysome and 80S peak and further quantified in the left panel (means ± SEM; n = 3 independent experiments; *P < 0.05, ratio paired t test). (B) Polysome profiling of WT and TSC2 KO cells was conducted after treatment with harringtonine for indicated times. The P/M ratio was determined and normalized to no harringtonine treatment per cell type (means ± SEM; n = 4 independent experiments; **P < 0.01, paired t test). (C) WT and TSC2 KO cells were pretreated with rapamycin followed by harringtonine treatment for indicated times before polysome profiling. The P/M ratio was determined and normalized to no harringtonine treatment (means ± SEM; n = 3 independent experiments; *P < 0.05, **P < 0.01, unpaired t test).

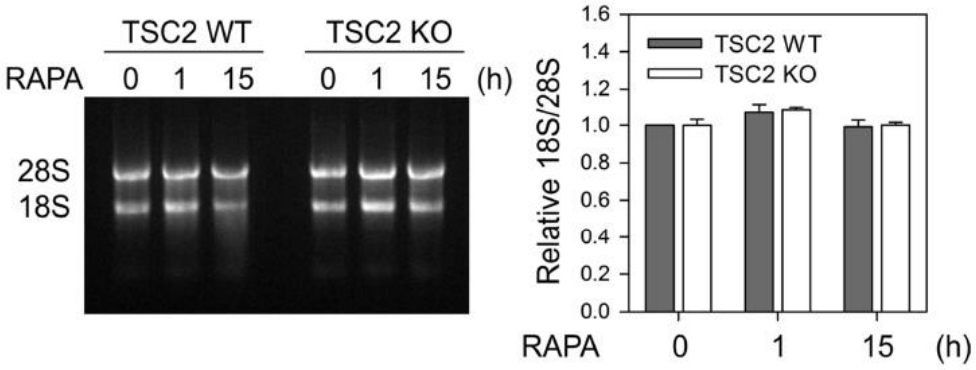

Figure 3-S7 **Ratio of 28S to 18S rRNAs in wild-type and TSC2 knockout cells.** RNA was extracted from wild-type and TSC2 knockout cells with or without 20 nM rapamycin treatment for the indicated times. RNA was run on a 1% agarose gel by electrophoresis (left panel). Relative ratios of 18S rRNA was compared to 28S rRNA (right panel) (mean ± SEM; n=3 independent experiments).

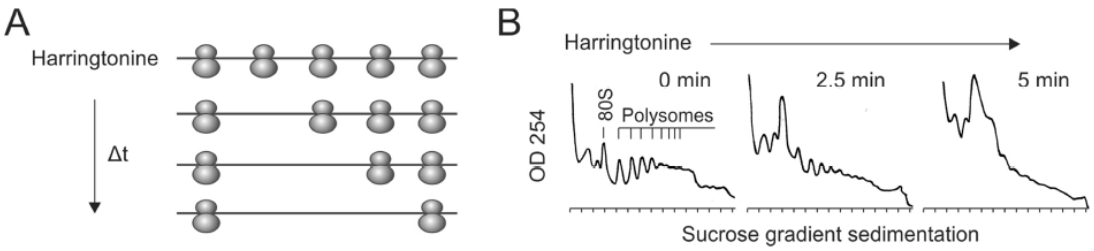

Figure 3-S8 **Measurement of ribosome dynamics during translation elongation.** (A) Schematic of ribosome run-off in the presence of harringtonine. (B) An example of polysome profiles of MEF cells in the presence of harringtonine (1mg/ml) at the indicated times. Monosome (80S) and polysomes are highlighted and the P/M ratio change is quantified in Fig. 6B.

mTORC1 controls cellular susceptibility to proteotoxic stress

mTORC1 signaling adversely affected the quality of newly synthesized proteins; therefore, we reasoned that cells with persistent mTORC1 signaling might be sensitive to proteotoxic stress. To test this possibility, we treated cells with MG132 to induce proteotoxic stress and compared the cell viability between wild-type and TSC2 knockout cells. MG132 treatment significantly reduced cell growth and caused about 10% cell death in wild-type cells (Fig. 7A). In contrast, more than 20% of cell death occurred in TSC2 knockout cells after the same treatment. Because proteotoxic stress triggers apoptosis, we analyzed molecular markers of apoptosis in these cells and detected increased caspase-3 cleavage in TSC2 knockout cells (Fig. 7B).

Adding rapamycin together with MG132 restored the cell viability of TSC2 null cells (Fig. 7, A B). Accordingly, there was a decrease in the proportion of cells undergoing apoptosis (Fig. 7B). These protective effects of rapamycin in response to proteotoxic stress might be attribute to the involvement of multiple pathways including macroautophagy (Zhou et al., 2009). Nevertheless, our results extend the benefits of rapamycin by showing that it alleviates proteotoxic stress by increasing the quality of newly synthesized proteins.

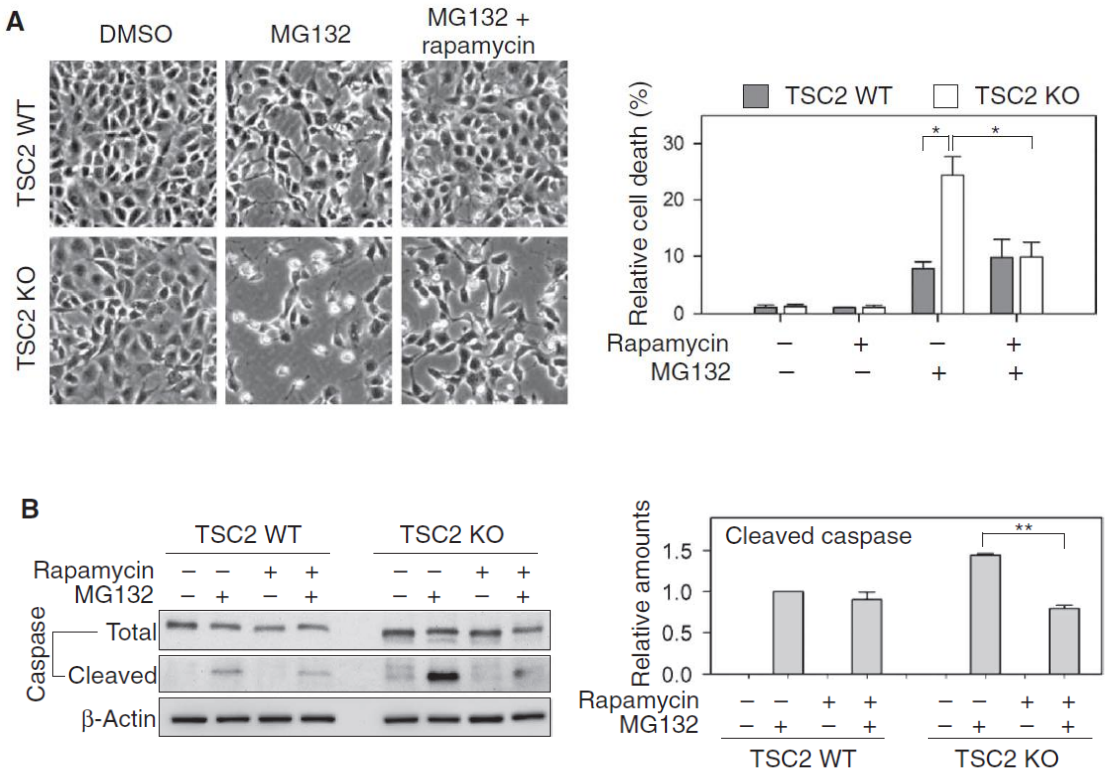

Figure 3-7. **mTORC1 regulates cellular susceptibility to proteotoxic stress.** (A) WT and TSC2 KO cells were treated with MG132 in the absence or presence of rapamycin. Cell viability and morphology were assessed by phase-contrast microscope images (left panel). Images were assessed for cell viability and quantified (right panel) (means ± SEM; n = 4 independent experiments; *P < 0.05, ratio paired t test). (B) Cell samples from (A) were lysed and immunoblotted using the indicated antibodies. The amount of cleaved caspase-3 relative to the total caspase-3 was quantified (right panel) (means ± SEM; n = 3 independent experiments; **P < 0.01, ratio paired t test).

3.4 Discussion

Studies conducted in rodents over the past seventy years have shown that life span is extended by caloric restriction (McCay et al., 1989). Similar to caloric restriction, mTORC1 inhibition also extends life span in various model organisms (Kapahi, et al, 2004; Kaeberlein et al., 2005; Powers et al., 2006), and administration of rapamycin to adult mice is sufficient to extend life span considerably (Harrison et al., 2009). However, how mTORC1 inhibition increases longevity in mammals remains an unresolved issue. Protein synthesis–dependent and protein synthesis–independent mechanisms have been proposed, and several models have been suggested to explain the potential benefits of reducing protein synthesis. First, a decrease of overall translational products could lower the cellular burden of erroneously synthesized polypeptides. This situation results in "spare" proteolytic and chaperone function in cells, which may contribute to the observed increase in organism stress resistance and life span (Hipkiss, 2007). Second, global suppression of protein synthesis may allow selective translation of a subset of mRNAs that exert a protective function (Zid et al., 2009). Here, we report that a global decrease in mRNA translation improves the fidelity of protein synthesis. Our observations not only extend the functional connection between mTORC1 and protein homeostasis (Fig. 8) but also suggest a molecular basis for how constitutively activemTORC1 signaling favors the development of age-related pathologies by disrupting protein homeostasis.

mTORC1 regulates mRNA translation at multiple stages. The regulatory mechanisms impinging on the initiation stage have received considerable attention, but accumulating evidence points to the elongation phase as another target of translational control (Proud, 2009). We monitored ribosome dynamics

in cells with altered mTORC1 signaling using the translation inhibitor harringtonine. Consistent with the positive role of mTORC1 in regulating eEF2 activity (Proud, 2011), TSC2 knockout cells exhibit faster ribosome runoff than the wild-type cells. Despite the wide belief that rapamycin suppresses general protein synthesis by acting primarily on translation initiation, we found that rapamycin does not disassemble the polysome, at least in the early stage. Thus, it is conceivable that rapamycin exerts additional impacts on elongation. Supporting this notion, rapamycin treatment reduces the elongation rate of ribosomes in both wild-type and TSC2 knockout cells.

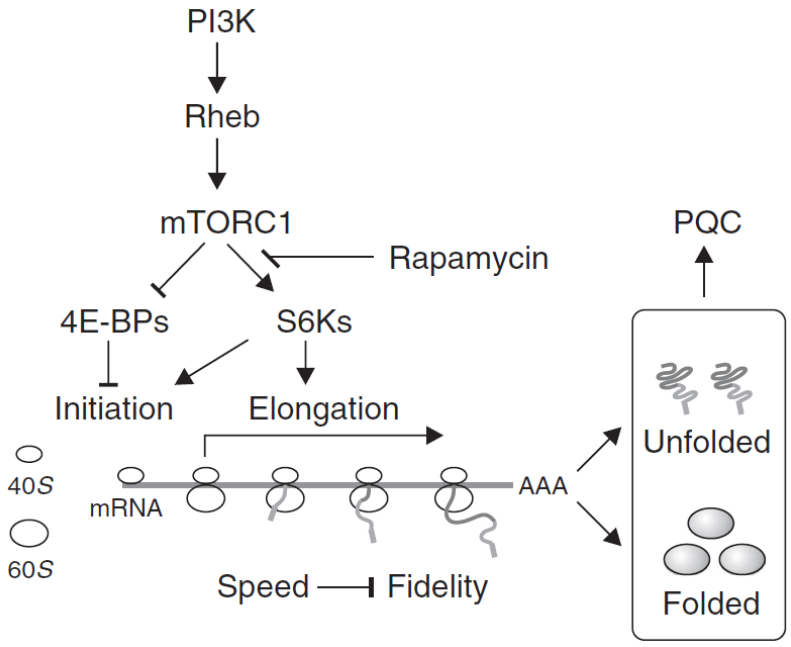

Figure 3-8. **Model for functional connection between mTORC1 and protein homeostasis.** mTORC1 regulates protein synthesis at multiple stages through different downstream targets. Whereas 4E-BPs control the initiation step, S6Ks mainly promote the elongation stage. The altered ribosome dynamics when mTORC1 signaling is deregulated results in protein dyshomeostasis and disruption of the protein quality control (PQC) network. Rapamycin restores protein homeostasis by enhancing translation fidelity through the S6Ks.

One unanticipated finding in this study is the distinct roles of mTORC1 downstream targets in translation fidelity. It appears that S6Ks, but not 4E-BPs, influence the quality of translational products, presumably through the regulation of elongation. This is in agreement with the finding that mice lacking S6K1 showed increased life span and resistance to age-related pathologies (Selman et al., 2009). In contrast, deleting 4EBPs mainly affected cell proliferation, but not cell growth (Dowling et al., 2010). In addition, only the phosphorylation of S6Ks, but not 4E-BPs, is sensitive to rapamycin treatment (Choo et al., 2008). The differential effects of rapamycin on mTORC1 downstream targets support the notion that the antiaging benefits of rapamycin occur through the elongation stage by S6Ks (Fig. 8).

How does an increased elongation rate affect translation fidelity? mRNA translation is an error-prone step in gene expression with about 1 in every 10^3 to 10^4 codons mistranslated (Gingold and Pilpel, 2011). Amino acid incorporation is a competitive process between the cognate and the near-cognate transfer RNAs (tRNAs) for a given codon. The increased elongation rate could potentially compromise the translational fidelity by promoting misincorporation of amino acids. Reduced elongation speed, on the other hand, allows for a relatively longer dwell time of the ribosome in its search for correct tRNA pairing. It is thus conceivable that an increased translation speed, such as that under constitutively active mTOR signaling, generates more aberrant translational products. In addition, variations of elongation speed may coordinate cotranslational folding of emerging polypeptides (Komar, 2009). The local discontinuous translation (ribosome pausing) temporally separates the translation of segments of the peptide chain and actively coordinates their cotranslational folding (Zhang et al., 2009). Supporting this notion, a study in *Escherichia coli* has demonstrated that

slowing translation speed enhances protein folding efficiency (Siller et al., 2010). The faster translation speed may eliminate the ribosome pausing necessary for cotranslational events. Supporting this notion, we observed an inverse correlation between elongation speed and the quality of nascent polypeptides in mammalian cells.

Ribosome biogenesis is largely controlled by mTORC1 at the level of translation because ribosomal subunits are encoded by TOP mRNAs (Thoreen et al., 2012; Hamilton et al., 2006). The reduced translation fidelity under constitutively active mTORC1 signaling could create errors in synthesized ribosomal proteins, which may cause an error catastrophe due to dysfunctional translation machinery. This catastrophe would create additional errors of newly synthesized polypeptides. We cannot exclude the possibility that this may account for the reduced quality of synthesized proteins. It remains to be investigated whether cells with unrestrained mTORC1 signaling contain defective ribosome subunits.

The observations described in this study have several implications. First, the critical role of mTORC1 in ribosome dynamics and translation quality extends the molecular linkage between mTORC1 and protein homeostasis. Second, the finding that an increase in protein synthesis is accompanied by a decrease in protein quality provides a plausible mechanism for how persistent mTORC1 signaling favors the development of age-related pathologies. With the most common feature of aging being an accumulation of misfolded proteins derived from erroneous biosynthesis and postsynthetic modification, protein homeostasis is an important mediator of rapamycin in longevity.

3.5 Materials & Methods

Cell lines and reagents- TSC2 wild-type and knockout MEFs were provided by D. J. Kwiatkowski (Harvard Medical School). 4E-BP wild-type and double-knockout MEFs were provided by N. Sonenberg (McGill University), and S6K wild-type and double-knockout MEFs by G. Thomas (University of Cincinnati). All cell lines were maintained in Dulbecco's modified Eagle's medium with 10% fetal bovine serum grown at 37°C with 5% CO2. Cycloheximide, rapamycin, and MG132 were purchased from Sigma, and harringtonine from LKT Laboratories. Dual-Luciferase Assay System, Luciferase Assay System, and Proteasome-Glo kit were purchased from Promega. D-Luciferin was purchased from Registech. Antibodies against phosphorylated and total S6 and caspase-3 were purchased from Cell Signaling Technology; β-actin from Sigma-Aldrich; myc from Santa Cruz; and polyubiquitin from Assay Designs. Anti-Fluc was purchased from Novus Biologicals.

Plasmids and transfection- The Fluc gene was directly removed from pGL3 vector (Promega) with Hind III and Xba I sites and then cloned into pcDNA3.1 (Invitrogen). Fluc mutants for fidelity assays were created from pGL3 vector with PCR Mutagenesis Kit (Agilent Technologies) with the following primers: Fluc(Stop), 5′-GGTCTGCCTAAAGGTGTCGCTTAGCCTCATAGAACTGCC-3′; Fluc(R218S), 5′-GCCTCATAGAACTGCCTGCGTGTCTTTCTCGCATGCCAGAGATCC-3′. Plasmids encoding Rheb-myc were provided by K.-L. Guan (University of California, San Diego). Transfection was performed with Lipofectamine 2000 (Invitrogen) according to the manufacturer's instructions.

mRNA in vitro transcription- mRNA with a m7G-cap was synthesized with the mMessage mMachine T7 Ultra Kit (Ambion), followed by purification with the

MEGAclear Kit (Ambion), according to the manufacturer's instructions. mRNA transfections were performed with Lipofectamine 2000 (Invitrogen) according to the manufacturer's instructions.

Luciferase assay- For real-time measurement of Fluc activity, cells were plated on 35-mm dishes and transfected with plasmid or mRNA containing the Fluc gene. Immediately after transfection, 1 mM luciferase substrate D-luciferin was added into the culture medium, and the Fluc activity was recorded at 37°C with 5% CO2 using Kronos Dio Luminometer (ATTO). For luciferase assay with cell lysates, Fluc activity was measured with a luciferase reporter assay (Promega) on a Synergy HT Multi-detection Microplate Reader (BioTek Instruments). For the fidelity assay, Fluc activity from Fluc mutants was normalized to Fluc activity derived from pGL3.

In vitro refolding assay- QuantiLum Recombinant Fluc (Promega) was diluted in lysis buffer at a concentration of 50 mg/ml and then split into two individual Eppendorf tubes. One tube was placed at 42°C for 15 min to denature Fluc, whereas the other was kept at room temperature. The denatured or nondenatured Fluc protein was then added to cell lysates for a final concentration of 16.5 mg/ml. Refolding was conducted at room temperature, and the Fluc activity was monitored every 15 min with the Promega Luciferase Assay System. Fluc activity in lysis buffer alone was measured in parallel to exclude spontaneous refolding of denatured Fluc. The nondenatured Fluc activity was used to normalize the denatured Fluc activity after cell lysate–mediated refolding.

Immunoblotting- Cells were lysed on ice in tris-buffered saline (TBS) buffer [50 mM tris-HCl (pH 7.5), 150 mM NaCl, 1 mM EDTA] containing protease inhibitor cocktail tablet (Roche) and 2% Triton X-100. After incubating on ice for

30 min with interval vortexing, the lysates were centrifuged for 5 min at 12,500 rpm, and an aliquot was removed for quantification by Bradford assay (Bio-Rad). Samples were adjusted to 1 mg/ml and heated for 5 min in SDS–polyacrylamide gel electrophoresis (SDS-PAGE) sample buffer [50 mM tris-HCl (pH 6.8), 100 mM dithiothreitol (DTT), 2% SDS, 0.1% bromophenol blue, 10% glycerol]. For fractionation analysis, the Triton X-100–soluble and Triton X-100–insoluble fractions were dissolved individually in SDS-PAGE sample buffer. Proteins were resolved on SDS-PAGE and transferred to Immobilon-Pmembranes (Millipore). Membranes were blocked for 30 min in TBS containing 5% blotting milk, followed by incubation with primary antibodies overnight. After several washes with TBS containing 0.1% Tween 20, the membrane was incubated with horseradish peroxidase–coupled secondary antibodies. Immunoblots were developed with enhanced chemiluminescence (ECL Plus, GE Healthcare). Individual Western experiments were quantified with ImageJ software and normalized to either β-actin or total protein of phosphorylated target as a loading control.

Reverse transcription PCR and qPCR- Total RNA was extracted from whole-cell lysates with TRIzol reagent (Invitrogen) according to the manufacturer's instructions. RNA quality was validated by NanoVue Spectrophotometer (GE Healthcare) and run on an agarose gel for integrity examination. Reverse transcription was performed with SuperScript III kit (Invitrogen) followed by PCR. The primers for the Fluc gene are 5′-ATTTATCGGAGTTGCAGTTGCGCC-3′ (forward) and 5′-CCAGCAGCGCACTTTGAATCTTGT-3′ (reverse), and the primers for 18S are 5′-CTTGGATGTGGTAGCCGTTT-3′ (forward) and 5′-TATGGTTCCTTTGGCGCTC-3′ (reverse). For qPCR, reverse transcription was performed with High Capacity cDNA Reverse Transcription Kit (Applied

Biosystems). qPCR was then conducted with Power SYBR Green PCR Master Mix (Applied Biosystems) according to the manufacturer's protocols. PCR was performed on a LightCycler 480 Real-Time PCR System (Roche Applied Science) with three technical replicates per sample per run. The primers for the Fluc gene are 5′-ATCCGGAAGCGACCAACGCC-3′ (forward) and 5′-GTCGGGAAGACCTGCCACGC -3′ (reverse), and the primers for β-actin are 5′-TTGCTGACAGGATGCAGAAG-3′ (forward) and 5′-ACTCCTGCTTGCTGATCCACAT-3′ (reverse).

Polysome profiling- A sucrose solution was prepared in polysome buffer [10 mM Hepes (pH 7.4), 100 mM KCl, 5 mM MgCl2, cycloheximide (100 mg/ml), 5 mM DTT]. A 15 to 45% sucrose density gradient was prepared in SW41 ultracentrifuge tubes (Fisher) with a Gradient Master (BioComp Instruments). Cells were treated with cycloheximide (100 mg/ml) for 3 min at 37°C in culture media followed by lysis in ice-cold polysome buffer containing 2% Triton X-100. Lysate was centrifuged for 10 min at 12,500 rpm, and 500 ml of supernatant was loaded onto sucrose gradient and centrifuged for 100 min at 38,000g at 4°C in a SW40 rotor. Gradients were fractioned at 0.75 ml/min with an automated fractionation system (ISCO), which continually monitors absorbance values at 254 nm. For rescue experiments, rapamycin was used at 20 nM for 3 hours before the addition of cycloheximide. For the ribosome runoff assay, cells were pretreated with harringtonine (1 mg/ml) with or without 20 nM rapamycin for up to 5 min before the addition of cycloheximide.

Proteotoxic stress and viability assay- TSC2 wild-type and knockout MEFs were treated with 10 mM MG132 overnight with or without 10 nM rapamycin. Multiple fields were selected for examination by a Nikon Eclipse Ti-S inverted

microscope. Cells were then collected and counted with trypan blue staining. Four counts were made per sample and averaged for viability assay.

Statistics- For each analysis, raw values were used when possible or raw values were normalized to an internal control from at least three biologically independent experiments. The data are expressed as means ± SEM. For each comparison, the relevant comparisons were chosen on the basis of the assay. A Bonferroni correction was used to adjust the P values for multiple comparisons within Fig. 3B. Statistical significance is denoted by *P <0.05 and **P < 0.01. Microsoft Excel, GraphPad Prism 6, and JMP software were used for statistical analyses.

3.6 Acknowledgements

We thank Qian laboratory members for helpful discussion of the manuscript and E. Ferrie for technical assistance. We are grateful to D. Kwiatkowski (Harvard), G. Thomas (University of Cincinnati), and N. Sonenberg (McGill University) for providing MEF cell lines and K.-L. Guan (University of California, San Diego) for Rheb plasmids. We also thank the Stover and Qi laboratories at Cornell for equipment accessibility. **Funding:** This work was supported by grants to S.-B.Q. from the NIH (1 DP2OD006449-01), the Ellison Medical Foundation (AG-NS-0605-09), and the Department of Defense Exploration-Hypothesis Development Award (W81XWH-11-1-0236). C.S.C. was partially supported by an NIH training grant for Cornell University Genetics, Genomics, and Development Graduate Program (T32GM00761). **Author contributions:** C.S.C. and S.-B.Q. conceived and designed the project; C.S.C. performed the experiments; and C.S.C. and S.-B.Q. wrote the manuscript.

CHAPTER 4

Detecting Co-translational Degradation *in Vivo*

This chapter is based on a new project written by Conn CS, to be placed together with previous work from Han Y, and analyzed in part by Liu B. With additional experiments, the manuscript will be completed by Conn CS and Qian S-B in 2013.

4.1 Abstract

Co-translational degradation of nascent polypeptides has been contemplated and debated for nearly thirty years. It has recently been reported that 12-15% of nascent polypeptides are ubiquinated in human cell culture and at least 1.1% in *S. cerevisiae*. To connect these recent findings with previous work studying ubiquinated residues, we used Ribo-Seq to monitor ribosome density along engineered nascent protein bearing an amino-terminal degradation signal (degron). In agreement with previous reports, we observed partial co-translational degradation of our degron sequence using Ribo-seq. Furthermore, the ribosomes remained intact along the mRNA transcript, suggesting that dissociation is not directly coupled with co-translational degradation.

4.2 Introduction

Protein synthesis is recognized as one of the highest error-prone steps in gene expression with approximately one in every $\sim 10^4$ codons mistranslated (Kirkwood et al., 1984). To balance the threat of aberrant protein products, cells have adapted intricate mechanisms of quality control. Synthesis, maturation, and

degradation of polypeptides are kept in check through a network of pathways to maintain this protein homeostasis. These quality control mechanisms begin at the birth of the polypeptide, as the amino-terminal end emerges from the ribosome exit tunnel. Once a controversial hypothesis, co-translational regulation has now become accepted with advances showing co-translational folding and potential degradation (Pechmann, et al., 2013; covered in Chapter 1).

Previous studies indicated that as high as 30% of newly synthesized polypeptides can be targeted for degradation (Schubert et al, 2000). This created a debate and even a schism in the field regarding why a cell would waste valuable products which require substantial consumption and are energetically demanding to yield (Yewdell and Nicchitta, 2006). Recent advances have narrowed down this percentage, stating that 12-15% of nascent polypeptides can be ubiquinated (Ub) in human cell culture and 1.1% in *S. cerevisiae* (Wang et al., 2013; Duttler et al., 2013). Furthermore, a disruption in protein homeostasis increasing mistranslation, increasing misfolding, or deleting quality control components enhanced the co-translational Ub in both organisms. The mechanisms of co-translational Ub at the ribosome leave much to uncover, including specificity for recognition and ribosome dynamics during degradation.

To expand on these recent advances, we engineered multi-domain substrates bearing an amino-terminal degradation signal (degron) to evaluate specificity of co-translational degradation using polysome profiling and sequencing (Ribo-Seq) (Bachmair and Varshavsky, 1989). Our data confirms a loss of ribosome reads within the coding sequence (CDS) of a degron that can be rescued by inhibition of the proteasome. Furthermore, the degradation of a targeted substrate does not alter the ribosome association along the mRNA transcript. These results support co-translational degradation in mammalian

cells and provide a strategy to monitor individual genes of interest for quality control at the ribosome.

4.3 Results

The degron technique was designed and perfected over the last thirty years to engineer substrates mimicking regulated polypeptides, which are short-lived *in vivo*. The sequence requires an Ub moiety for co-translational targeting of the substrate as well as essential lysine residues downstream for poly-Ub chain attachment (Lys-15, Lys-17, or multiple Lys sites) (Bachmair and Varshavsky, 1989). The C-terminal of Ub is cleaved co-translationally between the last two glycine residues then exposing the next amino acid as the new N-terminus. Varying amino acids in the N-terminus can create a range of stability noted as the N-end rule. For example, an exposed methionine residue may be stable over twenty hours *in vivo*, while an arginine residue, at the same position, might turn over in minutes (Bachmair et al., 1986). To evaluate the ribosome dynamics along a degron sequence, we generated monoclonal HEK293 cell lines stably expressing either the multi-domain transcript Ub-MFlag-Luc (M-Luc), Ub-RFlag-Luc (R-Luc), or UbvvRFlag-Luc (vvR-Luc) each with the first lysine residue of firefly luciferase (Luc) positioned as the optimal Lys-17 residue (Figure 4-1A, B). After Ub emerges from the exit tunnel, folding into the correct conformation, it will be recognized and cleaved at the C-terminus in the M-Luc construct, creating a relatively stable protein. In R-Luc, after cleavage, the product containing arginine in the N-terminus should be relatively unstable. However, within vvR-Luc the glycine residues recognized for cleavage were mutated to valine creating a constitutively targeted degron substrate remaining uncleaved (Figure 4-1B).

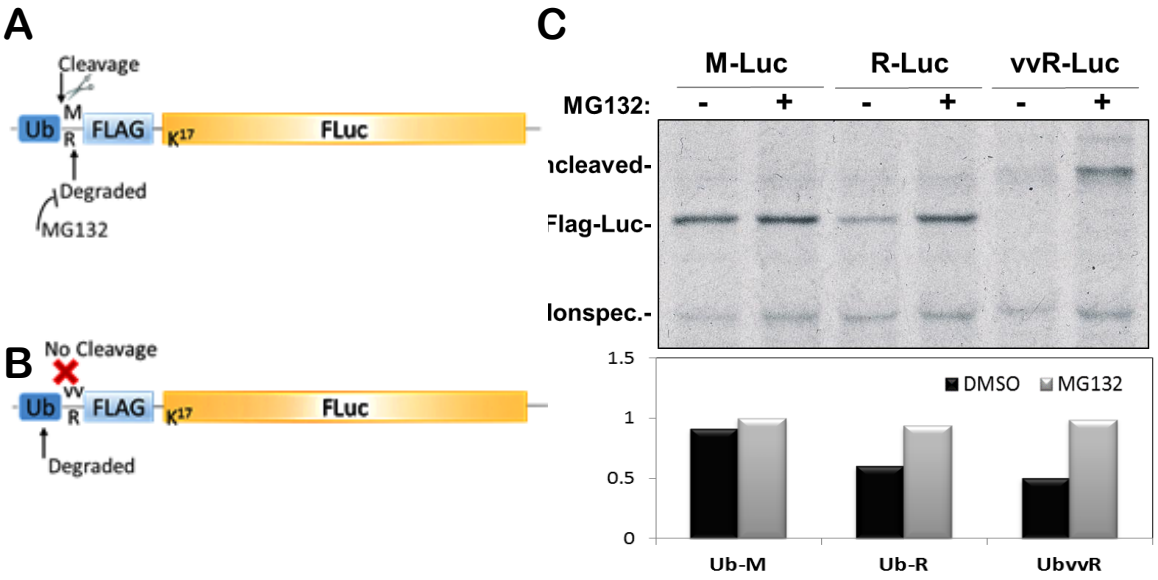

Figure 4-1. **Nascent polypeptides bearing an N-terminal degradation signal are quickly turned over *in vivo*.** (A) Schematic of amino-terminal degradation constructs (degrons) containing a targeted Ub domain followed by the N-end residue for stability, M, or instability, R. Flag allows for construct recognition, while firefly luciferase (FLuc) serves as a protein allowing for multi-Ub chains on Lys-17 (K^{17}) for optimal targeting. (B) Similar to A, though Ub is mutated to prevent cleavage creating a constitutively targeted degron construct. (C) Nascent polypeptides from degron constructs were recognized by pulse-labeling and IP from stably expressed HEK293 cells. MG132 at 20uM was added during pulse to prevent degradation of newly synthesized peptides. *Lower:* Quantification of band intensity to determine percent loss relative to Ub-M+MG.

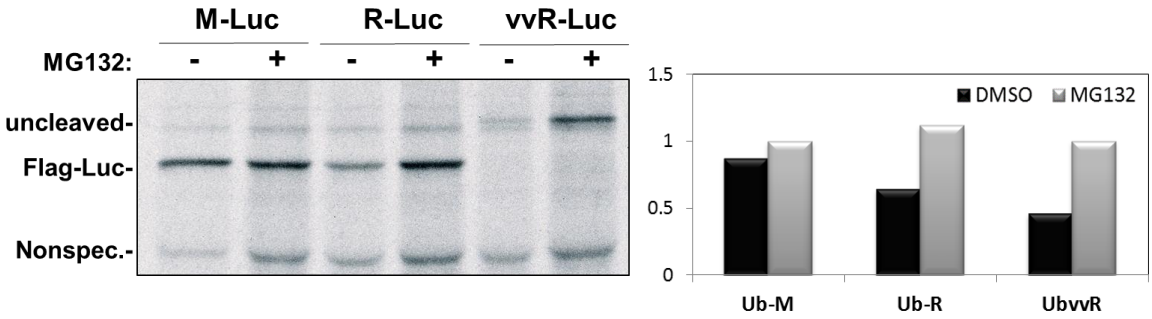

Figure 4-S1. **Nascent polypeptides bearing an N-terminal degradation signal are quickly turned over in MEF cells.** Nascent polypeptides from degron constructs recognized by pulse-labeling and IP from stably expressed WT MEF cells. MG132 at 20uM was added during pulse to prevent degradation of newly synthesized peptides. *Left panel:* Quantification of band intensity to determine percent loss relative to Ub-M+MG.

To verify the co-translational targeting of our degron sequences, we carried out radiolabeling followed by a Flag immunoprecipitation (IP) of our constructs. Cells were treated with or without MG132 to inhibit the proteasome for addressing stability of the nascent polypeptides (Figure 4-1C) and potential co-translational degradation. M-Luc showed an abundance of nascent proteins at the expected size after Ub cleavage, furthermore, MG132 had minimal effects on these stable polypeptides. R-Luc showed a loss of stability when compared to cells treated with MG132, suggesting the protein has a relatively high turnover during the radioactive pulse. The constitutive degron sequence, vvR-Luc, showed a higher molecular weight compared to the other constructs due to the fused mutated Ubvv moiety and had over 50% protein loss (Figure 4-1C). Similar results were also obtained in stable WT MEF cell lines expressing the same degron constructs (Figure 4-S1). The extent of stability loss in each of these constructs suggest that M-Luc indeed is long-lived, though a targeted substrate like UbvvR-Luc remains ubiquinated allowing for longer recognition for degradation co- and post-translation.

Distinguishing the separation of co- vs post-translational regulation requires sequencing of the protein of interest as it is bound by an actively translating ribosome. Ribosome sedimentation alone cannot address this issue due to the accumulation of ribosomal-protein complexes aggregating in granules throughout the cell or empty monosome complexes. For clear separation of co- vs post-translational degradation, we used polysome profiling followed by sequencing, Ribo-seq (Figure 4-2). Monitoring the positions of the ribosome along a given transcript allows for a dynamic reference during protein synthesis using ribosome protected mRNA fragments (RPFs). After collecting polysome fractions from the whole cell lysates, using sucrose sedimentation, we converted

the polysomes to single ribosomes by RNase I digestion. Ribosomes bearing the degron sequence were enriched by IP using anti-Flag mAb-coated beads. Flag tag-associated RPFs as well as total RPF reads from the sample pooled fractions were used to construct a cDNA library for Illumina high-throughput sequencing (Figure 4-2).

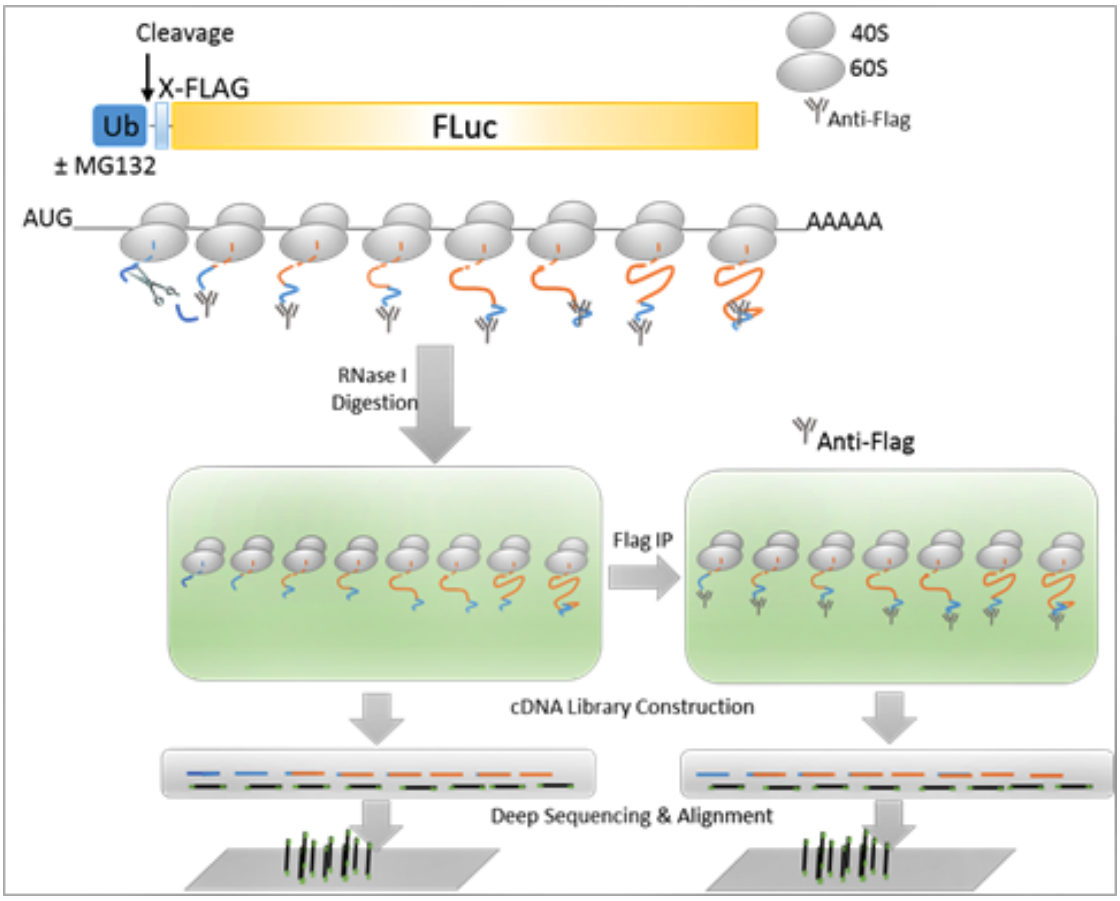

Figure 4-2. **Schematic for Ribo-Seq approach to enrich degron sequence.** Polysomes from HEK293/Ub(X)Flag-Luc cells, where (X) represents M or vvR residues, are converted into monosomes by RNase I digestion. To enrich for the degron sequence an IP with anti-Flag is done in the absence or presence of protein degradation (±MG132). RPFs are extracted for cDNA library construction. Deep sequencing results of RPFs are analyzed by transcriptome mapping.

Consistent with non-uniform mRNA translation rates, there were multiple sites along the Flag-Luc transcripts which showed enhanced RPF reads (Figure 4-3). These peaks may be due to ribosome pausing sites throughout the transcript, as an accurate codon is selected for or as the polypeptide emerges into the cellular environment finding the correct confirmation. The Flag tag presented at the N-terminus also allowed for Flag mAb-association throughout the elongation stages. Alignment of normalized RPF reads on the MFlag-Luc transcript, before and after Flag IP, revealed a similar pattern of ribosome density. As expected, when comparing the percent of ribosome density within a 100-nucleotide window, the RPFs from total reads and IP reads remained in similar ratios throughout the MFlag-Luc and vvRFlag-Luc transcript with only a drop in the first 100 nucleotide region due to Flag mAb capture (Figure 4-3, lower panels).

Alignment of normalized reads on the vvRFlag-Luc transcript from Total and Flag-IP showed a distinct pattern with only slight peak similarities (Figure 3, left panel). Due to the fused Ub moiety in this transcript, it is assumed that the degron sequence is constantly targeted for degradation. If the polypeptide emerges and is bound by additional factors for degradation, this may alter the binding of Flag mAb to the transcript. For example, at nucleotide position 883 there is a high peak that is also at the same location in the total samples, but with a greater pronunciation in the IP reads. When the ribosome reaches this position there may be a conformational rearrangement of the polypeptide allowing for optimal binding with the Flag mAb. This is likely the case due to the pronounced peak in the MFlag-Luc IP as well. Additional variation throughout the transcript, as elongation proceeds, may be due to a loss of reads within the vvRFlag-Luc transcript potentially from co-translational degradation.

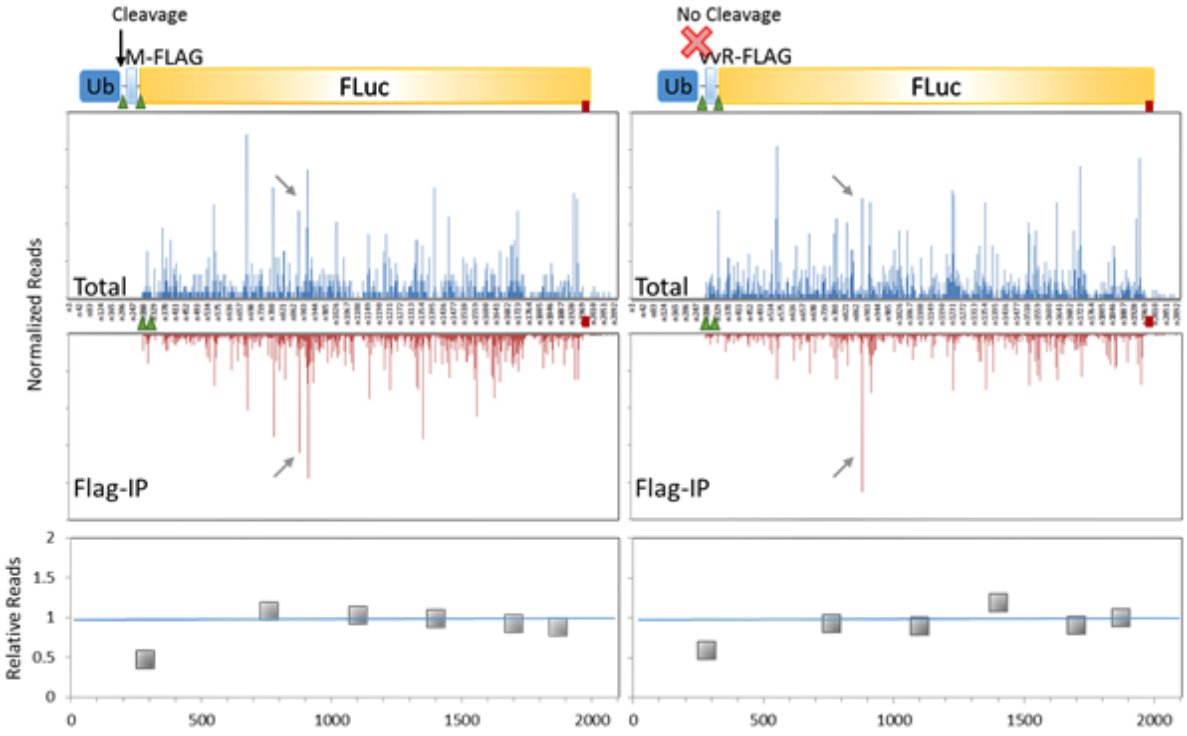

Figure 4-3. **Monitoring co-translational dynamics of degron Flag-Luc constructs in mammalian cells.** Comparison of RPF distribution along Flag-Luc transcript before and after anti-Flag IP. The total and IP reads are aligned based on sequence position of Ub(X)Flag-Luc, where X represents M or R (right and left panel, respectively). The green arrows represent the X location and FLuc start site. The red square represents FLuc stop codon and the nucleotide position at 883 is highlighted by the gray arrows. *Lower*: The RPFs sequence distribution was relatively compared between total and IP reads at six, 100-nucleotide based, windows including the first and last 100 nucleotides in the (X)Flag-Luc transcript as well as four other intra-transcript sequences.

To determine if vvRFlag-Luc is co-translationally degraded, we treated the cells with MG132 at 20uM for one hour before ribosome sedimentation and profiling. This treatment did not create a significant disruption on global translation as viewed by polysome profiles (data not shown). In addition, alignment of normalized RPF reads on the Flag-Luc transcript, before and after Flag IP, revealed a similar pattern of ribosome density that was disrupted in the absence of MG132 (Figure 4-4 compared to Figure 4-3, right panels).

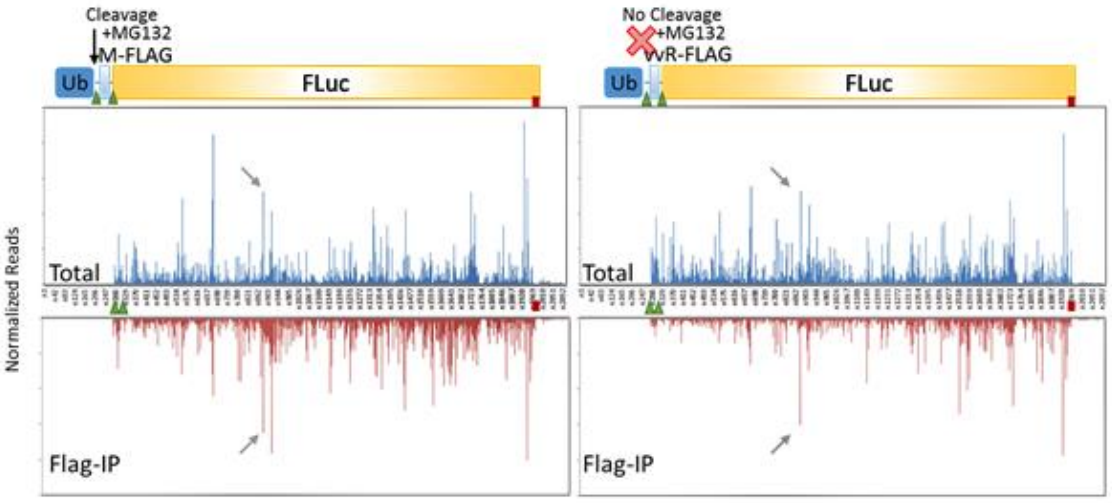

Figure 4-4. **Monitoring co-translational dynamics of degron Flag-Luc constructs with MG132 treatment.** Comparison of RPF distribution along Flag-Luc transcript before and after anti-Flag IP from cells treated with 20 μM MG132. The total and IP reads are aligned based on sequence position of Ub(X)Flag-Luc, where X represents M or R (right and left panel, respectively). The green arrows represent the X location and FLuc start site. The red square represents FLuc stop codon and the nucleotide position at 883 is highlighted by the gray arrows.

If co-translational degradation can occur on a targeted sequence it would lead to a loss of reads throughout the transcript. If the emerging polypeptide is recognized for degradation as it emerges there would also be a lower density of RPFs in the 3'end that could potentially be rescued by the inhibition of the

proteasome. Looking at a 75-nucleotide sliding window, we compared the RFP-density enriched in the Flag-IP with or without MG132 along the Flag-Luc transcript (Figure 4-5). Indeed there was an accumulation of reads in the 3'end of vvRFlag-Luc, though the stable MFlag-Luc showed a constant density with or without MG132. This suggest that vvRFlag-Luc reads can be rescued by inhibiting the proteasome or rather that they are targeted for degradation during synthesis.

Sequence specificity is also required for accurate quality control. An unstable targeted substrate should be recognized for co-translational degradation, while a stable sequence should remain intact. Flag IP enrichment differences between vvRFlag-Luc and MFlag-Luc were then compared in the absence or presence of MG132 (Figure 4-S2). If both transcripts are rescued by MG132 we should see no specificity between the two transcripts, however, an increase would suggest that UbvvR is specifically being targeted; the latter was seen. Furthermore, comparing the presence to the absence of MG132 for each construct and then looking at this rescue effect for sequence specificity gave noticeable results confirming co-translational degradation occurring on the degron construct vvRFlag-Luc (Figure 4-6).

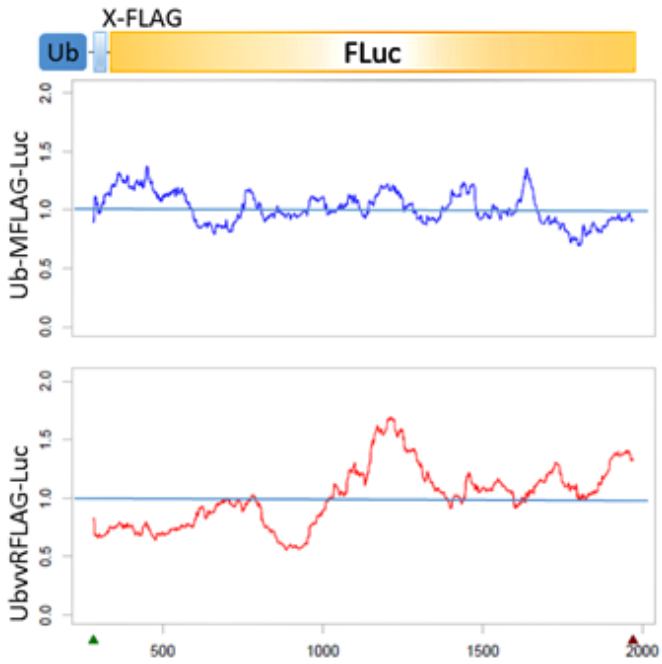

Figure 4-5. **Flag-IP enrichment rescued by MG132.** Pattern analysis of RPF distribution along Flag-Luc transcript before and after MG132 treatment within a 75-nucleotide sliding window. The reads are aligned based on sequence position of Ub(X)Flag-Luc, where X represents M or R (upper and lower panel, respectively). The green arrows represent the X location and the red represents FLuc stop codon.

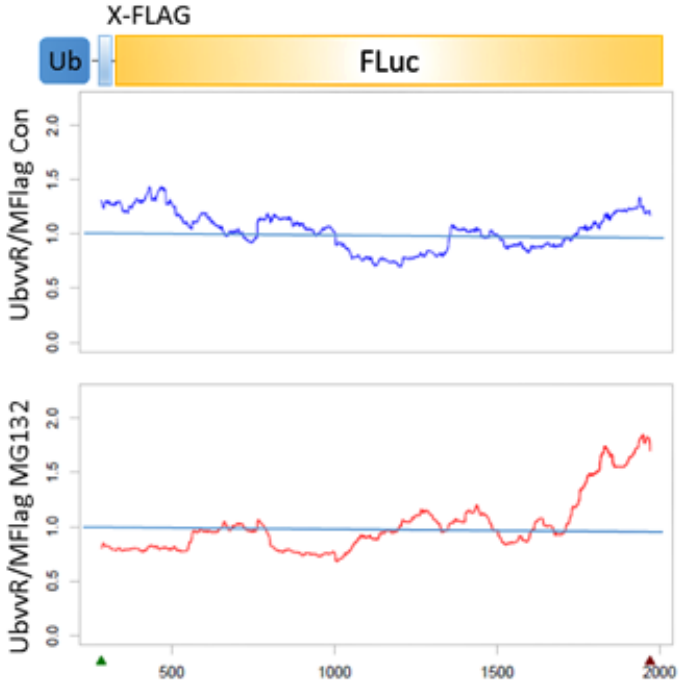

Figure 4-S2. **Flag-IP enrichment for substrate specificity between vvR- and M- Flag-Luc.** Pattern analysis of RPF distribution along Flag-Luc transcript between vvR- and M- Flag-Luc reads with or without MG132 treatment in a 120-nucleotide sliding window. The reads are aligned based on sequence position of Ub(X)Flag-Luc, where X represents M or R residues. The green arrows represent the X location and the red represents FLuc stop codon.

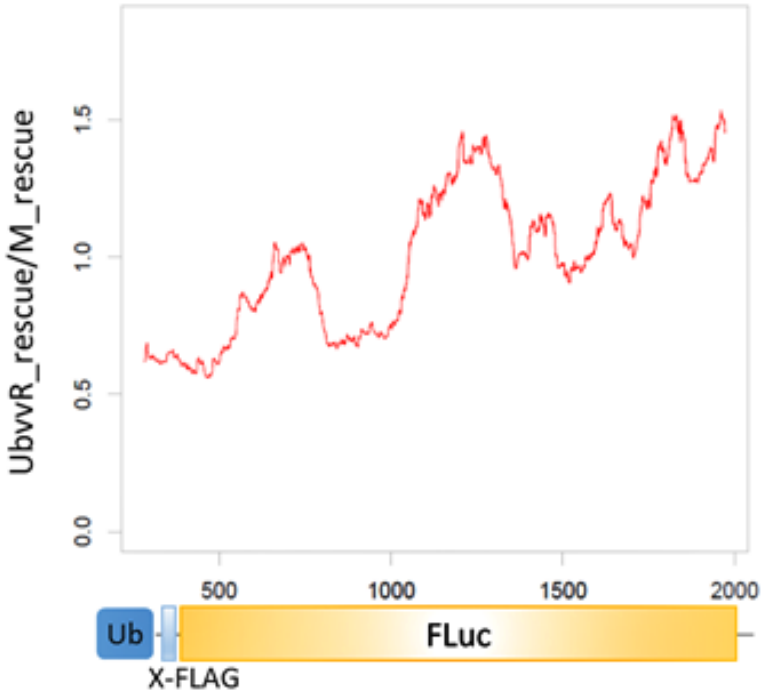

Figure 4-6. **Co-translational degradation shows substrate specificity.** Pattern analysis of RPF distribution along Flag-Luc transcript before and after MG132 treatment compared between vvR- and M-Flag-Luc substrates within a 120-nucleotide sliding window. The reads are aligned based on sequence position of Ub(X)Flag-Luc, where X represents M or R.

4.4 Discussion

Co-translational regulation for quality control is becoming an accepted dogma in the protein homeostasis field. Recent advanced in the past year have confirmed co-translational folding and confirmed co-translational ubiquination assumed to target newly synthesized peptides for degradation (Spencer et al., 2012; Liu et al., 2012; Kirstein-Miles et al., 2013; Duttler et al., 2013; Brandman et al., 2012). However, co-translational degradation *in vivo* has only directly been measured once, over a decade ago (Turner and Varshavsky, 2000). Their work established that ubiquitin targeted substrates, known to be degraded in the cell, have more than 50% co-translationally targeted. Their previous work also characterized substrates targeted for degradation, showing that an Ub target is required, an Ub-targeting specific proteolytic pathway is required, and the substrate targeted must be a minimum length to allow recognition for co-translation targeting (Bachmair and Varshavsky, 1989). Following their criteria, we engineered a degron sequence to accurately observe ribosome dynamics to detect degradation during mRNA translation.

We believe this is the first study to directly examine co-translational degradation on actively translating ribosomes. Using an exogenous degron reporter allowed us to map unique reads to observe a relative loss within the coding sequence, which could be rescued by inhibiting proteasome degradation. We note that the direct measurements of co-translational degradation within our engineered sequences and endogenous short-lived proteins remain to be established, however, our detection with Ribo-Seq shows specificity for a targeted degradation substrate. Looking at various reporters for ribosome-stalling (poly-basic rich regions), induced mis-folding (using mutant proteins or

inducing with AZC-proline-analog), and studying reporters for mistranslation and non-stop mediated decay will lead to a better understanding of co-translational degradation mechanisms. Eventually this technique can also be adapted to study endogenous short-lived proteins to examine their regulation at the ribosome. Overall, we confirm with Ribo-seq that co-translational degradation represents an additional mechanism for quality control necessary for protein homeostasis.

4.5 Materials & Methods

Cells and Reagents—HEK293 and WT MEF cells stably expressing UbMFlag-Luc, UbRFlag-Luc, and UbvvRFlag-Luc were maintained in Dulbecco's modified Eagle's medium (DMEM) with 10% fetal bovine serum (FBS) additionally maintained by selection with Geneticin (Gibco). Anti-Flag M2 affinity gel and IgG-Agarose were purchased from Sigma (A2220 and A0919). TRIzol LS reagent was purchased from Invitrogen.

Plasmids—Ubiquitin(X)Flag sequences were amplified by PCR, where X represents M or R and two reverse primers were utilized to have Ub or mutant Ub(vvR). The sequence was cloned to pcDNA3.1 with HindIII and EcoRV digestion sites. The *firefly luciferase* gene was amplified from PGL3 into the pcDNA3.1/*Ub(X)-Flag* plasmids using EcoRV and XbaI restriction sites. All constructs were validated by sequencing and meticulously checked.

Transfections—Plasmid transfections were initially performed using Lipofectamine 2000 (Invitrogen), according to the manufacturer's instructions.

Radioactive labeling—Cells were quickly centrifuged, media was aspirated, and cells were re-suspended in labeling media with or without 20uM MG132 (methionine free media supplemented with 10% FBS containing 10

μCi/mL [^{35}S] mix (Perkin Elmer)). After 1 hr pulse at 37°C, the samples were added to a pre-chilled Stop buffer (DMEM containing 1 mg/mL cold L-methionine, 1 mg/mL cold L-cystine and 100 μg/mL cycloheximide), centrifuged at 4°C 12,500 rpm for 5 min, and washed two times in ice-cold dPBS supplemented with 1 mg/mL of L-methionine and L-cystine with 100 μg/mL cycloheximide. Samples were re-centrifuged, all wash removed, and pellets stored -20°C till needed.

Radioactive Flag-IP—Pellets from radioactive labeling were lysed in 150 μL ice-cold TBS lysis buffer (50 mM tris-HCl (pH 7.5), 150 mM NaCl, 1 mM EDTA, 100 μg/ml cycloheximide, 2% Triton X-100, and proteasome inhibitor cocktail (Roche)) iced, vortexed, and centrifigued at 4°C 12,500 rpm for 5 min. For IP, 100 uL of sample were mixed with 30 μL of TBS equilibrated anti-Flag M2 affinity gel suspension and incubated at 4 °C for 2 hr rotating, followed by washing three times with TBS buffer, and elution in sample buffer (50 mM tris-HCl (pH 6.8), 100 mM dithiothreitol (DTT), 2% SDS, 0.1% bromophenol blue, 10% glycerol).

Ribosome Profiling—Sucrose solutions were prepared in polysome buffer (10 mM HEPES, pH 7.4, 100 mM KCl, 5 mM MgCl2, 100 μg/ml of cycloheximide, 5 mM DTT, 20 units/ml of SUPERase_In). Sucrose density gradients (15– 45% w/v) were prepared in SW41 ultracentrifuge tubes (Fisher) using a BioComp Gradient Master (BioComp Instruments) according to the manufacturer's instructions. Stable cell lines were pretreated with or without MG132 at 20μM for 1 hr, treated with cycloheximide (100 μg/ml) for 3 min at 37 °C, then lysed in ice-cold polysome lysis buffer (polysome buffer, 2% Triton, ETA-Free protease inhibitor cocktail (Roche), cycloheximide 100 μg/ml, ± MG132 20μM). Lysates were centrifuged 10 min at 12,000 rpm at 4 °C, ~600 μl of supernatant was loaded onto sucrose gradients, followed by centrifugation for 100 min at 38,000 x g at 4

°C in an SW41 rotor. Separate sample gradients were fractionated at 0.75 ml/min using a fractionation system (Isco), which continually monitored OD254 values. Fractions corresponding to 60 s intervals were collected.

Ribosome Purification—Polysome fractions per each sample were pooled together and pre-cleared by incubating the ribosome pooled samples with 30 µL protein IgG agarose pre-coated with 4% BSA for 1 h rotating at 4 °C. From pooled fractions, 300 µL was removed for 'total', and then each sample converted into monosomes using E. coli RNase I (Ambion) (750 U per 100 A260 units) rotating at 4 °C for 1 h. For IP using anti-Flag M2 affinity gel, 30 µL of gel suspension was used per sample first incubated at 4 °C for 1 h with 4% BSA for blocking the beads. The blocked anti-Flag affinity gel was then incubated with the pre-cleared ribosome samples at 4 °C for 1 h during the RNase I digestion, followed by washing with polysome lysis buffer three times. Total RNA extraction was performed by using TRIzol LS reagent according to manufacturer's protocol.

cDNA Library Construction of Ribosome-Protected mRNA Fragment—As explained previously (Han et al, 2012), purified RNA samples were dephosphorylated in a 15 µL reaction containing 1× T4 polynucleotide kinase buffer, 10 U SUPERase_In, and 20 U T4 polynucleotide kinase (NEB). Dephosphorylation was carried out for 1 h at 37 °C, and the enzyme was then heat-inactivated for 20 min at 65 °C. Dephosphorylated samples were mixed with a 2× Novex TBE-Urea sample buffer (Invitrogen) and loaded on a Novex denaturing 15% polyacrylamide TBE-urea gel (Invitrogen). The gel was stained with SYBR Gold (Invitrogen) to visualize RNA fragments. Gel bands containing RNA species corresponding to 25-35 nt were excised and physically disrupted by using centrifugation through the holes of a .5 ml tube within a 1.5 ml tube. RNA fragments were dissolved by soaking overnight in gel elution buffer at 4 °C (300

mM NaOAc, pH 5.5, 1 mM EDTA, 0.1 U/mL SUPERase_In). The gel debris was removed using a Spin-X column (Corning) and RNA was purified by using ethanol precipitation.

Purified RNA fragments were resuspended in 10 mM Tris (pH 8) and denatured briefly at 65 °C for 30 s. Poly-(A) tailing reaction was performed in a 8 µL with 1 × poly-(A) polymerase buffer, 1 mM ATP, 0.75 U/µL SUPERase_In, and 3 U E. coli poly-(A) polymerase (NEB). Tailing was carried out for 45 min at 37 °C. For reverse transcription, the following oligos containing barcodes were synthesized: MCA02, 5′-pCAGATCGTCGGACTGTAGAACTCTCAAGCAGAAGACGGCATACGATTTTTTTTTTTTT TTTTTTTTVN-3′; LGT03, 5′-pGTGATCGTCGGACTGTAGAACTCTCAAGCAGAAGACGGCATACGATT TTTTTTTTTTTTTTTTTTVN-3′; YAG04, 5′-pAGGATCGTCGGACTGTAGAACTCTCAAGCAGAAGACGGCATACGATT TTTTTTTTTTTTTTTTTTVN-3′; HTC05, 5′-pTCGATCGTCGGACTGTAGAACTCTCAAGCAGAAGACGGCATACGATT TTTTTTTTTTTTTTTTTTVN-3′.

Briefly, the tailed RNA product was mixed with 0.5 mM dNTP and 2.5 mM synthesized primer and incubated at 65 °C for 5 min, followed by incubation on ice for 5 min. The reaction mix was then added with 20 mM Tris (pH 8.4), 50 mM KCl, 5 mM MgCl, 10 mM DTT, 40 U RNaseOUT, and 200 U SuperScript III (Invitrogen). RT reaction was performed according to the manufacturer's instructions. RNA was eliminated from cDNA by adding 1.8 µL 1 M NaOH and incubating at 98 °C for 20 min. The reaction was then neutralized with 1.8 µL 1 M HCl. Reverse transcription products were separated on a 10% polyacrylamide TBE-urea gel as described earlier. The extended first-strand product band was

expected to be approximately 100 nt, and the corresponding region was excised. The cDNA was recovered as described above followed by using DNA gel elution buffer overnight (300 mM NaCl, 1 mM EDTA).

First-strand cDNA was circularized in 20 μL of reaction containing 1× CircLigase buffer, 2.5 mM MnCl2, 1 M Betaine, and 100 U CircLigase II (Epicentre). Circularization was performed at 60 °C for 1 h, and the reaction was heat-inactivated at 80 °C for 10 min. Circular single-strand DNA was relinearized with 20 mM Tris-acetate, 50 mM potassium acetate, 10 mM magnesium acetate, 1 mM DTT, and 7.5 U APE 1 (NEB). The reaction was carried out at 37 °C for 1 h. The linearized single-strand DNA was separated on a Novex 10% polyacrylamide TBE-urea gel (Invitrogen). The expected 100-nt product bands were excised and recovered as described above in DNA gel elution buffer overnight. cDNA was extracted and precipitated as described above and resolved in 10 μl of H_2O. Approximately half the cDNA sample was used as a template for PCR amplification using Phusion polyE ( ) with PCR procedure: 98°C 30sec; 98 °C 10 sec, 60 °C 20 sec, 72 °C 10 sec for 11 cycles; 72 °C 10 min. PCR products were separated on a non-denaturing 8% polyacrylamide TBE gel for 1 hr and the expected ~120 bp DNA amplicon excised and recovered overnight once more.

Data Analysis—As previously described (Han et al, 2012), the deep sequencing data of ribosome footprints was processed and analyzed by using a collection of custom Perl scripts. The barcoded multiplex sequencing output files were separated into individual sample datasets according to the first 2-nt barcodes. Second, the 3′ polyA tails allowing one mismatch were identified and removed. After that, the high-quality reads of length ranging from 25-35 nt were retained. The sequences of the longest transcript isoform for each human gene were downloaded from the Ensembl database to construct a human

transcriptome reference. In addition, the plasmid sequence of UbMFlag-Luc and UbvvRFlag-Luc were used as the reference. The 5′ end positions of aligned reads were mapped into the coding frame and the number of reads was counted at each codon ranging from −20 codon 5′ UTR to the stop codon for the downstream analysis.

To compare the RPF distribution on transcript before and after the affinity purification, the reads in the first 30-codon window were considered as the background because the polypeptides are still buried within the ribosome exit tunnel and cannot be accessed. The RPF density vs. background within a sliding window in the pull-down sample was calculated across the transcripts compared with the total sample. Based on the number of reads after the folding start point, the total and pull-down data were normalized to the same scale. The single codon peak ratio was calculated by dividing the normalized reads of pull-down sample to those of total sample at the same codon. The trend line of the single codon peak ratio was determined by locally estimated scatterplot smoothing (LOESS) by using SigmaPlot 11.0 (Systat).

4.6 Acknowledgements

We thank the previous Qian laboratory member Dr. Yan Han for establishing the Ribo-Seq system in our lab, Botao Liu for partial data analysis, Cornell University Life Sciences Core Laboratory Center for performing deep sequencing, and the Stover laboratory at Cornell for equipment accessibility.

CHAPTER 5

Concluding Remarks & Future Endeavors

The balance of protein synthesis, maturation, and degradation has historically been viewed as distinct mechanisms playing a larger part to maintain proteostasis. Researchers that had proclaimed otherwise were questioned for their judgment and ingenuity in experimental design, creating a schism in the field. However, the understanding of the proteostasis network has developed immensely in the past few decades due to the perseverance of a few. Combining historical methodology with bioinformatics and proteomics has answered age-old questions regarding protein regulation. Today, the proteostasis field has acknowledged the interlocking networks providing quality control from the start of mRNA translation through to the polypeptide turn-over, be it co- or post-translational regulation.

Protein synthesis itself is a complex branch of the proteostasis network, combining the translational apparatus, building blocks and energy for production, and selectivity to determine where and when an mRNA will be decoded. The mammalian (or mechanistic) Target of Rapamycin Complex 1 (mTORC1) is the metabolic hub essential for these signaling events. mTORC1 links the cellular environment to ribosome biogenesis, select mRNA recognition, and translation initiation. On one hand, mTORC1 signaling has become infamous for its role in multiple proteostasis diseases including cancer, neurological disorders, and diabetes. On the other hand, a decrease in mTORC1 activity is honored for organismal benefits including stress resistance and lifespan

extension. These alterations have raised many questions including: how could an increase in mTORC1 signaling or rather protein synthesis become detrimental to an organism and how could a decrease in these essential mechanisms become beneficial? By understanding the molecular signaling altered through mTORC1 activity we not only uncover targets to prevent or treat diseases states, but we elucidate the impact protein synthesis has on the proteostasis network from mRNA translation through to protein turn-over.

The work presented here encompasses two main stories focused on understanding the paradox of 'less is more', one regarding unique translation under stress and the other the detrimental effects of an increase in protein synthesis. In chapter 2, I used heat shock to study mTORC1 signaling in a cytosolic stress background. Initially, I naively believed that an increase in mRNA translation might allow for quicker recovery, producing more molecular chaperones necessary during cell stress. However, we discovered that an increase in cap-dependent synthesis attenuated the stress-induced translation of HSP70 eventually leading to cell death. Using real-time luciferase assays, we studied the unique translation through *Hsp70*'s 5'UTR while manipulating mTORC1 activity. Decreasing the PI3K-mTORC1 signaling pathway lead to an increase in HSP70 recovery during stress. Furthermore, we determined that HSP70 could be translated in a cap-independent mechanism unique of the typical IRES and enhanced by decreasing mTORC1 signaling through the downstream target 4E-BP. This suggested a competition between cap-dependent and cap-independent synthesis under stress, while creating a connection between mTORC1 signaling and the chaperone network previously unrecognized.

In Appendix I, I tried to find direct factors regulated downstream of the PI3K-mTORC1 signaling pathway that could influence the switch in protein

synthesis from cap-dependent to cap-independent recognition. I used an mRNA-pulldown of cap- or cap-independent *in vitro* transcribed *Hsp70* mRNA with or without the inhibition of the PI3K-mTORC1 signaling pathway by LY treatment. Unique factors that bound to the mRNA under conditions that would inhibit, activate, or may enhance cap-independent translation based on our previous results in Chapter 2 were selected for and analyzed by mass spectrometry analysis. I pursued the study of one individual helicase protein, DHX30, which bound cap-independent *Hsp70* mRNA with LY treatment, yet was absent in the control condition where *Hsp70* would be repressed. As a helicase protein, we imagined DHX30 bound the 5'UTR of cap-independent transcripts, similar to the helicase eIFA, working to unwind the secondary structures to increase initiation scanning by the 40S ribosomal subunit. Though the results were optimistic, the exact mechanism of DHX30 was not further elucidated nor were the other candidate factors.

Independently, I tried to address cap-independent translation by monitoring ribosomal proteins (RPs) that may or may not play an essential role in a translational switch. The ribosomal complex is created of ~79 RPs, most of which are sequestered to stress granules and aggregates during cell stress. To identify a 'cap-independent' ribosome or RPs with potential extra-ribosomal functions, we individually knocked down each ribosomal protein with a lentiviral system discussed further in Appendix II. Our data confirmed that at least 36 RPs are essential, however, there were many that were knocked down with very little physiological effect on the cells. Using a bi-cistronic luciferase reporter stably expressed in HEK293 cells we monitored cap- and cap-independent translation, but very few knock-downs showed a conclusive reproducible result within our experimental set-up. This may be due to insufficient knockdown or knockdown

levels. One of the proteins, RPL8, consistently showed a unique structural cell morphology during knock-down and was also essential for cell viability. However, knocking down RPL8 increased both cap and cap-independent translation suggesting a regulatory role in monitoring protein synthesis. This protein is further being studied as an independent thesis by my undergraduate students to reproduce our initial findings and uncover a mechanism of action behind the observed phenotypes.

Currently, another member of our lab has successfully identified a stress-induced mitochondria ribosomal protein, mRPL18, that is necessary for HSP70 synthesis and interacts within the cytosolic ribosome in what we are terming a 'stress' ribosome. I used radio-active labeling to monitor global cell recovery when mRPL18 was knocked down and I observed clear attenuation of newly synthesized HSP70 and potentially global recovery. It is hard to determine if the effect is strictly HSP70 related or global due the necessity of HSP70 in cell recovery. It will be interesting to identify other unique factors involved in this selective mRNA translation or stress-induced ribosome complex. Hopefully, by incorporating ribosome sedimentation assays followed by immunoprecipation of mRPL18 within the ribosome, we can identify other factors required for stress-induced translation. I look forward to seeing if any of my previous candidate factors in Appendix I are further validated. Ribo-Seq coupled with immunoprecipitaion, will also provide a more detailed list of mRNA transcripts synthesized through the stress-ribosome showing the relevance of regulation starting from mRNA selection.

In my second story, presented in Chapter 3 and Appendix III, I further try and understand the perplexing relationship between mTORC1 activity and the thought that 'less is more'. Hyperactive mTORC1 signaling universally leads to an

increase in newly synthesized proteins, however, when utilizing reporter proteins I consistently saw less activity with no effect on the mRNA transcript. By inhibiting the proteasome activity I could capture the accumulation of the reporters in the insoluble fractions and there was an increase in global proteins targeted for ubiquitin, suggesting a loss of protein quality. Interestingly, by partially inhibiting mTORC1 with rapamycin or knocking-down mTORC1 components, I decreased the amount of protein made, but could rescue the stable reporters. My work further determined the loss of protein quality was through a decrease in translation fidelity through S6K signaling. Using polysome profiling, I developed a novel way to monitor translation elongation using the drug harringtonin to create screen-shots of polysome run-offs. Hyperactive mTORC1 signaling lead to faster elongation rates, creating a disruption in protein quality control at the ribosome, eventually leading to mistranslation and proteotoxic stress. Rapamycin was able to rescue cell death under proteotoxic stress, slow-down elongation rates, and decrease the fidelity errors. This work created the first molecular explanation for how mTORC1 creates dys-homeostasis during protein synthesis not only by disrupting initiation, but specifically elongation

It would be interesting to monitor which residues or transcript domains are specifically disrupted during hyperactive mTORC1 signaling. For example the 5'TOP mRNA sequence, utilized by RPs, are shown to be highly regulated by mTORC1 activity. If an increase in mTORC1 signaling disrupts protein fidelity, is it due to translational errors in the ribosomal machinery specifically or is it a global effect? Looking further downstream of mTORC1 by directly monitoring S6K signaling will also provide a more direct target to rescue these effects. In Appendix III I show that rapamycin can specifically increase or decrease the

phosphorylation of elongation factor eEF2, a downstream target of S6K, potentially slowing down elongation by sequestering eEF2 will also be beneficial.

One remaining puzzle from studying the effects of hyperactive mTORC1 on protein quality, was the unexplained loss of the protein or quickly degraded proteins. We reasoned that an increase in protein synthesis may be balanced by the proteasome system or may saturate the molecular chaperones, however I saw no direct effects on the activity of either through multiple independent experiments. Additionally, I could never capture the loss of aberrant proteins even using sensitive assays; including pulse-chase. I was able to capture an increase in poly-ubiquination at the ribosomes under an increase in mTORC1 activity, but I couldn't decipher if the nascent polypeptides were modified or the ribosomes directly. We reasoned that the decrease in translation fidelity lead to an increase in co-translational quality control.

In Chapter 4, I set out to explore the debated concept of co-translational degradation. Novel applications including Ribo-Seq give the ability to utilize genome-wide analysis to monitor protein synthesis at single-nucleotide resolution. We utilized this technique, coupled with a domain specific antibody, to determine the exact sequence of ribosome pausing for further identification of co-translational processing *in vivo*. Following the clever design of our predecessors, I engineered an amino-targeted degradation construct allowing us to monitor stable polypeptides in the presence or absence of degradation. We were able to observe co-translational degradation within actively translating ribosomes by comparing specificity of a targeted degron sequence to a stable expressed construct. Utilizing, these methods we can begin to elucidate signaling events promoting or disrupting co-translational quality control.

Here I presented evidence that hyperactive mTORC1 can lead to a global increase in translation, yet the attenuation of stress-regulated translation necessary for cell recovery. Mechanistically, I demonstrated that hyperactive mTORC1 increases translational errors that could be rescued through rapamycin treatment. The increase in protein quantity, through mTORC1 signaling, is at the expense of the protein quality likely favoring disease-related states associated with hyperactive mTORC1. Collectively, my *ex vivo* results used to manipulate mTORC1 activity uncover multiple molecular events highlighting mTORC1 as a key component of the proteostasis network. It seems mTORC1 activity needs to be finely tuned during protein synthesis to produce high quality products and, furthermore, to maintain balance in protein homeostasis especially under stress conditions. Additional *in vivo* research is necessary to understand how mTORC1 effects specific mRNA sequences, what factors are targeted downstream to play additional assistance in quality control, and when this assistance occurs physiologically during development and disease-related states. The research touched upon here provides novel insights into individual and global protein synthesis regulation through mTORC1 signaling, and will shed light on understanding the molecular events in pathological conditions in future studies.

APPENDIX I

PI3K-mTORC1 Regulated Factors for Cap-independent Hsp70 Translation

This work was conducted by Conn CS in 2010 to identify factors that may be involved in cap-independent synthesis and further be regulated by PI3K-mTORC1 signaling. This work was also the basis of her A-exam proposal titled *PI3K-mTOR Signaling Regulates a Translation-Switch to Promote Cell Survival*.

Summary

The regulation of Eukaryotic gene expression allows for protein synthesis to be signaled at unique times required for development and cell survival. The PI3K-mTORC1 pathway plays a pivotal role in this translational regulation as a sensor of the cellular environment; monitoring nutrients, energy and stress conditions. However, it has long been known that under cellular stress some proteins continue to be synthesized though global translation is compromised. It is speculated that mRNAs transcribed during stress recruit distinct RNA-binding factors to confer a preferred translation status, or lack elements promoting repression of protein synthesis (Anderson and Kedersha, 2009). One prominent example is the selective translation of induced heat shock proteins (HSPs).

Our previous results show that stress-induced translation of *Hsp70* is negatively regulated by PI3K-mTORC1 signaling and can be synthesized by a cap-independent mechanism (Chapter 2; Sun et al, 2011). Therefore, if the PI3K-mTORC1 pathway becomes hyperactive the cellular stress response is impaired,

which is known to associate with disease states including inflammation, cancer, and aging (Inoki et al., 2005). We hypothesized that the PI3K-mTORC1 pathway regulates a translational switch to ensure cell survival. To identify factors required for stress induced translation, I completed an mRNA-affinity pull-down under specific parameters followed by mass spectrometry (MS). I began examining the direct interaction of various candidate factors with *Hsp70* mRNA to determine their role in stress induced, cap-independent translation.

The following preliminary results suggest one of the candidate factors, DHX30 (an ATP-dependent DExD/H family RNA helicase), is beneficial for cap-independent translation specifically when PI3K-mTORC1 signaling is inhibited. I was able to validate that DHX30 binds to Hsp70 full mRNA and binding is enhanced when PI3K-mTORC1 is inhibited. Additionally, over expressing a helicase dead mutant of DHX30(AAVH) may compete with endogenous DHX30 to bind *Hsp70* mRNA hampering HSP70 recovery. However, overexpressing WT DHX30 enhanced HSP70 recovery. Using ribosome profiling fractions, I also was able to see DHX30 in fractions corresponding with the 40S, 60S and monosome peaks suggesting a potential role in mRNA recognition or initiation. Additional experiments are required to validate this interaction, as well as other candidate cap-independent translation factors, and the mechanisms involved.

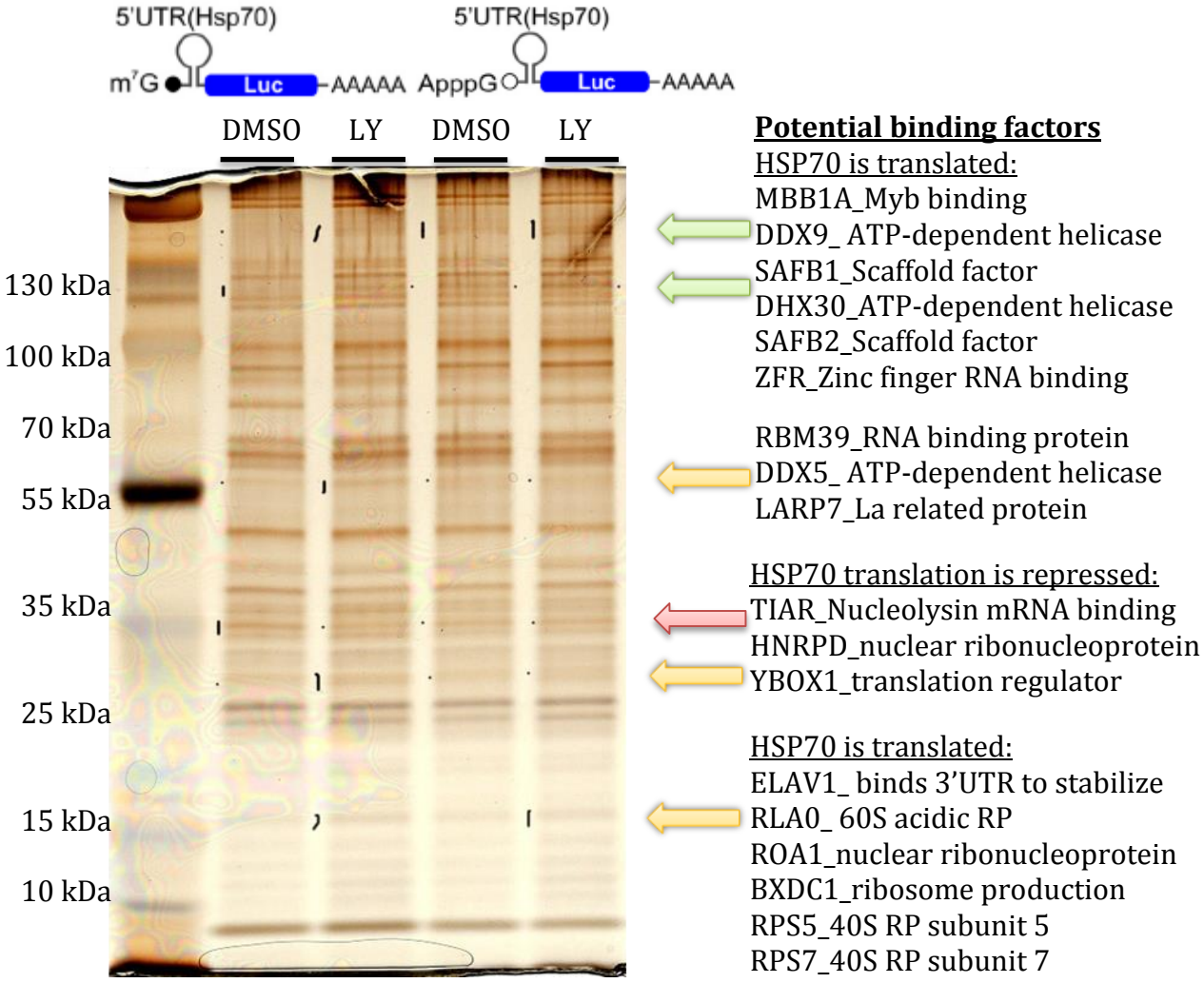

Figure AI-1. **Identification of Hsp70 mRNA candidate binding factors.** A mRNA biotin pulldown assay was performed with TSC2 WT lysates treated with or without LY. Elution was run on acrylamide gel followed by silver staining for unique band identification. Bands of interest are highlighted and were cut and sent to MS for identification. The top hits and potential roles are listed to the right of the stained gel.

Table AI-1. **Candidate Hsp70 mRNA binding factors.** A list of candidate Hsp70 mRNA binding factors with or without LY treatment was compiled from MS identification. mRNA type, treatment, and predicted size are labelled to signify the band cut (Figure A1-1). Factors of the wrong size, likely due to contamination, or with low protein score were removed for simplicity.

TABLE A1-1. CANDIDATE HSP70 MRNA BINDING FACTORS.						
APG- 5'UTR LY TREATED CELLS (BAND ~ 130-200 KDA) –VISUALIZED IN ALL, HIGHEST IN LY						
HIT #	**PROT_ACC**	**PROT_DESCRIPTION**	**SIZE KD**	**SCORE**	**MASS**	**COVER**
2	MBB1A_ MOUSE	Myb-binding protein 1A	152	3500	152854	34.7
7	DHX9_ MOUSE	ATP-dependent RNA helicase A	150	1217	150692	22.5
10	DHX9_ BOVIN	ATP-dependent RNA helicase A	143	691	143223	16
11	MBB1A_ RAT	Myb-binding protein 1A	153	512	153046	10.6
16	VIGLN_ MOUSE	Vigilin - binds HDL	142	435	142225	14.3
31	YTDC2_ HUMAN	Probable ATP-dependent RNA helicase YTHDC2	162	149	161573	4.1
37	RRP12_ MOUSE	RRP12-like protein	144	111	144295	0.8
46	PLCZ1_ MOUSE	1-PI-4,5-bisphosphate phosphodiesterase	75	58	75137	1.2
48	SF3B1_ HUMAN	Splicing factor 3B subunit	146	54	146479	2.7
52	FCSD2_ HUMAN	FCH and double SH3 domains protein	85	39	84737	1.5
54	SMRC1_ HUMAN	SWI/SNF complex subunit SMARCC1	123	38	123303	0.8
APG- 5'UTR LY TREATED CELLS (BAND ~ 100-200 KDA) –VISUALIZED IN M7G-LY, APG-DMSO, AND APG-LY						
HIT #	**PROT_ACC**	**PROT_DESCRIPTION**	**SIZE KD**	**SCORE**	**MASS**	**COVER**
9	ZCH18_ MOUSE	Zinc finger CCCH domain	106	941	105859	22.7
10	CISY_ PIG	Citrate synthase, mitochondrial	105	715	51882	38.8
11	SAFB1_ RAT	Scaffold attachment factor B1	105	643	104960	11.4
14	**DHX30**_ RAT	Putative ATP-dependent RNA helicase	135	589	134997	11.4
15	PYC_ MOUSE	Pyruvate carboxylase, mitochondrial	130	568	130344	13.7
17	DHE3_ HUMAN	Glutamate dehydrogenase 1, mitochondrial	115-180	527	61701	24.9
18	DHE4_	Glutamate dehydrogenase	115-180	471	61689	12.2

	PONPY	2, mitochondrial				
19	SAFB2_ MOUSE	Scaffold attachment factor B2	112	439	112398	9.5
20	ZFR_ MOUSE	Zinc finger RNA-binding protein	118	373	117926	10.2
23	MDHM_ BOVIN	Malate dehydrogenase, mitochondrial	110	214	36102	15.1
26	SMCA5_ MOUSE	SWI/SNF-related matrix-associated regulator	122	180	122291	7.5
28	SR140_ HUMAN	U2-associated protein	120	165	118675	11
30	CPSF1_ MOUSE	Cleavage and polyadenylation factor	160	145	162027	1.9
38	SP16H_ MOUSE	FACT complex subunit	120	96	120320	7.4
39	HNRPU_ HUMAN	Heterogeneous nuclear ribonucleoprotein	91	91	91269	1.8
40	CEBPZ_ MOUSE	CCAAT/enhancer-binding protein	121	89	120928	2.1
42	RC3H1_ MOUSE	Roquin RING ligase, implicated in mRNA translation	126	84	126269	4.5
43	HYOU1_ MOUSE	Hypoxia up-regulated protein	111	83	111340	3.6
45	LARP1_ MOUSE	La-related, appears to bind mRNA	123	80	121476	4.8
47	MBB1A_ MOUSE	Myb-binding protein 1A	153	68	152854	0.8
48	DHX9_ MOUSE	ATP-dependent RNA helicase	151	64	150692	2.2
50	SF3B2_ HUMAN	Splicing factor 3B subunit	98	53	97710	1.4
53	SYLC_ MOUSE	Leucyl-tRNA synthetase, cytoplasmic	134	46	135360	2
M7G- 5'UTR LY TREATED CELLS (BAND ~ 50-100 KDA) –VISUALIZED IN ALL, STRONGEST IN M7G-LY						
HIT #	**PROT_ACC**	**PROT_DESCRIPTION**	**SIZE KD**	**SCORE**	**MASS**	**COVER**
2	RFA1_ MOUSE	Replication protein A 70 kDa	70	3085	69621	44.5
6	RBM39_ PONAB	RNA-binding protein 39	59	1835	58905	45.4
7	HNRPM_ MOUSE	Heterogeneous nuclear ribonucleoprotein	78	1386	77940	22.5
8	NOP56_	Nucleolar protein 56	65	860	64880	28.8

	MOUSE					
11	DDX5_ MOUSE	Probable ATP-dependent RNA helicase	70	590	69790	29
16	LARP7_ MOUSE	La-related protein 7	65	287	65218	13.7
17	SPAS2_ MOUSE	Spermatogenesis-associated serine-rich	60	286	59319	13.8
21	FXR1_ CRIGR	Fragile X mental retardation syndrome-related	70	235	70005	12.2
24	DDX3X_ MOUSE	ATP-dependent RNA helicase	74	216	73455	9.1
25	ELAV1_ HUMAN	ELAV-like protein 1	36	210	36240	7.4
27	IF2B2_ MOUSE	Insulin-like growth factor 2 mRNA-binding	66	170	65657	7.9
29	TKT_MOUSE	Transketolase	68	165	68272	10.8
36	IF2B1_ MOUSE	Insulin-like growth factor 2 mRNA-bindingp	63	122	63753	10.7
38	POTE1_ MOUSE	Protection of telomeres protein	72	90	71902	2.2
39	HNRPQ_ HUMAN	Heterogeneous nuclear ribonucleoprotein	69	90	69788	1.9
46	CPSF6_ BOVIN	Cleavage & polyadenylation specificity factor	60	45	59447	2.5
48	DDX55_ MOUSE	ATP-dependent RNA helicase	69	41	68934	2
50	RIOK2_ MOUSE	Serine/threonine-protein kinase	63	40	62907	4.4
M7G- 5'UTR DMSO TREATED CELLS (BAND ~35- 50 KDA) –VISUALIZED IN ALL, STRONGEST IN M7G-DMSO (INHIBITOR?)						
HIT #	**PROT_ACC**	**PROT_DESCRIPTION**	**SIZE KD**	**SCORE**	**MASS**	**COVER**
2	TIAR_ HUMAN	Nucleolysin TIAR binds mRNA rich in adenine	42	5350	41906	53.9
10	HNRPD_ HUMAN	Heterogeneous nuclear ribonucleoprotein	39	985	38581	31.5
12	TIA1_ MOUSE	Nucleolysin TIA-1 cytotoxic granule-associated	43	724	43115	27.7
14	YBOX1_ BOVIN	regulation of translation between mRNA and eIFs	36	526	35903	34.6
22	RBMS2_ MOUSE	RNA-binding motif, single-stranded-interacting	41	319	40926	16.2

24	ILF2_ HUMAN	Interleukin enhancer-binding factor	43	288	43263	23.1
25	PRS10_ HUMAN	26S protease regulatory subunit, cleave peptides	45	278	44430	12.1
27	LC7L2_ HUMAN	Putative RNA-binding protein Luc7-like	47	232	46942	10.2
28	DC12_ MOUSE	UPF0361 protein DC12 homolog	41	230	40770	25.5
31	SHLB1_ BOVIN	Endophilin-B1, recruit other proteins to membranes	41	171	41037	8.8
34	RL3_MOUSE	60S rp L3	46	154	46380	9.2
35	RL3_BOVIN	60S ribosomal protein L3	46	148	46280	6.9
36	PAWR_ MOUSE	PRKC apoptosis WT1 regulator	36	141	36058	4.8
37	PPID_ MOUSE	40 kDa peptidyl-prolyl cis-trans isomerase	41	132	41116	10
40	THIM_ MOUSE	3-ketoacyl-CoA thiolase	42	113	42288	8.6
45	THIL_ MOUSE	Acetyl-CoA acetyltransferase, mito.	45	85	45129	2.8
46	RPAC1_ MOUSE	DNA-directed RNA polymerases I and III subunit	39	82	39279	7.5
47	RINI_ HUMAN	Ribonuclease inhibitor	51	81	51766	3.3
48	ACADL_ MOUSE	Long-chain specific acyl-CoA dehydrogenase	48	75	48277	2.8
50	PSMD6_ BOVIN	26S proteasome non-ATPase regulatory subunit	46	73	45789	4.6
51	RT27_ MOUSE	28S ribosomal protein S27, mitochondrial	48	73	48220	8
52	CSN3_ BOVIN	COP9 signalosome complex subunit	48	72	48338	2.6
56	RM38_ BOVIN	39S ribosomal protein L38, mitochondrial	45	65	44936	5
57	ROA3_ HUMAN	Heterogeneous nuclear ribonucleoprotein A3	40	65	39799	6.9
60	DJB11_ BOVIN	DnaJ homolog subfamily B member 11	41	60	40764	3.1
62	LUC7L_ HUMAN	Putative RNA-binding protein Luc7-like	44	56	44100	5.7
64	AHSA1_ HUMAN	Activator of 90 kDa heat shock protein ATPase	49	52	38421	3
68	RBMS1_ BOVIN	RNA-binding motif, single-stranded-interacting	44	38	44312	4.7

71	RAD_MOUSE	GTP-binding protein RAD	34	37	33544	3.9
M7G- 5'UTR LY TREATED CELLS (BAND ~ 20-40 KDA) –VISUALIZED IN ALL, STRONGEST IN M7G-LY						
HIT #	**PROT_ACC**	**PROT_DESCRIPTION**	**SIZE KD**	**SCORE**	**MASS**	**COVER**
2	ELAV1_ MOUSE	binds mRNA, Involved in 3'UTR stabilization	36	5134	36217	49.1
3	ELAV1_ HUMAN	ELAV-like protein 1	36	5081	36240	47.2
4	RLA0_ MOUSE	60S acidic RP, neutral phosphoprotein	34	1690	34366	60.6
6	RALY_MOUSE	RNA-binding protein Raly	33	1464	33309	41.7
10	ROA1_BOVIN	Heterogeneous nuclear ribonucleoprotein	34	807	34289	39.7
15	BXDC1_ MOUSE	ribosome production factor 2	35.5	501	35512	25.2
19	RL5_HUMAN	60S ribosomal protein, binds 5S RNA	35	403	34569	37.7
25	RS3_BOVIN	40S ribosomal protein S3	27	349	26842	28.4
26	EF1D_ MOUSE	Elongation factor 1-delta	31	342	31388	30.2
30	RSSA_BOVIN	40S ribosomal protein SA	33	286	32977	12.9
33	RL6_MOUSE	60S ribosomal protein L6	33.3	245	33546	23.6
44	SMN_BOVIN	Survival motor neuron	32	136	31592	4.5
45	PP1G_BOVIN	Serine/threonine-protein phosphatase PP1	38	135	37701	12.7
50	SCAM3_ BOVIN	Secretory carrier-associated membrane protein	38.7	107	38652	4.6
52	IF2A_BOVIN	eIF2 factor 2 subunit 1	36	103	36371	7
60	PSDE_ HUMAN	26S proteasome non-ATPase regulatory subunit	34	78	34726	4.2
61	LRC59_ HUMAN	Leucine-rich repeat-containing protein 59	35	73	35308	7.2
67	CSN5_ HUMAN	COP9 signalosome complex subunit	38	58	37783	3
75	SSRA_BOVIN	Translocon-associated protein subunit alpha	32	44	32034	3.8
76	ZN346_ MOUSE	Zinc finger protein 346	33	43	33361	4.4
78	SYSM_ HUMAN	Seryl-tRNA synthetase, mitochondrial	58	41	58702	1.4
80	NUP37_ MOUSE	Nucleoporin Nup37	37	40	37101	2.1

84	SGTA_MOUSE	Small glutamine-rich tetratricopeptide repeat	34.5	36	34529	2.9
85	PP2AA_BOVIN	Serine/threonine-protein phosphatase 2A	36	35	36142	2.6
M7G- 5'UTR LY TREATED CELLS (BAND ~ 20-30 KDA) –VISUALIZED IN ALL, IN STRONGEST IN LY SAMPLES						
HIT #	**PROT_ACC**	**PROT_DESCRIPTION**	**SIZE KD**	**SCORE**	**MASS**	**COVER**
7	RS5_BOVIN	40S ribosomal protein S5	23	881	23033	37.7
8	RL24_BOVIN	60S ribosomal protein L24	18	691	17882	31.8
9	RS7_BOVIN	40S ribosomal protein S7	22	660	22113	59.8
11	RL21_CAPHI	60S ribosomal protein L21	19	545	18652	36.2
12	RL11_BOVIN	60S ribosomal protein L11	20	504	20468	41
15	SFRS3_BOVIN	Splicing factor, arginine/serine-rich	20	444	19546	39.6
16	RSSA_BOVIN	40S ribosomal protein SA	33	439	32977	12.9
17	RL18A_MOUSE	60S ribosomal protein L18a	21	347	21004	31.8
20	RS9_BOVIN	40S ribosomal protein S9	22.5	326	22635	36.6
21	RL18_MOUSE	60S ribosomal protein L18	21.5	290	21688	22.9
28	ELAV1_HUMAN	ELAV-like protein 1	36	215	36240	7.4
31	RL9_MOUSE	60S ribosomal protein L9	22	177	21982	22.9
35	RLP24_MOUSE	Probable ribosome biogenesis protein RLP24	20	158	19883	16.6
36	RL12_BOVIN	60S ribosomal protein L12	18	142	17979	18.8
40	PSB6_MOUSE	Proteasome subunit beta type-6	25.5	137	25591	13
45	PEBP1_MOUSE	Phosphatidylethanolamine-binding protein 1	21	122	20988	11.2
47	RT25_MOUSE	28S ribosomal protein S25, mitochondrial	20	119	20135	9.9
48	RAB1B_BOVIN	Ras-related protein Rab-1B	22	118	22359	20.9
49	CP080_BOVIN	UPF0468 protein C16orf80 homolog	23	114	22905	11.9
51	ATP5H_MOUSE	ATP synthase subunit d, mitochondrial	18.8	110	18795	16.1
55	RAB7A_CANFA	Ras-related protein Rab-7a	24	97	23790	16.9
62	RAB2A_CANFA	Ras-related protein Rab-2A	24	84	23702	6.6
65	TCTP_MOUSE	Translationally-controlled tumor protein	19.5	70	19564	22.1

69	EIF3K_BOVIN	Eukaryotic translation initiation factor 3 subunit	25	66	25343	5
70	RL17_BOVIN	60S ribosomal protein L17	21.6	64	21611	5.4
72	TI23B_HUMAN	Mito. import inner membrane translocase	28	61	28315	3.9
73	CBX3_HUMAN	Chromobox protein homolog	21	61	20969	7.7
78	ATPO_CALMO	ATP synthase subunit O, mitochondrial	23.4	57	23438	6.6
79	SAR1A_BOVIN	GTP-binding protein SAR1a	22.5	57	22509	15.7
81	RL8_BOVIN	60S ribosomal protein L8	28	53	28235	4.3
82	PSB2_BOVIN	Proteasome subunit beta type-2	23	50	22996	10.4
86	RS11_BOVIN	40S ribosomal protein S11	18.5	46	18590	6.3
89	RAB18_BOVIN	Ras-related protein Rab-18	23	40	23262	5.3
93	RM21_MOUSE	39S ribosomal protein L21, mitochondrial	23	37	23466	5.7

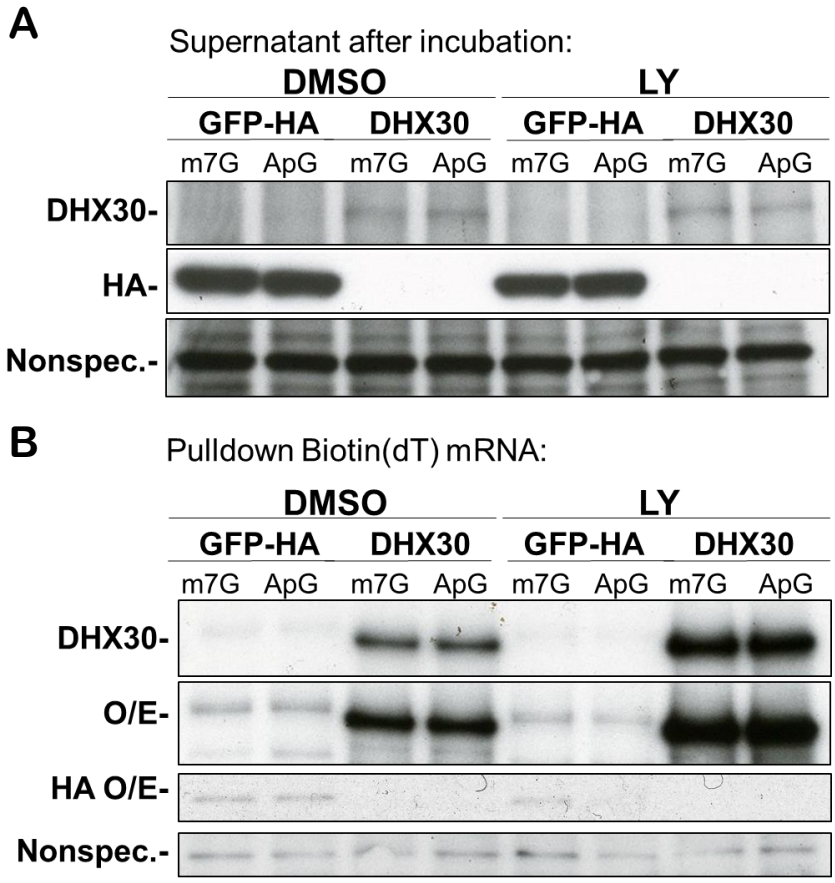

Figure AI-2. **DHX30 binds cap and cap-independent Hsp70 mRNA, enhanced under PI3K-mTORC1 inhibition.** TSC2 WT MEFs were transfected with GFP-HA or DHX30 plasmids for 24 hr followed by DMSO or LY treatment. Cell lysates were then run over a resin with m7G-Full Hsp70 or ApppG-full Hsp70 pre-bound at 4°C for pulldown assay. The supernatant (A) and the eluted mRNA Biotin (dT) binding factors (B) were run by gel electrophoresis and immunoblotted with the indicated antibodies

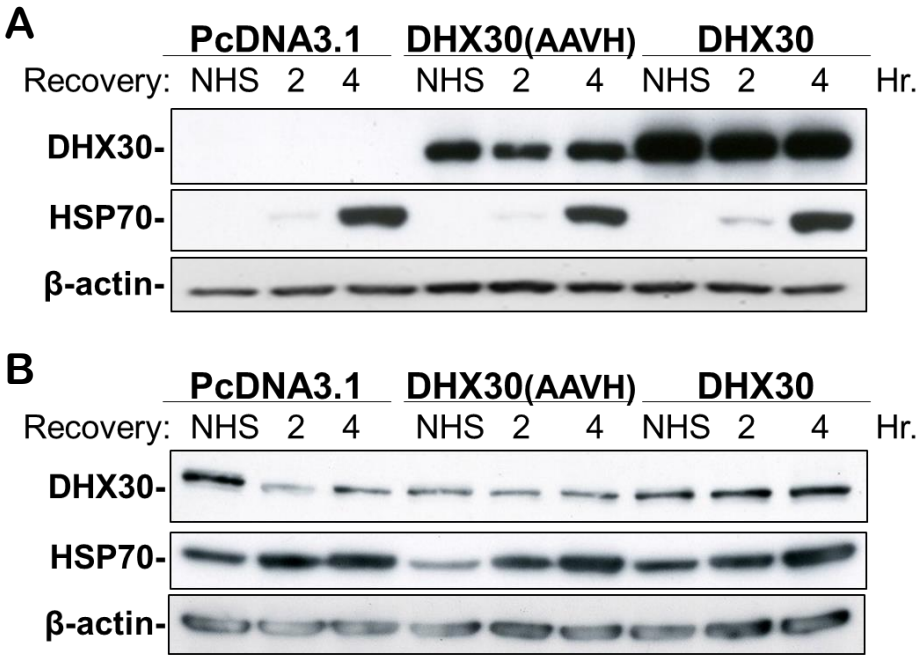

Figure AI-3. **DHX30 overexpression enhances HSP70 translation in recovery, but DHX30(AAVH) attenuates expression.** (A) TSC2 WT MEFs were transfected with empty vector or DHX30 plasmids, one (AAVH) has a catalytically dead helicase, the other WT. After 24 hr, the cells were subjected to 42°C HS 1hr followed by recovery at 37°C for times indicated. Cell lysates were run by gel electrophoresis and immunoblotted with the indicated antibodies. (B) Hela cells were treated as in (A), but HS at 43°C. Note, endogenous DHX30 is also apparent in human cell lysates.

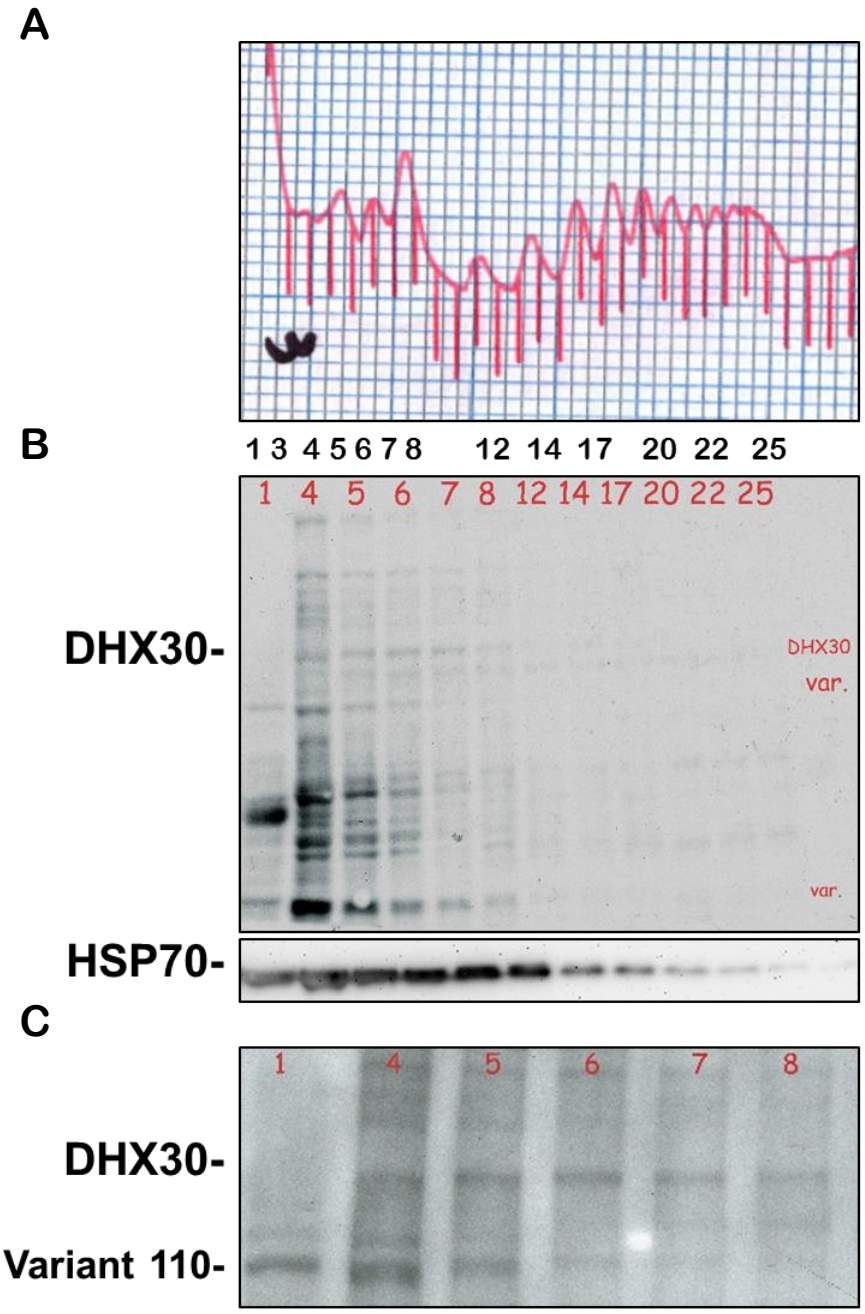

Figure AI-4. **DHX30 interacts at the ribosome potentially for recognition or initiation of mRNA.** (A) A ribosome profile of HEK293 cells under basal condition. Fractions of interest are numbered. (B) Fractions from (A) were immunoblotted with the indicated antibodies, DHX30 to look for correspondence at the ribosome and HSP70 as a positive control. Variant DHX30 bands are marked. (C) Fractions of interest were re-ran to identify DHX30 within the 40S-monosome bound fractions; note the free pool lacks DHX30 showing specificity (lane 1).

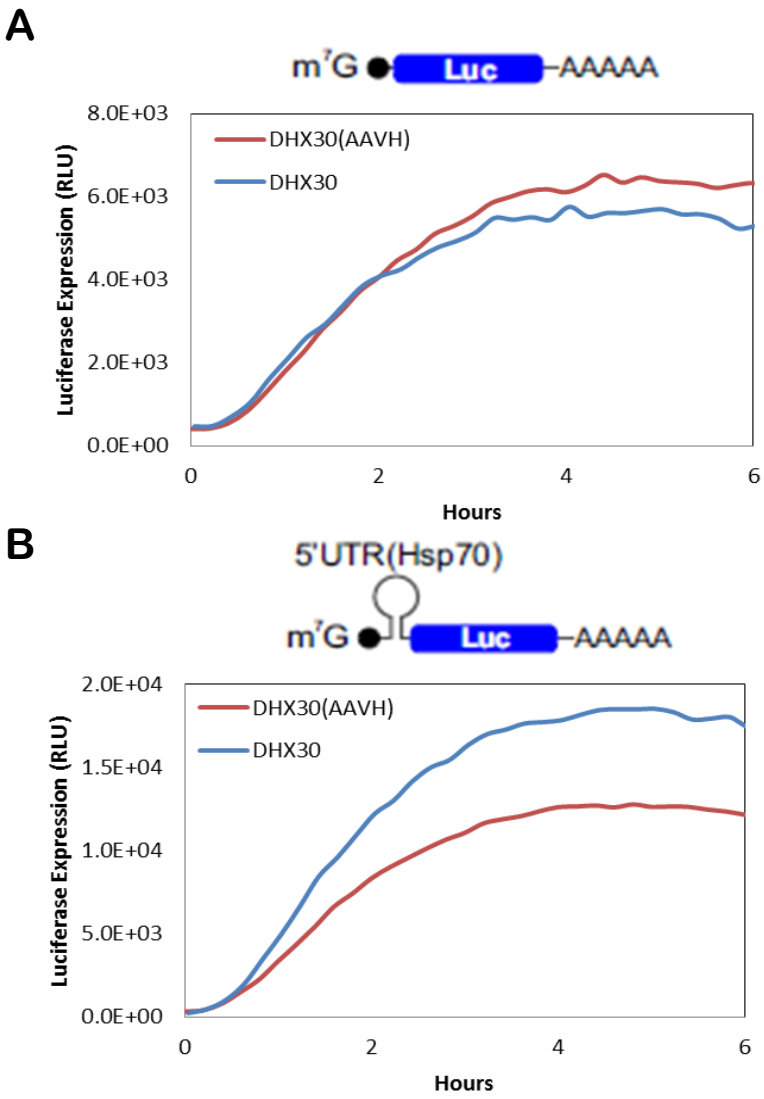

Figure AI-4. **Hsp70 5'-UTR responds to the helicase domain of DHX30. (**A) Luciferase mRNA (Luc) was synthesized using *in vitro* transcription followed by 5' end capping and 3' end polyadenylation. mRNA transfection was performed on TSC2 WT pre-transfected with either DHX30(AAVH) or DHX30 for 24hr. Real time luciferase activity was recorded immediately after mRNA transfection. (B) Luc mRNA containing the 5'UTR of Hsp70 mRNA was transfection and treated as in (A).

APPENDIX II

Screening for Specialized Ribosomes and Potential Extra-ribosomal functions

This work was conducted by Conn CS in 2011-2012 with Haerin Paik and Xiaoxing (Alva) Shen to identify essential ribosomal proteins that may be involved in cap-independent or stress induced translation. Phenotypes were also recorded for potential extra-ribosomal functions.

Summary

mRNA transcripts or rather the "blueprints" of the cell are decoded by the ribosome complex, a massive ribonucleoprotein. The ribosome is composed of four rRNAs –5S, 5.8S, 18S, 28S, ~80 ribosomal proteins (RPs), and additional interacting proteins, which play a role in assembly and stabilization of the complete complex. In mammals, there are 47 large subunit ribosomal proteins (RPL) which associate with the 60S complex and 33 small subunit ribosomal proteins (RPS) which associate with the 40S complex. The 40S subunit is the main regulatory site of protein synthesis functioning to decode the codons of the mRNA, while the 60S ribosomal subunit mediates the peptidyl transferase reaction for elongation.

Ribosomal proteins are tightly regulated group of proteins which sense the status of the cell and act in a coordinated manner (Meyuhas and Perry, 1980). Ribosomal proteins are regulated by many upstream factors as well; one of which is the mammalian target of rapamycin complex 1 (mTORC1), a kinase that promotes cell growth in response to the cellular environment. The fact that ribosomal proteins are fairly well conserved among species with similar size, sequence, and functions

suggests that this regulatory network of genes plays a crucial role in regulation of cell processes and ribosome biogenesis itself

If protein synthesis and ribosome biogenesis are the only functions of RPs then they should be found in equimolar amounts with rRNAs in the cytoplasm, the synthesis site of RPs, and in the nucleolus where RPs are imported from cytoplasm for ribosomal biogenesis. However, the excess and varied levels of RPs suggest that they have extra-ribosomal functions in the cell (Lindstrom, 2009). These function include a wide spectra of events related to cellular homeostasis and viability including cellular apoptosis, mRNA processing, DNA repair, and regulation in transcription. Individual ribosomal proteins also may play distinct roles in translation and the hypothesis of unique ribosomal complexes is also under investigation.

In order to validate and explore the importance of each ribosomal protein on overall cell viability, and to identify new RPs for unique roles in the cell, a ribosomal protein lentiviral shRNA library was constructed to knockdown each ribosomal protein genes. We began our screening by measuring cell viability via a Cell Death Assay (CCK8) and using a bi-cistronic dual-luciferase assay to measure the ratio of cap-dependent to cap-independent translation. RT-PCR was completed to validate knockdown where no phenotype was observed.

Table AII-1. **Cell death assay depicts essential ribosomal proteins knocked down by lentivirus.** A list of RPs monitored on four independent days during knockdown, with biological replicates averaged for the noted value, measure using CCK-8 assay. Cell death was normalized relative to the control scramble sequence knockdown.

	Day5	Day6	Day8	Day10
scramble	100	100	100	100
RPSa	48	3	5	7
RPS2	48	72	58	80
RPS3	57	54	67	37
RPS3A	26	31	48	4
RPS4X	60	57	72	47
RPS4Y	50	39	39	54
RPS5	76	54	41	35
RPS6	95	53	51	22
RPS7	112	137	89	89
RPS8	69	57	24	17
RPS9	66	30	7	14
RPS10	58	41	53	33
RPS11	71	51	34	20
RPS12	95	88	98	74
RPS13	95	101	89	63
RPS14	65	44	23	13
RPS15	85	86	37	12
RPS15A	93	80	55	34
RPS16	64	54	39	20
RPS17	72	80	61	42
RPS18	52	49	19	11
RPS19	92	92	40	19
RPS20	95	99	84	63
RPS21	58	84	14	35
RPS23	77	48	21	10
RPS24	44	57	47	34
RPS25	86	36	31	8
RPS26	50	40	19	13
RPS27	76	82	62	46
RPS27A	72	65	67	29
RPS28	85	62	36	17
RPS29	56	40	20	20
RPS30	85	94	88	49

Very Healthy:80%-100%
Healthy:60%-80%
Average:40%-60%
Dying:20%-40%
Dead 0-20%

	Day5	Day6	Day8	Day10
scramble	100	100	100	100
RPL0	68	56	24	24
RPLP1	112	100	89	80
RPLP2	105	95	65	66
RPL3	82	82	60	62
RPL4	86	82	34	19
RPL5	73	106	53	58
RPL6	87	80	30	11
RPL7	71	59	42	39
RPL7A	78	82	55	22
RPL8	76	42	20	9
RPL9	83	84	76	55
RPL10	72	88	87	70
RPL10A	89	57	55	47
RPL11	106	103	72	54
RPL12	76	89	60	36
RPL13	75	51	51	34
RPL13A	83	83	38	19
RPL14	70	48	41	41
RPL15	71	73	73	71
RPL17	67	83	114	93
RPL18	89	68	65	20
RPL18A	74	109	114	57
RPL19	79	63	54	26
RPL21	95	111	95	50
RPL22	100	106	89	53
RPL23	53	75	21	10
RPL23A	33	22	4	6
RPL24	72	66	50	22
RPL26	77	93	114	46
RPL27	70	39	22	23
RPL27A	75	61	54	51
RPL28	66	72	86	51
RPL29	84	81	70	26
RPL30	73	83	68	47
RPL31	93	75	70	52
RPL32	76	112	93	103
RPL34	75	79	58	45
RPL35	70	86	34	35
RPL35A	71	50	35	16
RPL36	83	56	41	35
RPL36A	69	71	53	18
RPL37	43	29	19	10
RPL37A	80	64	60	26
RPL38	79	72	47	33
RPL39	89	95	108	78
RPL40	55	57	48	32
RPL41	60	59	38	21

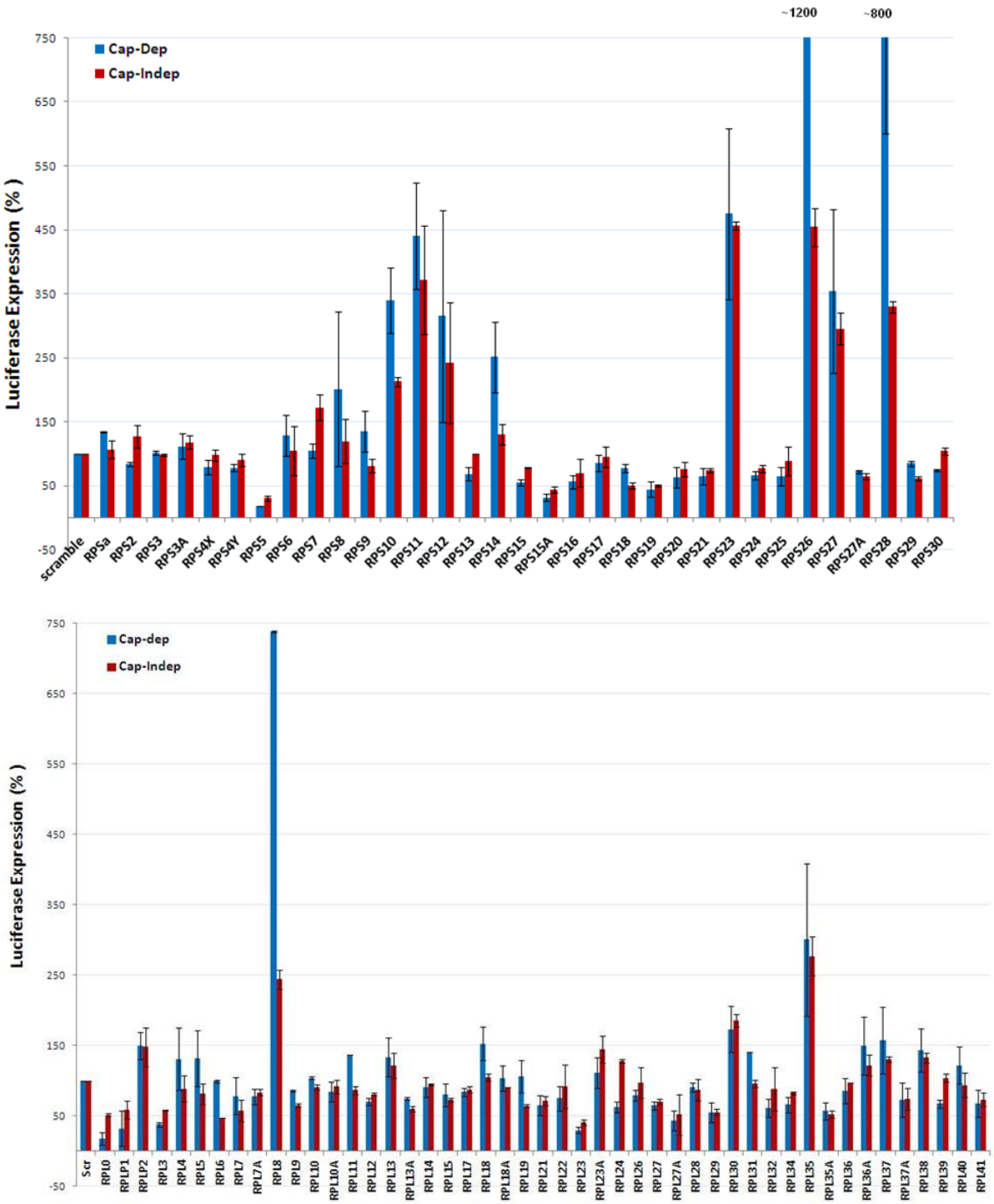

Figure AII-1. **Bi-cistronic dual-luciferase assay monitors cap-dependent and independent translation.** Relative luciferase expression between knockdown RPs and scramble control in a stable dual-luciferase bicistronic HEK293 cell line. *Upper*: small subunit RPs, *lower*: large subunit RPs. n=2

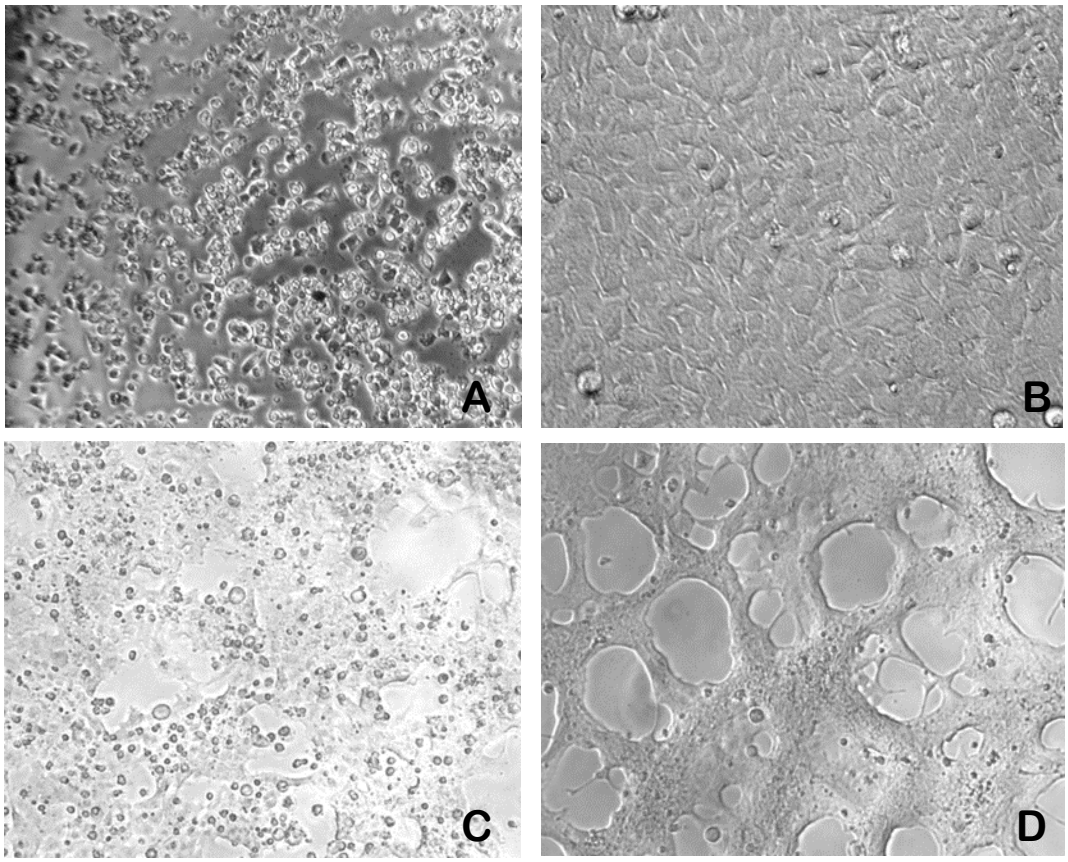

Figure AII-2. **Morphology of specific knockdown HEK293 cells.** (A) Negative control after puromycin selection of lentivirus day 3 (B) Scramble KD after selection day 5 (C) RPL6 KD after selection day 5 (D) RPL8 KD after selection day 5.

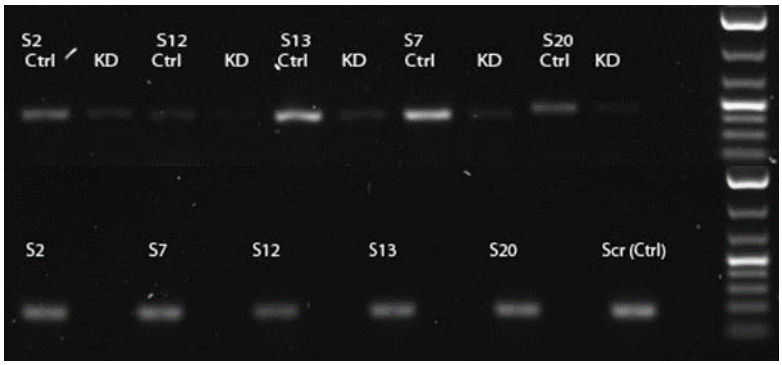

Figure AII-3. **Validating RP knockdown with RT-PCR.** *Upper*: RT-PCR for primers labeled by RPs side by side with PCR from Scramble KD cDNA (left). *Lower*: GAPDH primers for cDNA check and normalization. Analyzed by imageJ to have a 45-95% efficient KD.

APPENDIX III

Hyperactive mTORC1 increase Global Protein Synthesis with No Influence on Half-life, yet an Increase in Co-translational Ubiquination

This work was conducted by Conn CS in 2011-2012 to further characterize hyperactive mTORC1 signaling and the effects on protein synthesis and turnover.

Summary

mTORC1 signaling promotes protein synthesis, but at the expense of protein quality (Chapter 3). To elucidate the mechanism, I monitored various aspects of the proteostasis network in regards to hyperactive mTORC1 signaling. This work was excluded from the main manuscript for simplicity, but added here to answer any lingering concerns.

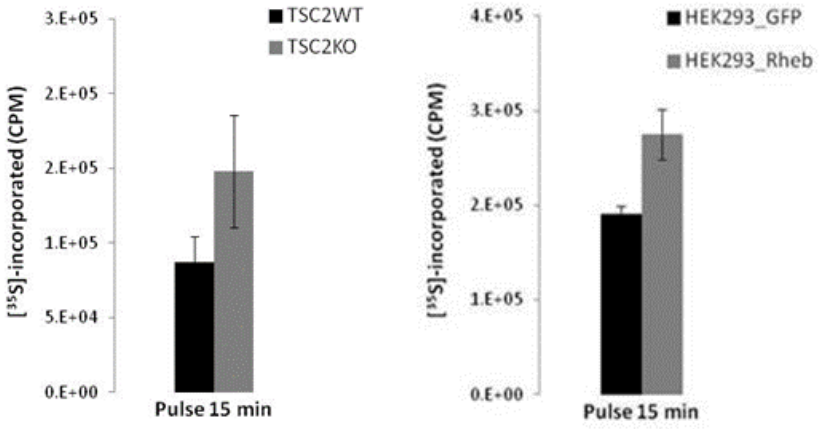

Figure AIII-1. **Hyperactive mTORC1 increases global newly synthesized nascent polypeptides.** *Left*: TSC2 MEFs were radioactive pulsed for 15 min, followed by lysis, and scintillation counting. *Right*: HEK293 cells overexpressing GFP or Rheb for 24 hr were radioactive pulsed for 15 min, followed by lysis, and scintillation counting.

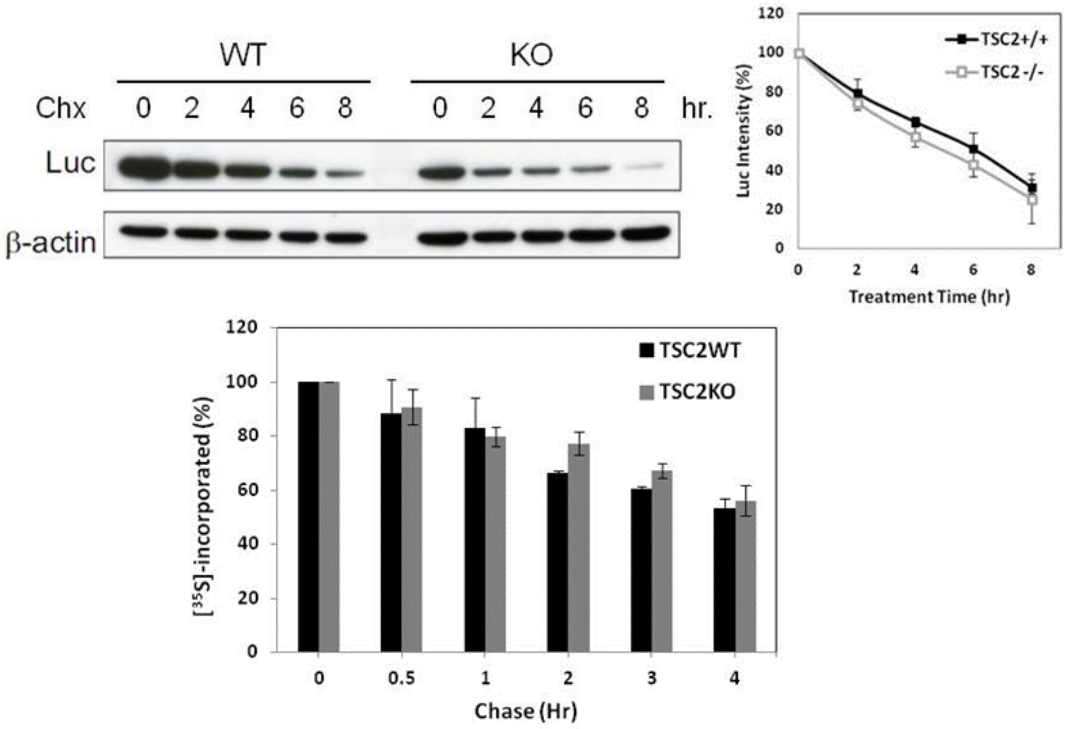

Figure AIII-2. **Hyperactive mTORC1 does not affect Luc protein half-life or global protein turnover.** *Upper left*: TSC2 MEFs expressing Luc were given a cycloheximide chase for the indicated times. *Upper Right*: quantification of Luc half-life ~5 hr (n=3). *Lower:* Radioactive pulse-chase in TSC2 MEFs (n=3).

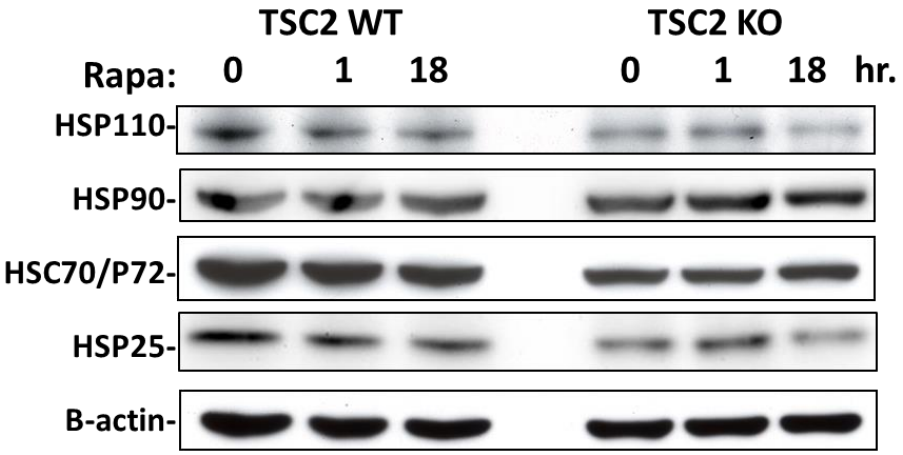

Figure AIII-3. **Molecular chaperone expression is unaffected by mTORC1 activity under basal conditions.** TSC2 MEFs treated with or without rapamycin at 20nM for the indicated times, were immunoblotted as indicated.

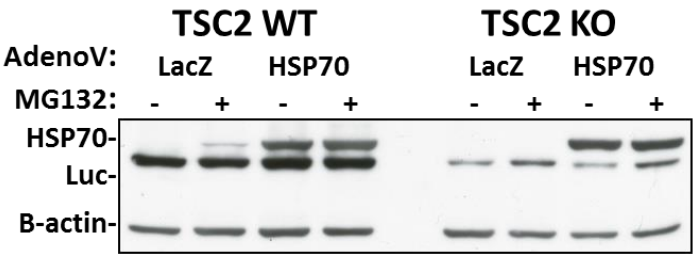

Figure AIII-4. **Overexpressing HSP70 failed to recover stable Luc in TSC2 KO cells.** TSC2 MEFs expressing Luc were treated with or without MG132 at 20 μM with the indicated adenovirus expression. Cell lysates were immunoblotted with the indicated antibodies.

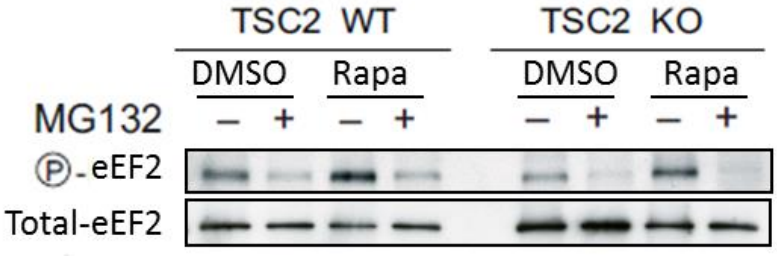

Figure AIII-5. **Hyperactive mTORC1 has a decrease in eEF2 phosphorylation, which releases inhibition for translocation.** TSC2 MEFs treated with or without MG132 at 20 μM and rapamycin 20 nM were immunoblotted with the indicated antibodies.

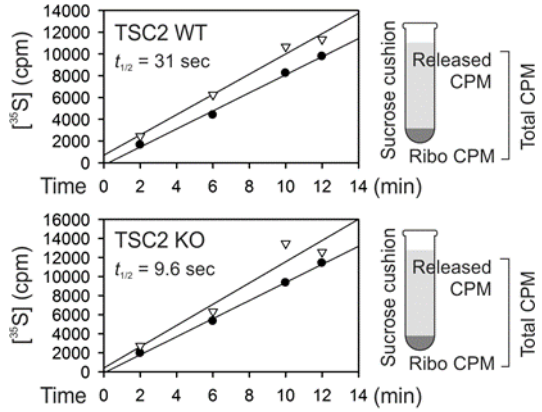

Figure AIII-6. **Hyperactive mTORC1 increases elongation speed measured by transit time.** The measurement of ribosomal half-transit time in TSC2 MEFs. *Open triangle*: total CPM; *black circle*: released CPM

REFERENCES

Anderson P and Kedersha N. (June 2009) RNA granules: post-trascriptional and epigenetic modulators of gene expression. Nature Rev.Mol Cell Bio 10: 430-435.

Andreev DE, Dmitriev SE, Terenin IM, Prassolov VS, Merrick WC, Shatsky IN. (2009). Differential contribution of the m7G-cap to the 5' end-dependent translation initiation of mammalian mRNAs. Nucleic Acids Res. 37 (18): 6135-47.

Averous J and Proud CG. (2006). When translation meets transformation: the mTOR story. Oncogene 25(48): 6423-6435.

Avruch J, Hara K, Lin Y, Liu M, Long X, Ortiz-Vega S, and Yonezawa K. (2006). Insulin and amino-acid regulation of mTOR signaling and kinase activity through the Rheb GTPase. Oncogene 25:6361-6372.

Bukau B, Weissman J, and Horwich A. (2006). Molecular chaperones and protein quality control. Cell 125: 443–451.

Bachmair A, Finley D, and Varshavsky A. (1986). In vivo half-life of a protein is a function of its amino-terminal residue. Science. 234(4773): 179-86.

Bachmair A and Varshavsky A. (1989). The degradation signal in a short-lived protein. Cell. 56(6): 1019-32.

Balch WE, Morimoto RI, Dillin A, and Kelly JW. (2008). Adapting proteostasis for disease intervention. Science 319: 916–919.

Ben-Sahra I, Howell JJ, Asara JM, and Manning BD. (2013). Stimulation of de novo pyrimidine synthesis by growth signaling through mTOR and S6K1. Science 339: 1323–8.

Browne GJ and Proud CG. (2004). A Novel mTOR-Regulated Phosphorylation Site in Elongation Factor 2 Kinase Modulates the Activity of the Kinase and Its Binding to Calmodulin. Molecular and Cellular Biology 24(7): 2986-2997.

Belin S, Beghin A, Solano-Gonzàlez E, Bezin L, Brunet-Manquat S, Textoris J, Prats AC, Mertani HC, Dumontet C, and Diaz JJ. (2009). Dysregulation of ribosome biogenesis and translational capacity is associated with tumor progression of human breast cancer cells. PLoS One. 4(9):e7147.

Bengtson MH and Joazeiro CAP. (2010). Role of a ribosome-associated E3 ubiquitin ligase in protein quality control. Nature 467: 470-473.

Brandman O, Stewart-Ornstein J, Wong D, Larson A, Williams CC, Li GW, Zhou S, King D, Shen PS, Weibezahn J, Dunn JG, Rouskin S, Inada T, Frost A, and Weissman JS. (2012). A ribosome-bound quality control complex triggers degradation of nascent peptides and signals translation stress. Cell. 151 (5): 1042-54.

Brugarolas J, Lei K, Hurley RL, Manning BD, Reiling JH, Hafen E, Witters LA, Ellisen LW, and Kaelin WJ Jr. (2004). Regulation of mTOR function in response to hypoxia by REDD1 and the TSC1/TSC2 tumor suppressor complex. Genes Dev. 18: 2893–2904.

Buchan JR and Stansfield I. (2007). Halting a cellular production line: Responses to ribosomal pausing during translation. Biol. Cell 99: 475–487.

Cabrita LD, Hsu S-TD, Launay H, Dobson CM and Christodoulou J. (2009). Probing ribosome-nascent chain complexes produced in vivo by NMR spectroscopy. Proc Natl Acad Sci. 106: 22239-44.

Chen EJ and Kaiser CA. (2003). LST8 negatively regulates amino acid biosynthesis as a component of the TOR pathway. J. Cell Biol. 161: 333–347.

Choo AY, Yoon SO, Kim SG, Roux PP, and Blenis J. (2008). Rapamycin differentially inhibits S6Ks and 4E-BP1 to mediate cell-type-specific repression of mRNA translation. Proc. Natl. Acad. Sci. U.S.A. 105: 17414–17419.

Chou MM, and Blenis J. (1995). The 70 kDa S6 kinase: regulation of a kinase with multiple roles in mitogenic signalling. Curr.Opin.Cell Biol. 7:806-81425.

Ciryam P, Morimoto RI, Vendruscolo M, Dobson CM, and O'Brien EP. (2013). In vivo translation rates can substantially delay the cotranslational folding of the Escherichia coli cytosolic proteome. Proc. Natl. Acad. Sci. U.S.A. 110(2): E132-40.

Clemens MJ. (2001). Translational regulation in cell stress and apoptosis. Roles of the eIF4E binding proteins. J.Cell Mol.Med. 5:221-239.

Cohen E and Dillin A. (2008). The insulin paradox: aging, proteotoxicity and neurodegeneration. Nature Reviews Neuroscience 9(10): 759-767.

Cohen E, Paulsson JF, Blinder P, Burstyn-Cohen T, Du D, Estepa G, Adame A, Pham HM, Holzenberger M, Kelly JW, Masliah E, Dillin A. Reduced IGF-1 signaling delays age-associated proteotoxicity in mice. (2009). Cell (6): 1157-69.

Conn CS and Qian S-B. mTOR signaling in protein homeostasis: Less is more? (2011). Cell Cycle 10(12): 1940-7.

Conn CS and Qian S-B. Nutrient Signaling in protein homeostasis: increase in protein quantity at the expense of quality. (2013). Science Signaling 6(271): ra24.

Dan HC, Sun M, Yang L, Sui RM, Yeung RS, Halley DJJ, Nicosia SV, Pledger WJ and Cheng JQ. (2002). PI3K/Akt pathway regulates TSC tumor suppressor complex by phosphorylation of tuberin. J. Biol. Chem. 277: 35364–35370.

Dann SG, Selvaraj A, and Thomas G. (2007). mTOR Complex1-S6K1 signaling: at the crossroads of obesity, diabetes and cancer. Trends Mol Med. (6):252-9.

Damgaard CK and Lykke-Andersen J. (2011). Translational coregulation of 5′TOP mRNAs by TIA-1 and TIAR. Genes Dev 25: 2057–2068.

Dibble CC, Elis W, Menon S, Qin W, Klekota J, Asara JM, Finan PM, Kwiatkowski DJ, Murphy LO, and Manning BD. (2012). TBC1D7 is a third subunit of the TSC1-TSC2 complex upstream of mTORC1. Mol Cell 47: 535–546.

Dowling RJ, Topisirovic I, Alain T, Bidinosti M, Fonseca BD, Petroulakis E, Wang X, Larsson O, Selvaraj A, Liu Y, Kozma SC, Thomas G, Sonenberg N. (2010). mTORC1-mediated cell proliferation, but not cell growth, controlled by the 4E-BPs. Science 328(5982): 1172-6.

Duttler S, Pechmann S and Frydman J. (2013). Principles of cotranslational ubiquitination and quality control at the ribosome. Mol. Cell 50(3):379-93.

Fedorov AN and Baldwin TO. (1997). Cotranslational protein folding. J. Biol. Chem. 272: 32715–32718.

Fedyukina DV and Cavagnero S. (2011). Protein folding at the exit tunnel. Annu. Rev. Biophys. 40, 337–359.

Feldman DE and Frydman J. (2000). Protein folding in vivo: the importance of molecular chaperones. Curr Opin Struct Biol. (1): 26-33.

Fontana L. (2009). The scientific basis of caloric restriction leading to longer life. Curr. Opin. Gastroenterol. 25: 144–150.

Foster DA and Toschi A. (2009) Targeting mTOR with rapamycin: one dose does not fit all. Cell Cycle 8:1026-9.

Frias MA, Thoreen CC, Jaffe JD, Schroder W, Sculley T, Carr SA and Sabatini DM. (2006). mSin1 is necessary for Akt/PKB phosphorylation, and its isoforms define three distinct mTORC2s. Curr. Biol. 16, 1865-1870.

Frydman J, Erdjument-Bromage H, Tempst P, and Hartl FU. (1999). Co-translational domain folding as the structural basis for the rapid de novo folding of firefly luciferase. Nat. Struct. Biol. 6: 697–705.

Fuda NJ, Ardehali MB, and Lis JT. (2009). Defining mechanisms that regulate RNA polymerase II transcription in vivo. Nature 461:186-192.

Ghosh HS, McBurney M, Robbins PD. (2010). SIRT1 negatively regulates the mammalian target of rapamycin. PLoS One 5: e9199.

Gingold H and Pilpel Y. (2011). Determinants of translation efficiency and accuracy. Mol Syst Biol. 7:481.

Gingras AC, Raught B, and Sonenberg N. (1999). eIF4 initiation factors: effectors of mRNA recruitment to ribosomes and regulators of translation. Annu. Rev. Biochem. 68:913-963.27.

Goto J, Talos DM, Klein P, Qin W, Chekaluk YI, Anderl S, Malinowska IA, Di Nardo A, Bronson RT, Chan JA, Vinters HV, Kernie SG, Jensen FE, Sahin M, and Kwiatkowski DJ. (2011). Regulable neural progenitor-specific Tsc1 loss yields giant cells with organellar dysfunction in a model of tuberous sclerosis complex. Proc Natl Acad Sci U S A. 108(45):E1070-9.

Guertin DA, Stevens DM, Thoreen CC, Burds AA, Kalaany NY, Moffat J, Brown M, Fitzgerald KJ and Sabatini DM. (2006). Ablation in mice of the mTORC components raptor, rictor, or mLST8 reveals that mTORC2 is required for signaling to Akt-FOXO and PKCalpha, but not S6K1. Dev. Cell 11, 859-871.

Gupta R, Kasturi P, Bracher A, Loew C, Zheng M, Villella A, Garza D, Hartl FU, and Raychaudhuri S. (2011).Firefly luciferase mutants as sensors of proteome stress. Nat. Methods 8: 879–884.

Hahn JS, Hu Z, Thiele DJ, and Iyer VR. (2004). Genome-wide analysis of the biology of stress responses through heat shock transcription factor. Mol.Cell Biol. 24:5249-5256.

Hamilton TL,Stoneley M, Spriggs KA, and Bushell M. (2006). TOPs and their regulation. Biochem. Soc. Trans. 34, 12–16.

Han Y, David A, Liu B, Magadán JG, Bennink JR, Yewdell JW, and Qian S-B. (2012). Monitoring co-translational protein folding in mammalian cells at codon resolution. Proc. Natl. Acad. Sci. U.S.A. 109(31): 12467–12472.

Hannan KM, Brandenburger Y, Jenkins A, Sharkey K, Cava-naugh A, Rothblum L, Moss T, Poortinga G, McArthur GA, Pearson RB, and Hannan RD. (2003). mTOR-dependent regulation of ribosomal gene transcription requires

S6K1 and is mediated by phosphorylation of the carboxy-terminal activation domain of the nucleolar transcription factor UBF. Mol. Cell. Biol. 23:8862–8877.

Hansen M, Taubert S, Crawford D, Libina N, Lee SJ, and Kenyon C. (2007). Lifespan extension by conditions that inhibit translation in Caenorhabditis elegans. Aging Cell 6: 95–110.

Hara K, Yonezawa K, Weng QP, Kozlowski MT, Belham C, and Avruch J. (1998). Amino acid sufficiency and mTOR regulate p70 S6 kinase and eIF-4E BP1 through a common effector mechanism. J. Biol. Chem., 273:14484–14494.

Hara K, Maruki Y, Long X, Yoshino K, Oshiro N, Hidayat S, Tokunaga C, Avruch J, and Yonezawa K. (2002) Raptor, a binding partner of target of rapamycin (TOR), mediates TOR action. Cell 110: 177-189.

Harrison DE, Strong R, Sharp ZD, Nelson JF, Astle CM, Flurkey K, Nadon NL, Wilkinson JE, Frenkel K, Carter CS, Pahor M, Javors MA, Fernandez E, and Miller RA. (2009). Rapamycin fed late in life extends lifespan in genetically heterogeneous mice. Nature. 460(7253):392-5.

Hartl FU and Hayer-Hartl M. (2009). Converging concepts of protein folding in vitro and in vivo. Nat Struct Mol Biol. 16, 574-581.

Hartl FU, Bracher A, and Hayer-Hartl M. (2011). Molecular chaperones in protein folding and proteostasis. Nature 475: 324–332.

Hay N and Sonenberg N. (2004). Upstream and downstream of mTOR. Genes Dev. 18:1926-1945.

Heublein S, Kazi S, Ögmundsdóttir MH, Attwood EV, Kala S, Boyd CAR, Wilson C, and Goberdhan DCI. (2010). Proton-assisted amino-acid transporters are conserved regulators of proliferation and amino-acid-dependent mTORC1 activation. Oncogene 29, 4068–4079.

Hipkiss AR. (2006). Accumulation of altered proteins and ageing: Causes and effects. Experimental Gerontology 41(5): 464-473.

Hipkiss AR. (2007). On why decreasing protein synthesis can increase lifespan. Mech. Ageing Dev. 128: 412–414.

Hipkiss AR. (2008). Error-protein metabolism and ageing. Biogerontology 10(4): 523-529.

Holcik M and Sonenberg N. (2005). Nat. Rev. Mol. Cell. Biol. 6, 318–327.

Holz MK, Ballif BA, Gygi SP, and Blenis J. (2005). mTOR and S6K1 mediate assembly of the translation preinitiation complex through dynamic protein interchange and ordered phosphorylation events. Cell 123: 569-80.

Hsieh AC, Liu Y, Edlind MP, Ingolia NT, Janes MR, Sher A, Shi EY, Stumpf CR, Christensen C, Bonham MJ, Wang S, Ren P, Martin M, Jessen K, Feldman ME, Weissman JS, Shokat KM, Rommel C, and Ruggero D. (2012). The translational landscape of oncogenic mTOR signaling controls distinct cancer cell behaviors including metastasis. Nature 485(7396):55-61.

Hsu AL, Murphy CT, and Kenyon C. (2003). Regulation of aging and age-related disease by DAF-16 and heat-shock factor. Science 300:1142-1145.

Huang J. and Manning BD. (2008). The TSC1–TSC2 complex: A molecular switchboard controlling cell growth. Biochem. J. 412: 179–190.

Ingolia NT, Ghaemmaghami S, Newman JR and Weissman JS. (2009). Genome-wide analysis in vivo of translation with nucleotide resolution using ribosome profiling. Science 324: 218–213.

Inoki K, Li Y, Zhu T, Wu J and Guan KL. (2002). TSC2 is phosphorylated and inhibited by Akt and suppresses mTOR signalling. Nat. Cell Biol. 4:648-657.

Inoki K, Corradetti MN and Guan KL. (2005) Dysregulation of the TSC-mTOR pathway in human disease. Nat.Genet. 37:19-24.

Inoki K and Guan KL. (2006). Complexity of the TOR signaling network. Trends Cell Biol. 16:206-212.

Inoki K, Ouyang H, Zhu T, Lindvall C, Wang Y, Zhang X, Yang Q, Bennett C, Harada Y, Stankunas K, Wang CY, He X, MacDougald OA, You M, Williams BO, and Guan KL. (2006). TSC2 integrates Wnt and energy signals via a coordinated phosphorylation by AMPK and GSK3 to regulate cell growth. Cell 126: 955-968.

Jackson RJ, Hellen CU, and Pestova TV. (2010). The mechanism of eukaryotic translation initiation and principles of its regulation. Nat.Rev.Mol.Cell Biol. 11, 113-127.

Jaiswal H, Conz C, Otto H, Wölfle T, Fitzke E, Mayer MP, and Rospert S. (2011). The Chaperone Network Connected to Human Ribosome-Associated Complex. Mol. Cell. Biol. (6):1160-73.

Jewell JL and Guan KL. (2013). Nutrient signaling to mTOR and cell growth. Trends Biochem Sci. (5):233-42.

Johannes G and Sarnow P. (1998). Cap-independent polysomal association of natural mRNAs encoding c-myc, BiP, and eIF4G conferred by internal ribosome entry sites. RNA 4(12):1500-13.

Kaeberlein M, Powers RW III, Steffen KK, Westman EA, Hu D, Dang N, Kerr EO, Kirkland KT, Fields S, and Kennedy BK. (2005). Regulation of yeast replicative life span by TOR and Sch9 in response to nutrients. Science 310: 1193–1196.

Kapahi P, Zid BM, Harper T, Koslover D, Sapin V, and Benzer S. (2004). Regulation of lifespan in Drosophila by modulation of genes in the TOR signaling pathway. Curr. Biol. 14: 885–890.

Kapahi P, Chen D, Rogers AN, Katewa SD, Li PW, Thomas EL, and Kockel L. (2010). With TOR, less is more: A key role for the conserved nutrient-sensing TOR pathway in aging. Cell Metab. 11: 453–465.

Kenyon C. (2005). The plasticity of aging: Insights from long-lived mutants. Cell 120: 449–460.

Kim DH, Sarbassov DD, Ali SM, King JE, Latek RR, Erdjument-Bromage H, Tempst P and Sabatini D.M. (2002). mTOR interacts with raptor to form a nutrient-sensitive complex that signals to the cell growth machinery. Cell 110: 163-175.

Kirstein-Miles J, Scior A, Deuerling E, and Morimoto RI. (2013). The nascent polypeptide-associated complex is a key regulator of proteostasis. EMBO J. 32(10):1451-68.

Kirkwood TB, Holliday R, and Rosenberger RF. (1984). Stability of the Cellular Translation Process. 92: 93-132.

Klemenz R, Hultmark D, and Gehring WJ. (1985). Selective translation of heat shock mRNA in Drosophila melanogaster depends on sequence information in the leader. EMBO J. 4(8):2053-60.

Koga H, Kaushik S and Cuervo AM. (2011). Protein homeostasis and aging: The importance of exquisite quality control. Ageing Research Reviews 10(2): 205-215.

Komar AA. (2009). A pause for thought along the co-translational folding pathway. Trends Biochem Sci.34 (1), 16–24.

Kramer G, Boehringer D, Ban N, and Bukau B. (2009). The ribosome as a platform for co-translational processing, folding and targeting of newly synthesized proteins. Nat Struct Mol Biol. 16, 589-597.

Kwiatkowski DJ and Manning BD. (2005).Tuberous sclerosis: A GAP at the crossroads of multiple signaling pathways. Hum. Mol. Genet. 14: R251–R258.

Laplante M and Sabatini DM. (2012). mTOR signaling in growth control and disease. Cell 149: 274–293.

Levinthal C. (1968). Are there pathways for protein folding? J.Chim.Phys. 65:44–5.

Li H, Tsang CK, Watkins M, Bertram PG, and Zheng XF. (2006). Nutrient regulates Tor1 nuclear localization and association with rDNA promoter. Nature. 442(7106):1058-61.

Li S, Sonenberg N, Gingras AC, Peterson M, Avdulov S, Polunovsky VA, and Bitterman PB. (2002). Translational control of cell fate: availability of phosphorylation sites on translational repressor 4E-BP1 governs its proapoptotic potency. Mol. Cell Biol. 22:2853-2861.

Lindstorm MS. (2009). Emerging functions of ribosomal proteins in gene-specific transcription and translation. Biochem. Biophys. Res. Commun. 379: 167–170.

Lindquist S and Craig EA. (1988). The heat-shock proteins. Annu. Rev. Genet. 22:631-677.

Liu B, Han Y, and Qian S-B. (2012). Cotranslational response to proteotoxic stress by elongation pausing of ribosomes. Mol Cell 49: 453–463.

Liu B, Conn CS, and Qian S-B. (2012). Viewing folding of nascent polypeptide chains from ribosomes. Expert Rev Proteomics 9(6):579-81.

Loewith R, Jacinto E, Wullschleger S, Lorberg A, Crespo JL, Bonenfant D, Oppliger W, Jenoe P, and Hall MN. (2002). Two TOR complexes, only one of which is rapamycin sensitive, have distinct roles in cell growth control. Mol. Cell 10: 457-468.

Long X, Ortiz-Vega S, Lin Y, and Avruch J. (2005). Rheb binding to mammalian target of rapamycin (mTOR) is regulated by amino acid sufficiency. J Biol Chem. Jun 24; 280(25):23433-6.

Lu ZH, Shvartsman MB, Lee AY, Shao JM, Murray MM, Kladney RD, Fan D, Krajewski S, Chiang GG, Mills GB, and Arbeit JM. (2010). "Mammalian Target of Rapamycin Activator RHEB Is Frequently Overexpressed in Human Carcinomas and Is Critical and Sufficient for Skin Epithelial Carcinogenesis." Cancer Research 70(8): 3287-3298.

Ma L, Chen Z, Erdjument-Bromage H, Tempst P and Pandolfi PP. (2005). Phosphorylation and functional inactivation of TSC2 by Erk: implications for tuberous sclerosis and cancer pathogenesis. Cell 121, 179–193.

Ma XM and Blenis J. (2009). Molecular mechanisms of mTOR-mediated translational control. Nat. Rev. Mol. Cell Biol. 10, 307-318.

Malik AR, Urbanska M, Macias M, Skalecka A, and Jaworski J. (2012). Beyond control of protein translation: What we have learned about the non-canonical regulation and function of mammalian target of rapamycin (mTOR). Biochim Biophys Acta.

Mathews MB, Sonenberg N, and Hershey JWB. (2002). Origins and principles of translational control. *Translational Control of Gene Expression*. 1-31. CSHL press.

Mayer C, Zhao J, Yuan X, and Grummt I. (2004). mTOR-dependent activation of the transcription factor TIF-IA links rRNA synthesis to nutrient availability. Genes Dev. 18: 423–434.

Mayer MP, Brehmer D, Gässler CS, and Bukau B. (2001). Hsp70 chaperone machines. Adv Protein Chem. 59:1-44.

Meyuhas O and Perry RP. (1980). Construction and identification of cDNA clones for mouse ribosomal proteins: application for the study of r-protein gene expression, Gene 10: 113–129.

McCay CM, Crowell MF, and Maynard LA. (1989). The effect of retarded growth upon the length of life span and upon the ultimate body size. 1935. Nutrition 5: 155–171.

McClellan AJ, Tam S, Kaganovich D, and Frydman J. (2005). Protein quality control: chaperones culling corrupt conformations. Nat Cell Biol 7(8):736-41.

McGarry TJ and Lindquist S. (1985). The preferential translation of Drosophila hsp70 mRNA requires sequences in the untranslated leader. Cell 42:903-911. 45.

Meriin AB, Mense M, Colbert JD, Liang F, Bihler H, Zaarur N, Rock KL, Sherman MY. (2012). A novel approach to recovery of function of mutant proteins by slowing down translation. J Biol Chem. 287(41):34264-72.

Morimoto RI. (1998). Regulation of the heat shock transcriptional response: cross talk between a family of heat shock factors, molecular chaperones, and negative regulators. Genes Dev. 12: 3788-379626.

Morimoto RI. (2008). Proteotoxic stress and inducible chaperone networks in neurodegenerative disease and aging. Genes Dev. 22: 1427–1438.

Morimoto RI and Cuervo AM. (2009). Protein Homeostasis and Aging: Taking Care of Proteins from the Cradle to the Grave. The Journals of Gerontology Series A: Biological Sciences and Medical Sciences 64A (2): 167-170.

Morley JF and Morimoto RI. (2004). Regulation of longevity in Caenorhabditis elegans by heat shock factor and molecular chaperones. Mol.Biol.Cell 15:657-664.

Moseley PL, Wallen ES, McCafferty JD, Flanagan S, and Kern JA. (1993). Heat stress regulates the human 70-kDa heat-shock gene through the 3'-untranslated region. Am. J. Physiol 264:L533-L537.

Mosser DD, Caron AW, Bourget L, Meriin AB, Sherman MY, Morimoto RI, and Massie B. (2000). The chaperone function of hsp70 is required for protection against stressinduced apoptosis. Mol.Cell Biol. 20:7146-7159.

Neef DW and Thiele DJ. (2009). Enhancer of decapping proteins 1 and 2 are important for translation during heat stress in Saccharomyces cerevisiae. Mol. Microbiol. 73:1032-1042.

O'Brien EP, Vendruscolo M, and Dobson CM. (2012). Prediction of variable translation rate effects on cotranslational protein folding. Nat Commun. 3:868.

Oh WJ and Jacinto E. (2011). mTOR complex 2 signaling and functions, Cell Cycle. 10: 2305–2316.

Orgel LE. (1963). The maintenance of the accuracy of protein synthesis and its relevance to aging. Proc. Natl. Acad. Sci. U.S.A. 49: 517-21.

Ozcan U, Ozcan L, Yilmaz E, Duvel K, Sahin M, Manning BD and Hotamisligil GS. (2008). Loss of the tuberous sclerosis complex tumor suppressors triggers the unfolded protein response to regulate insulin signaling and apoptosis. Mol. Cell 29:541-551.

Pan KZ, Palter JE, Rogers AN, Olsen A, Chen D, Lithgow GJ, and Kapahi P. (2007). Inhibition of mRNA translation extends lifespan in Caenorhabditis elegans. Aging Cell 6(1): 111-119.

Panniers R. (1994). Translational control during heat shock. Biochimie 76, 737–747.

Parsell DA and Lindquist S. (1993). The function of heat-shock proteins in stress tolerance: degradation and reactivation of damaged proteins. Annu Rev Genet. 27: 437-96.

Pearce LR, Huang X, Boudeau J, Pawlowski R, Wullschleger S, Deak M, Ibrahim A, Gourlay R, Magnuson MA, and Alessi DR. (2007). Identification of Protor as a novel Rictor-binding component of mTOR-complex-2, Biochem. J. 405: 513–522.

Pechmann S, Willmund F, and Frydman J. (2013). The ribosome as a hub for protein quality control. Mol Cell. 49(3): 411-21.

Pelletier J and Sonenberg N. (1988). Internal initiation of translation of eukaryotic mRNA directed by a sequence derived from poliovirus RNA. Nature 334: 320-325.

Pende M, Um SH, Mieulet V, Sticker M, Goss VL, Mestan J, Mueller M, Fumagalli S, Kozma SC, and Thomas G. (2004). S6K1(-/-)/S6K2(-/-) mice exhibit perinatal lethality and rapamycin-sensitive 5'-terminal oligopyrimidine mRNA translation and reveal a mitogenactivated protein kinase-dependent S6 kinase pathway. Mol. Cell Biol. 24:3112-3124.

Petersen RB and Lindquist S. (1989). Regulation of HSP70 synthesis by messenger RNA degradation. Cell Regul. 1:135-49.

Peterson TR, Laplante M, Thoreen CC, Sancak Y, Kang SA, Kuehl WM, Gray NS and Sabatini DM. (2009). DEPTOR is an mTOR inhibitor frequently overexpressed in multiple myeloma cells and required for their survival. Cell 137: 873-886.

Powers RW III, Kaeberlein M, Caldwell SD, Kennedy BK, and Fields S. (2006). Extension of chronological life span in yeast by decreased TOR pathway signaling. Genes Dev. 20: 174–184.

Prats AC, Mertani HC, Dumontet C, and Diaz JJ. (2009). Dysregulation of ribosome biogenesis and translational capacity is associated with tumor progression of human breast cancer cells. PLoS One 4, e7147.

Proud CG. (2007). Signalling to translation: how signal transduction pathways control the protein synthetic machinery. Biochem J. 403(2):217-34.

Proud CG. (2009). mTORC1 signalling and mRNA translation. Biochem. Soc. Trans. 37: 227–231.

Proud CG. (2011). mTOR signalling in health and disease. Biochem. Soc. Trans. 39: 431–436.

Qian S-B, Ott DE, Schubert U, Bennink JR, and Yewdell JW. (2002).Fusion proteins with COOH-terminal ubiquitin are stable and maintain dual functionality in vivo. J. Biol. Chem. 277: 38818–38826.

Qian S-B, Bennink JR, and Yewdell JW. Quantitating defective ribosome products. (2005). Methods Mol Biol. 301:271-81.

Qian S-B, McDonough H, Boellmann F, Cyr DM, and Patterson C. (2006). CHIP-mediated stress recovery by sequential ubiquitination of substrates and Hsp70. Nature. 440(7083): 551-5.

Qian S-B, Princiotta MF, Bennink JR, and Yewdell JW. (2006). Characterization of rapidly degraded polypeptides in mammalian cells reveals a novel layer of nascent protein quality control. J Biol Chem 281(1):392-400.

Qian S-B, Zhang X, Sun J, Bennink JR, Yewdell JW, and Patterson C. (2010) mTORC1 links protein quality and quantity control by sensing chaperone availability. J Biol Chem 285(35):27385-95.

Qin X and Sarnow P. (2004). Preferential translation of internal ribosome entry site-containing mRNAs during the mitotic cycle in mammalian cells. J Biol Chem. 279(14):13721-8.

Rakwalska M and Rospert S. (2004). The ribosome-bound chaperones RAC and Ssb1/2p are required for accurate translation in Saccharomyces cerevisiae. Mol. Cell. Biol. 24: 9186–9197.

Reiling J and Sabatini DM. (2006). Stress and mTORture Signaling. Oncogene 25, 6373-83.

Richardson CJ, Bröenstrup M, Fingar DC, Jülich K, Ballif BA, Gygi S, Blenis J. (2004). SKAR is a specific target of S6 kinase 1 in cell growth control. Curr Biol.14 (17):1540-9.

Rogers AN, Chen D, McColl G, Czerwieniec G, Felkey K, Gibson BW, Hubbard A, Melov S, Lithgow GJ, and Kapahi P. (2011). Life span extension via eIF4G

inhibition is mediated by posttranscriptional remodeling of stress response gene expression in C. elegans. Cell Metab. 14(1):55-66.

Rosner M, Hanneder M, Siegel N, Valli A, and Hengstschläger M. (2008) The tuberous sclerosis gene products hamartin and tuberin are multi-functional proteins with a wide spectrum of interacting partners. Mutation Res.Rev. 658: 3, 234-246.

Rospert S, Dubaquie Y and Gautschi M. (2002). Nascent-polypeptide-associated complex. Cell. Mol. Life Sci. 59, 1632–1639.

Rubtsova MP, Sizova DV, Dmitriev SE, Ivanov DS, Prassolov VS, and Shatsky IN. (2003). Distinctive properties of the 5'-untranslated region of human hsp70 mRNA. J Biol Chem. 278(25): 22350-6.

Sahin M. and Kwiatkowski DJ. (2011). Regulable neural progenitor-specific Tsc1 loss yields giant cells with organellar dysfunction in a model of tuberous sclerosis complex. Proc. Natl. Acad. Sci. U.S.A. 108: E1070–E1079.

Sancak Y, Thoreen CC, Peterson TR, Lindquist RA, Kang SA, Spooner E, Carr SA and Sabatini DM. (2007). PRAS40 is an insulin-regulated inhibitor of the mTORC1 protein kinase. Mol. Cell 25: 903-915.

Sancak Y, Peterson TR, Shaul YD, Lindquist RA, Thoreen CC, Bar-Peled L, and Sabatini DM. (2008). The Rag GTPases bind raptor and mediate amino acid signaling to mTORC1. Science 320: 1496–1501.

Sancak Y, Bar-Peled L, Zoncu R, Markhard AL, Nada S, and Sabatini DM. (2010). Ragulator–Rag complex targets mTORC1 to the lysosomal surface and is necessary for its activation by amino acids. Cell 141: 290–303.

Sarbassov DD, Ali SM, Kim D-H, Guertin DA, Latek RR, Erdjument-Bromage H, Tempst P, and Sabatini DM. (2004) Rictor, a novel binding partner of mTOR, defines a rapamycin-insensitive and Raptor-independent pathway that regulates the cytoskeleton. Curr. Biol. 14: 1-20.

Sarbassov DD, Ali SM, Sabatini DM. (2005). Growing roles for the mTOR pathway. Curr Opin Cell Biol. (6): 596-603.

Sarbassov DD, Ali SM, Sengupta S, Sheen JH, Hsu PP, Bagley AF, Markhard AL and Sabatini DM. (2006). Prolonged rapamycin treatment inhibits mTORC2 assembly and Akt/PKB. Mol. Cell 22: 159-168.

Sarnow P, Cevallos RC, Jan E. (2005). Takeover of host ribosomes by divergent IRES elements. Biochem Soc Trans. 33(Pt 6):1479-82.

Schubert U, Antón LC, Gibbs J, Norbury CC, Yewdell JW, and Bennink JR. (2002). Rapid degradation of a large fraction of newly synthesized proteins by proteasomes. Nature 404: 770–774.

Schwanhäusser B, Busse D, Li N, Dttmar G, Schuchhardt J, Wolf J, Chen W, and Selbach M. (2011). Global quantification of mammalian gene expression control. Nature 473(7347): 337-342.

Selman C, Tullet JM, Wieser D, Irvine E, Lingard SJ, Choudhury AI, Claret M, Al-Qassab H, Carmignac D, Ramadani F, Woods A, Robinson ICA, Schuster E, Batterham RL, Kozma SC, Thomas G, Carling D, Okkenhaug K, Thornton JM, Partridge L, Gems D, and Withers DJ. (2009). Ribosomal Protein S6 Kinase 1 Signaling Regulates Mammalian Life Span. Science 326(5949): 140-144.

Shahbazian D, Roux PP, Mieulet V, Cohen MS, Raught B, Taunton J, Hershey JW, Blenis J, Pende M, and Sonenberg N. (2006). The mTOR/PI3K and MAPK pathways converge on eIF4B to control its phosphorylation and activity. EMBO J.25:2781-91.

Shalgi R, Hurt AH, LKrykbaeva I, Taipale M, Lindquist S, and Burge CB. (2012). Widespread regulation of translation by elongation pausing in heat shock. Mol Cell 49: 439–452.

Sherman MY and Goldberg AL. (2001). Cellular defenses against unfolded proteins: A cell biologist thinks about neurodegenerative diseases. Neuron 29: 15–32.

Shi Y, Mosser DD, and Morimoto RI. (1998). Molecular chaperones as HSF1-specific transcriptional repressors. Genes Dev. 12(5): 654-66.

Shubert U, Antón LC, Gibbs J, Norbury CC, Yewdell JW, and Bennink JR. (2000). Rapid degradation of a large fraction of newly synthesized proteins by proteasomes. Nature. 404(6779): 770-774.

Siller E, DeZwaan DC, Anderson JF, Freeman BC, Barral JM. (2010). Slowing bacterial translation speed enhances eukaryotic protein folding efficiency. J Mol Biol. 396(5):1310-8.

Sonenberg N and Hinnebusch AG. (2007). New modes of translational control in development, behavior, and disease. Mol. Cell 28:721-729.

Sonenberg N and Hinnebusch AG. (2009). Regulation of translation initiation in eukaryotes: Mechanisms and biological targets. Cell 136: 731–745.

Spencer PS, Siller E, Anderson JF, and Barral JM. (2012). Silent substitutions predictably alter translation elongation rates and protein folding efficiencies. J. Mol. Biol. 422: 328-335.

Spriggs KA, Stoneley M, Bushell M, and Willis AE. (2008). Re-programming of translation following cell stress allows IRES-mediated translation to predominate. Biol Cell. 100(1): 27-38.

Stanfel MN, Shamieh LS, Kaeberlein M, and Kennedy BK. (2009). The TOR pathway comes of age. Biochimica et Biophysica Acta (BBA) 1790(10): 1067-1074.

Sun J, Conn CS, Han Y, Yeung V, and Qian S-B. PI3K-mTORC1 attenuates stress response by inhibiting cap-independent Hsp70 mRNA translation. (2011). J Biol Chem. 286(8):6791-800.

Syntichaki P, Troulinaki K, and Tavernarakis N. (2007). "eIF4E function in somatic cells modulates ageing in Caenorhabditis elegans." Nature 445(7130): 922-926.

Tang H, Hornstein E, Stolovich M, Levy G, Livingstone M, Templeton D et al. (2001). Amino acid-induced translation of TOP mRNAs is fully dependent on phosphatidylinositol 3-kinase-mediated signaling, is partially inhibited by rapamycin, and is independent of S6K1 and rpS6 phosphorylation. Mol Cell Biol 21: 8671–8683.

Tee AR and Blenis J. (2005). mTOR, translational control and human disease. Semin Cell Dev Biol. 16(1): 29-37.

Thoreen CC, Kang SA, Chang JW, Liu Q, Zhang J, Gao Y, Reichling LJ, Sim T, Sabatini DM, and Gray NS. (2009). An ATP-competitive mammalian target of rapamycin inhibitor reveals rapamycin-resistant functions of mTORC1. J Biol Chem. 284 (12): 8023-32.

Thoreen CC, Chantranupong L, Keys HR, Wang T, Gray NS, and Sabatini DM. (2012). A unifying model for mTORC1-mediated regulation of mRNA translation. Nature. 485(7396):109-13.

Tsang CK, Bertram PG, Ai W, Drenan R, and Zheng XF. (2003). Chromatin-mediated regulation of nucleolar structure and RNA Pol I localization by TOR. EMBO J.; 22:6045–6056.

Tsang CK, Liu H, and Zheng XF. (2010). mTOR binds to the promoters of RNA polymerase I- and III-transcribed genes. Cell Cycle. 9(5): 953–957.

Tuller T, Carmi A, Vestsigian K, Navon S, Dorfan Y, Zaborske J, Pan T, Dahan O, Furman I, Pilpel Y. (2010). An Evolutionarily Conserved Mechanism for Controlling the Efficiency of Protein Translation. Cell 141(2): 344-354.

Turner GC and Varshavsky A. (2000). Detecting and measuring cotranslational protein degradation in vivo. Science 289: 2117–2120.

Vander Haar E, Lee SI, Bandhakavi S, Griffin TJ and Kim DH. (2007). Insulin signalling to mTOR mediated by the Akt/PKB substrate PRAS40. Nat. Cell Biol. 9, 316-323.

Vellai T, Takacs-Vellai K, Zhang Y, Kovacs AL, Orosz L, Müller F. (2003). Genetics: influence of TOR kinase on lifespan in C. elegans. Nature. 426(6967): 620.

Voisine C, Pedersen JS, and Morimoto RI. (2010). Chaperone networks: Tipping the balance in protein folding diseases. Neurobiology of Disease 40(1): 12-20.

Wang F, Durfee LA and Huibregtse JM. (2013). A cotranslational ubiquitination pathway for quality control of misfolded proteins. Mol. Cell 50(3):368-78.

Wang X, Li W, Williams M, Terada N, Alessi DR, and Proud CG. (2001). Regulation of elongation factor 2 kinase by p90 (RSK1) and p70 S6 kinase. EMBO J. 20 (16): 4370–9.

Wang X and Proud C. (2006). The mTOR pathway in the control of protein synthesis. Physiology 21:362-369.

Wang X, Larsson O, Selvaraj A, Liu Y, Kozma SC, Thomas G, and Sonenberg N. (2010). mTORC1-mediated cell proliferation, but not cell growth, controlled by the 4E-BPs. Science 328: 1172–1176.

Warner JR. (1999). The economics of ribosome biosynthesis in yeast. Trends Biochem Sci 24: 437–440.

Wegele H, Müller L, and Buchner J. (2004). Hsp70 and Hsp90--a relay team for protein folding. Rev Physiol Biochem Pharmacol. 151:1-44.

Wilson MA, Meaux S, and van Hoof A. (2007). A genomic screen in yeast reveals novel aspects of nonstop mRNA metabolism. Genetics. (2):773-84.

Wu C. Heat shock transcription factors: structure and regulation. (1995). Annu Rev Cell Dev Biol. 11: 441-69.

Wullschleger S, Loewith R, and Hall MN. (2006).TOR signaling in growth and metabolism. Cell 124: 471–484.

Xiao, L. and Grove, A. (2009). Coordination of ribosomal protein and ribosomal RNA gene expression in response to TOR signaling. Current Genomics 10: 198-205.

Yang, HS, Jansen, AP, Komar, AA, Zheng X, Merrick WC, Costes S, Lockett SJ, Sonenberg N, and Colburn NH. (2003). The transformation suppressor Pdcd4 is a novel eukaryotic translation initiation factor 4A binding protein that inhibits translation. Mol. Cell. Biol. 23: 26–37.

Yang Q, Inoki K, Kim E, and Guan KL. (2006). TSC1/TSC2 and Rheb have different effects on TORC1 and TORC2 activity. Proc Natl Acad Sci U S A. (18): 6811-6.

Yang X, Yang C, Farberman A, Rideout T, de Lange C, France J, and Fan MZ. (2009). The mammalian target of rapamycin-signaling pathway in regulating metabolism and growth. J. Anim. Sci. 86.36-47.

Yam AY, Xia Y, Lin HT, Burlingame A, Gerstein M, and Frydman J. (2008). Defining the TRiC/CCT interactome links chaperonin function to stabilization of newly made proteins with complex topologies. Nat Struct Mol Biol 15: 1255-62.

Yewdell JW and Nicchitta CW. (2006). The DRiP hypothesis decennial: support, controversy, refinement and extension. Trends Immunol 27: 368–373.

Zhang G, Hubalewska M, and Ignatova Z. (2009). Transient ribosomal attenuation coordinates protein synthesis and co-translational folding. Nature Structural &; Molecular Biology 16(3): 274-280.

Zhou X, Ikenoue T, Chen X, Li L, Inoki K, and Guan KL. (2009).Rheb controls misfolded protein metabolism by inhibiting aggresome formation and autophagy. Proc. Natl. Acad. Sci. U.S.A. 106, 8923–8928.

Zid BM, Rogers AN, Katewa SD, Vargas MA, Kolipinski MC, Lu TA, Benzer S, and Kapahi P. (2009). 4E-BP Extends Lifespan upon Dietary Restriction by Enhancing Mitochondrial Activity in Drosophila. Cell 139(1): 149-160.

Zoncu R, Bar-Peled L, Efeyan A, Wang S, Sancak Y, and Sabatini DM. (2011). mTORC1 senses lysosomal amino acids through an inside-out mechanism that requires the vacuolar H(+)-ATPase. Science 334, 678–683.

Zoncu R, Efeyan A and Sabatini DM. (2011). mTOR: from growth signal integration to cancer, diabetes and ageing. Nature Rev. Mol. Cell Biol. 12, 21–35.